Journal of CO2 Utilization 90 (2024) 102986

Contents lists available at ScienceDirect

Journal of CO2 Utilization

journal homepage: www.elsevier.com/locate/jcou

Carbon sequestration, performance optimization and environmental impact assessment of functional materials in cementitious composites

Kailun Chen [a], Fulin Qu [a], Zihui Sun [b], Surendra P. Shah [c], Wengui Li [a,*]

[a] Centre for Infrastructure Engineering and Safety, School of Civil and Environmental Engineering, The University of New South Wales, NSW 2052, Australia
[b] Department of Civil and Environmental Engineering, University of Louisville, KY 40292, USA
[c] Center for Advanced Construction Materials, Department of Civil Engineering, The University of Texas at Arlington, TX 76019, USA

ARTICLE INFO

Keywords:
Carbon sequestration
Nano-TiO_2
Graphene oxide
Wollastonite
Biochar, Cellulose fiber

ABSTRACT

This paper reviews the mechanisms of carbon sequestration, methods for testing carbon sequestration capacity, and the performance of functional materials, including wollastonite, titanium dioxide nanoparticles (Nano-TiO_2), graphene oxide (GO), biochar, and cellulose fibers (CS), as well as their performance in cement-based materials. A system boundary model has been developed to facilitate a comprehensive analysis of the environmental impact associated with preparing these materials as concretes. It is demonstrated that wollastonite reacts with atmospheric carbon dioxide (CO_2) to form carbonate minerals, contributing to carbon sequestration. Nano-TiO_2 and GO absorb and transform CO_2 through light-excited charge carriers to generate redox reactions and oxide functional groups on their surfaces and edges, respectively. Biochar achieves carbon sequestration through physical and chemical stability, while the carbon sequestration mechanism in cellulose fibers is related to their structural properties as plant materials. In cement-based materials, wollastonite significantly enhances mechanical properties by filling pores and bridging microcracks. Nano-TiO_2 and GO enhance mechanical properties by providing nucleation sites and template effects, among other mechanisms. An appropriate amount of biochar improves densification and strength, while cellulose fibers facilitate the cement hydration process, thus enhancing mechanical properties. Additionally, Life Cycle Assessment (LCA) analyses demonstrate that wollastonite and cellulose fibers offer sustainable environmental benefits in producing low-carbon concrete due to their low Global Warming Potential (GWP) and minimal negative impacts on the environment and human health. This review emphasizes the pivotal role of these functional construction materials in mitigating climate change.

1. Introduction

Amid global climate change, CO_2 emissions stand as one of the primary drivers of the greenhouse effect. Its environmental impact is profound, particularly in accelerating temperature rises across both marine and terrestrial ecosystems [1], as depicted in Fig. 1(a). Furthermore, an increasing body of evidence highlights the direct risks posed to human health by elevated CO_2 concentrations in the environment [2], as illustrated in Fig. 1(b). Short-term exposure to high levels of CO_2 (2000–4000 ppm) can result in chronic inflammation and cognitive impairment, while prolonged exposure (above 3000 ppm) may lead to systemic inflammation and conditions such as osteoporosis. The construction industry, known for its high energy consumption and emissions, is a significant contributor to global CO_2 output. It is estimated that construction activities account for roughly 39 % of the world's annual CO_2 emissions [3], as shown in Fig. 1(c). In both developed and developing countries, the sector's energy consumption and carbon emissions exceed one-third of the total. Notably, materials commonly used in construction, including cement, steel, glass, and aluminium, leave a substantial carbon footprint during production, as indicated in Fig. 1(d), due to their high Global Warming Potential (GWP) [4–6]. In addition to the large amount of energy consumed in their production, the chemical processes involved directly emit CO_2, making them significant sources of carbon emissions. In recent years, as the focus on global sustainability intensifies, the development of technologies and materials to reduce the construction sector's carbon footprint has become an urgent priority.

Carbon Capture and Storage (CCS) is regarded as one of the most effective solutions to combat climate change. In the construction industry, researchers are focused on developing innovative cement-based

* Corresponding author.
E-mail address: wengui.li@unsw.edu.au (W. Li).

https://doi.org/10.1016/j.jcou.2024.102986
Received 21 September 2024; Received in revised form 1 November 2024; Accepted 25 November 2024
Available online 4 December 2024

materials that can capture and sequester atmospheric CO_2, ultimately achieving carbon-negative building materials. Recent advancements in CCS materials include the modification of cement-based composites with new additives such as wollastonite, titanium dioxide nanoparticles (Nano-TiO_2), and graphene oxide (GO). Recent studies have highlighted the effectiveness of wollastonite when combined with cementitious materials for carbon capture [7,8]. Wollastonite, a calcium silicate mineral, reacts with atmospheric CO_2 after carbonation, forming stable calcium carbonate ($CaCO_3$). This reaction not only sequesters carbon but also strengthens the cement matrix by filling pores and enhancing durability. Wollastonite can achieve a high carbon sequestration rate, with up to 70 % of the mineral transforming into $CaCO_3$ under optimal conditions in a short period [9]. Similarly, Nano-TiO_2 and GO show promising potential in enhancing the carbon capture capabilities of cementitious materials. Nano-TiO_2, known for its photocatalytic properties, is highly effective in environmental applications such as carbon sequestration. When incorporated into cement-based materials, Nano-TiO_2 facilitates photocatalytic reactions under light exposure, capturing CO_2 from the atmosphere and converting it into stable carbonates [10,11]. This not only reduces carbon emissions but also significantly improves the performance of cementitious materials. Also, GO, a two-dimensional material, exhibits excellent adsorption capabilities due to its high surface area and abundant oxygen-containing functional groups. These properties enable GO to effectively capture CO_2 when integrated into cement. Additionally, GO enhances the mechanical properties of the cement matrix by acting as nucleation sites during hydration, strengthening the matrix and reducing porosity. GO-modified cement composites have demonstrated higher CO_2 capture efficiency, contributing to the production of more durable and functional building materials [12].

On the other hand, recent studies [13,14] have shown that biochar can be effectively used in cement-based materials to enhance carbon capture, primarily through the process of mineral carbonation. Biochar is produced by the pyrolysis of organic residues, such as agricultural waste, and its highly porous structure allows it to capture and sequester atmospheric CO_2. This CO_2 reacts with calcium compounds in cement to form stable $CaCO_3$, thus storing carbon in a solid form. The addition of biochar not only aids in carbon capture but also improves the mechanical and thermal properties of the cement, making it more durable and energy efficient.

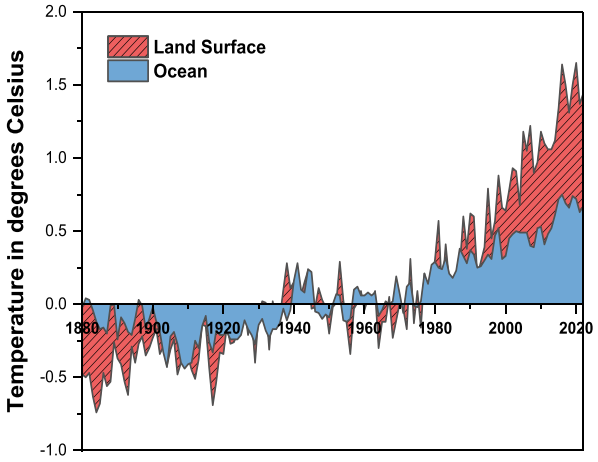

(a) CO_2 impacts on the environment

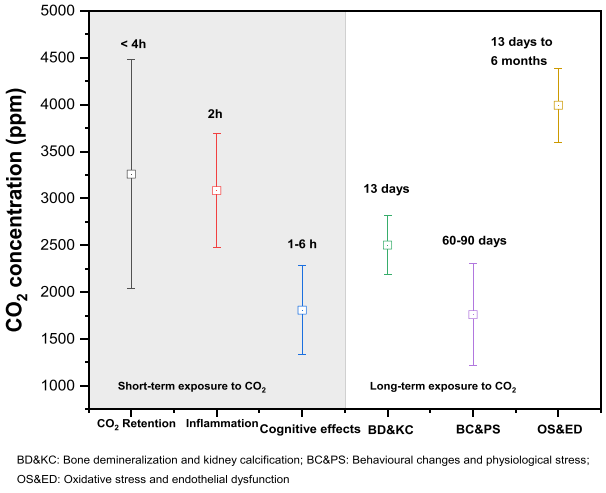

(b) CO_2 impacts on human health

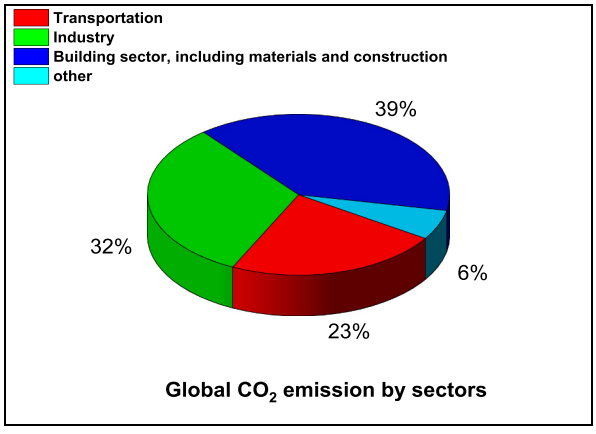

(c) CO_2 emissions from different sectors

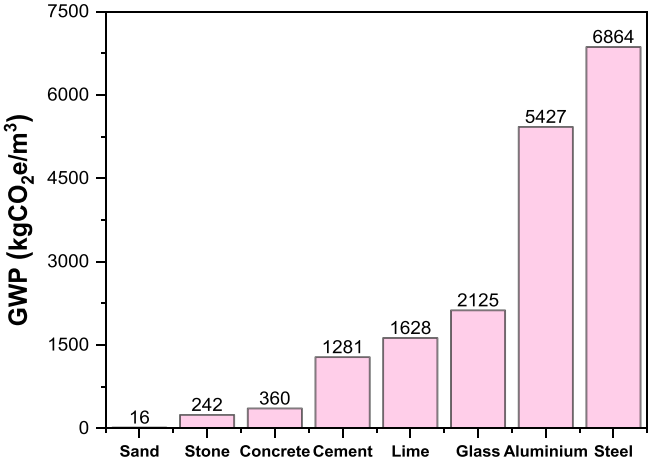

(d) GWP values of different building materials

Fig. 1. Global Building Materials Industry Overview: CO_2 Emissions, Health Impacts and Market Trends [1–6].

Similarly, cellulose fibers, another reinforcement for cement-based materials, significantly enhance carbon capture efficiency through mineral precipitation. These plant-derived fibers not only improve the structural strength and crack resistance of the cement matrix but also provide nucleation sites for carbonation reactions. In this process, atmospheric CO_2 reacts with calcium hydroxide in cement to form $CaCO_3$, permanently sequestering carbon [15–17]. This process not only reduces the carbon footprint of cement-based materials but also significantly improves their durability and structural integrity, making cellulose fibers a highly promising sustainable material for carbon capture in construction [18–21].

This paper thoroughly examines the pivotal role of functional construction materials in carbon sequestration technologies, offering an in-depth analysis of materials suitable for carbon sequestration in cement-based systems, including wollastonite, nano-TiO_2, GO, biochar, and cellulose fibers [22–24]. The potential of these materials to enhance carbon sequestration efficiency, improve the structural properties of cement-based materials, and boost environmental performance and durability is assessed. Furthermore, their overall environmental impact is analyzed through Life Cycle Assessment (LCA). This paper provides researchers with practical guidelines and strategies for utilizing these advanced materials to achieve sustainable development goals in the construction industry, while also exploring their contribution to reducing GWP, offering new research directions for sustainable development in construction.

2. Wollastonite: a novel approach to carbon sequestration

2.1. Definition of wollastonite and mechanism of carbon sequestration

Wollastonite is a naturally occurring mineral that contains silicates, including silicon, oxygen, calcium, and magnesium. It plays a crucial role in carbon sequestration through mineral carbonation or mineral sequestration, which involves the chemical reaction of CO_2 in the environment to produce carbonate minerals [25–27]. The $CaSiO_3$ structure of wollastonite was discovered in 1886 by WH Wollaston, a British mineralogist and chemist. Wollastonite is formed through the reaction of silica and limestone at high temperatures (400–450 °C), as shown in Eq. (1) [28].

$$CaCO_3 + SiO_2 \rightarrow CaSiO_3 + CO_2 \quad (1)$$

Wollastonite's needle-like crystal structure gives it a white appearance, as shown in Fig. 2. This material contains β-CaO-SiO_2, which imparts excellent properties such as biocompatibility, low dielectric constants and losses, low coefficient of thermal expansion, low thermal conductivity, good thermal stability, and properties that facilitate melting [29–31]. Wollastonite is a highly cost-effective material that can be effortlessly ground into a fine powder. Its extensive use in various fields, including agricultural carbon sequestration, soil improvement, and concrete manufacturing [32–34], is a testament to its exceptional properties.

Wollastonite is an excellent candidate for carbon sequestration due to its natural origin and environmentally friendly mining and processing methods. Its use results in significantly less pollution compared to synthetic building materials. Wollastonite is a naturally occurring and abundant material, making it an excellent sustainable building material. Its use in cement and concrete allows for the absorption of CO_2 through carbonation, which sequesters atmospheric CO_2 in the form of $CaCO_3$ solids Eqs. (2) to (4) [36]. This process is highly effective in reducing atmospheric CO_2 levels. Research has shown that wollastonite can significantly reduce greenhouse gas emissions when used as a substitute for cement [37]. By replacing 20 wt% of cement with wollastonite in the production of 1 m^3 of CO_2-cured cement blocks, GWP can be reduced from 419 kg CO_2 equivalent for Ordinary Portland Cement (OPC) to 292 kg CO_2-eq. It confidently demonstrates that wollastonite is an effective material for reducing CO_2 emissions and lowering its levels in the environment when used as a partial replacement for cement. Moreover, increasing the amount of wollastonite replacement is likely to

Fig. 2. Morphologies of wollastonite martials: (a) wollastonite ore; (b) wollastonite powder; (c) and (d) micrographs of coarse and fine wollastonite particles [35].

further enhance its positive impact on the environment, underscoring the significant advantages of wollastonite's carbon sequestration capacity. Wollastonite not only serves as a green building material, but also plays a crucial role in carbon sequestration and mitigating global warming.

$$H_2O + CO_2 \rightarrow CO_3^{2-} + 2H^+ \quad (2)$$

$$Ca(OH)_2 + CO_3^{2-} + 2H^+ \rightarrow CaCO_3 + 2H_2O \quad (3)$$

$$CaO \bullet SiO_2 + CO_3^{2-} + H^+ \rightarrow CaCO_3 + SiO_2 \bullet nH_2O \quad (4)$$

In summary, wollastonite is a highly promising green building material with significant potential for environmental protection and sustainable development. Its unique ability to react with atmospheric CO_2 to form carbonate minerals positions it as a key player in carbon sequestration technology, which is essential for reducing greenhouse gas emissions. Wollastonite is an ideal building material for enhancing the durability and environmental resilience of structures due to its physical and chemical properties. Its biocompatibility and low coefficient of thermal expansion are particularly noteworthy.

2.2. Carbon sequestration capacity of wollastonite in cement-based materials

Cement-based materials have been studied as a potential solution for storing CO_2 [38–41], with their CO_2 storage capacity being dependent on their chemical composition, specifically the oxide content [36]. The Eq. (5) can be used to predict the maximum amount of CO_2 that can be stored in a cement-based material based on its oxide content [42].

$$CO_2(\%, Max) = 0.785(CaO - 0.7SO_3) + 1.091MgO + 1.420Na_2O + 0.935K_2O \quad (5)$$

However, evaluating the ability of wollastonite to sequester carbon in cement-based materials involves various methods. Wollastonite has the potential to absorb CO_2, and its carbon sequestration efficiency can be confidently evaluated through surface area measurements, thermogravimetric analysis (TGA), and X-ray diffraction (XRD) analysis. These methods provide detailed and reliable information about the structure of wollastonite, its surface activity, and its capacity to absorb CO_2. Incorporating wollastonite into cement-based materials requires a comprehensive assessment of its microstructure, physical properties, and chemical composition to fully evaluate its potential for carbon sequestration. This evaluation will aid in optimizing the formulation of cement-based materials to maximize their efficiency in storing CO_2.

Huang et al. [43] conducted a study using the device shown in Fig. 3 to investigate the carbon fixation ability of wollastonite in cement-based materials. The carbon sequestration performance of wollastonite was evaluated by measuring the pressure difference and temperature change in the surge chamber before and after the reaction. The carbon sequestration capabilities of these materials were found to be exceptional under mild environmental conditions (0.5–2.5 MPa, 40 °C), with CO_2 absorption reaching approximately 20 wt% after a 2-hour curing process. The study confirms that cement-based materials containing wollastonite minerals can significantly enhance the storage capacity of cement samples for CO_2, providing clear advantages over OPC. The carbon sequestration of wollastonite in cement-based materials is significantly higher than other composites, such as MgO-fly ash-OPC paste (15.57 %) [44], OPC-limestone paste (14.22 %) [45], steel slag block (6.60 %) [46], and waste concrete aggregate (3.88 %) [47]. Also, Li et al. [48] explored the performance of low-calcium silicate materials in carbon sequestration within cementitious materials, with a particular focus on the significant role of wollastonite during the carbonation process. The carbonation curing process (under conditions of 20 % CO_2 concentration and high humidity) accelerated the reaction between cementitious materials and CO_2, generating stable products such as $CaCO_3$ and silica gel, as shown in Fig. 3(b). Low-calcium silicate minerals like wollastonite exhibit high carbonation reactivity, effectively capturing CO_2 and forming $CaCO_3$, which enhances the strength and durability of the materials. The experimental results showed that the maximum CO_2 absorption rate for the carbonated samples was 25.3 %, demonstrating the considerable potential of wollastonite for carbon sequestration in cementitious materials.

Kashim et al. [49] conducted carbonation experiments using an autoclave reactor equipped with a piston-assisted high-pressure accumulator (refer to Fig. 4). Following a period of 10 days, suspension samples of wollastonite and water were collected, dried, and turned into powder samples. These samples were then subjected to TGA. The study unequivocally demonstrates that wollastonite has a remarkable capacity for CO_2 storage. Specifically, 10 g of wollastonite can sequester 3.42 g of CO_2. Importantly, there is a strong positive statistical correlation between the amount of wollastonite consumed and the amount of CO_2 stored. For example, to sequester 1 metric ton of CO_2 annually, 5.160 metric tons of wollastonite would be required.

Saxena et al. [50] explored the carbon sequestration potential of wollastonite as a partial replacement (1–5 wt%) for limestone in cement production. Using TGA, they found that wollastonite exhibited low weight loss (4.67 %) due to chemical dissociation, indicating its stability. Cement with 1 wt% wollastonite emitted 0.013 t CO_2/t less CO_2 than conventional cement, demonstrating its ability to significantly reduce emissions and offering a greener alternative for the cement industry.

In summary, Wollastonite shows significant potential for carbon sequestration in cementitious materials. Under optimal conditions, its

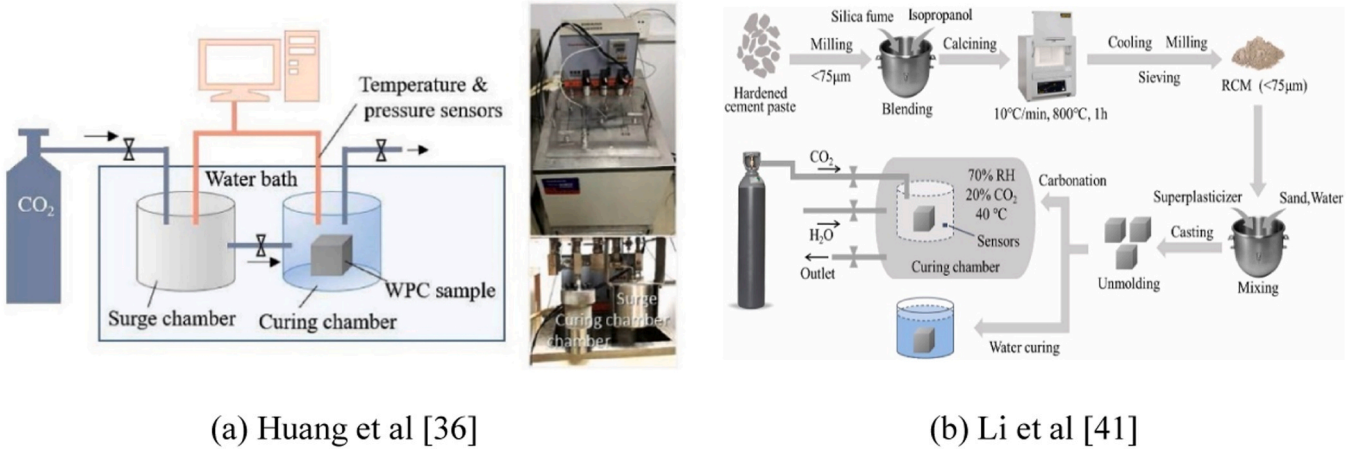

(a) Huang et al [36] (b) Li et al [41]

Fig. 3. Cement-based materials containing wollastonite carbon sequestration capacity test device.

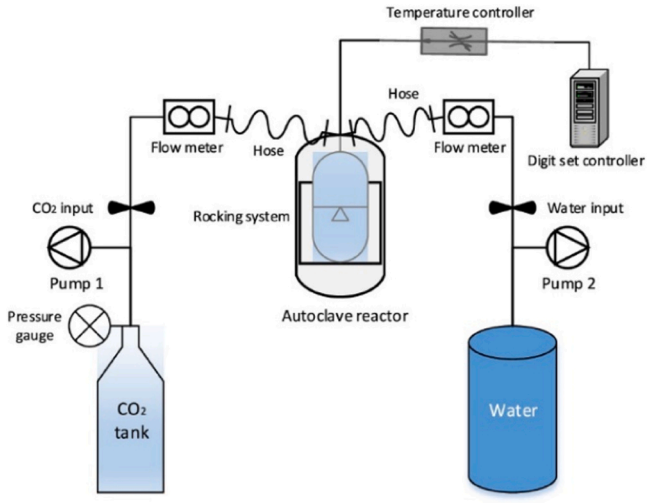

Fig. 4. Schematic of the rocking-batch experimental setup [49].

CO_2 absorption rate can reach up to 25.3 %, and even in milder environmental conditions, wollastonite remains a stable and effective CO_2 absorbent, making it a valuable material for reducing carbon emissions in cement production. Several research methods, including TGA, pressure and temperature monitoring, and autoclave carbonation, have been employed to evaluate its performance, each offering unique insights into its carbon sequestration capabilities. TGA effectively quantifies CO_2 absorption by tracking the weight changes of wollastonite as it reacts with CO_2. While TGA provides precise data on CO_2 absorption, it is less effective at capturing the detailed microstructural changes that occur during carbonation. In contrast, pressure and temperature monitoring allows real-time tracking of the carbonation process, offering a dynamic view of carbon sequestration. However, this method requires specialized equipment and strict environmental control, which limits its broader application. Autoclave carbonation, on the other hand, provides valuable insights into large-scale carbon sequestration under industrial conditions, though it may not fully replicate the milder conditions typical of cement applications. Each method has its strengths and limitations: TGA is ideal for accurate CO_2 absorption measurements, pressure monitoring captures real-time reaction kinetics, and autoclave carbonation demonstrates scalability for industrial use.

2.3. Effect of wollastonite on the mechanical properties of cement-based materials

The introduction of wollastonite as a supplementary cementitious material in cement-based systems can effectively enhance microstructural optimization, significantly improving the mechanical properties of the material. Table 1 lists several recent studies on the impact of wollastonite-cement composite systems on mechanical properties. Yücel et al. [51] prepared green mortars using 3–15 wt% wollastonite as the replacement of cement. This study showed that for the mechanical strength of the mortar, both compressive and flexural strengths increased with increasing wollastonite content, with an optimum substitution ratio of 9 wt%. The increase in compressive strength is mainly attributed to the pore filling benefits of wollastonite, while the development of flexural strength is attributed to the microfiber capacity of wollastonite minerals, which helps to bridge microcracks by achieving a higher load bearing capacity in the cement aggregate. Similarly, Zhu et al. [52] found that the optimum replacement of cement by wollastonite should not exceed 10 wt% and that a higher replacement would have an unacceptable effect on the compressive strength of the mortar. The compressive strength of the samples with 10 wt% wollastonite was increased by 106.22 % compared to the compressive strength of conventional cement mortar. Notably, this study also showed that the wollastonite particle size (3μm-12μm) had little effect on the compressive strength, with samples containing 10 wt% wollastonite and 3 mm particle size (D50) exhibiting the best mechanical properties. However, the effect of wollastonite on flexural strength was slightly greater than that of wollastonite on compressive strength; in particular, smaller sized wollastonite microfibers act as both a bridging agent for the fibers and a filler for the fine aggregates, while wollastonite of larger particle sizes has similar properties to the coarser fibers and acts mainly as a bridging agent for the fibers, effectively cushioning and absorbing the energy generated by the matrix fracture, which effectively cushions and absorbs

Table 1
Contribution of wollastonite to the mechanical strength of cement-based materials.

Refs.	Chemical composites of wollastonite	Control variable (replaced by wollastonite wt %)	Sample types	Mechanical properties	
				Compressive strength (MPa)	Flexural strengths (MPa)
[51]	CaO (46.5 %) SiO_2(50.1 %) Al_2O_3(0.7 %)	3–15 wt% of cement	Mortar	43–60 (7 days) 47–66 (28 days)	7–9 (7 days) 8–11 (28 days)
[52]	CaO (45.1 %) SiO_2 (51.4 %) Al_2O_3 (0.7 %)	0–20 wt% of cement	Mortar	52–58 (28 days)	8–12 (28 days)
[55]	—	0–50 wt% of cement	Mortar	25–47 (7 days) 30–47 (28 days)	—
[56]	—	2–8 wt% of cement	Mortar	22–30 (7 days) 33–45 (28 days)	4–5 (7 days) 5–6 (28 days)
[57]	—	0–25 wt% of cement	Concrete	w/b (0.55):34–38 (90 days) w/b (0.5):37–43 (90 days) w/b (0.45):43–50(90 days)	w/b (0.55):4.1–4.7 (90 days) w/b (0.5):3.9–4.7 (90 days) w/b (0.45):4.3–4.7 (90 days)
[58]	CaO(45.6 %); SiO_2(48 %); Al_2O_3(1.4 %)	A: 10 wt% of total cementitious materials B: 10 wt% of sand	Concrete	A:26 (7 days) 37 (28 days) B:40 (7 days) 53 (28 days)	A:5 (28 days) 6 (56 days) B:6 (28 days) 7 (56 days)
[59]	—	0–8 wt% of cement	Concrete	26–35 (7 days) 34–47 (28 days)	3.5–4.7 (7 days) 4.7–5.7 (28 days)
[60]	—	0–0.5 wt% of mass	Concrete	19–20 (7 days) 20–35 (28 days)	5–6.4 (7 days) 4.5–6.1 (28 days)
[61]	CaO (48 %) SiO_2 (52 %) Al_2O_3 (3 %)	0–15 wt% of cement	Concrete	23–24 (7 days) 41–43 (28 days)	Split tensile strength: 2.6–3.2 (7days) 3–3.5(28 days)

the impact forces, thereby improving the brittleness and flexural strength of the matrix [53,54]. Furthermore, Khan et al. [55] investigated the effect of wollastonite particle size on cement hydration as well as compressive strength, the results show the additional nucleation sites and packing effect that wollastonite with a particle size of 3.5 μm can be provided to the hydration products, which can accelerate the hydration of cement; whereas the gain effect at later stages of the hydration process is due to the dilution effect. In addition, it was found that wollastonite, as an inert material, appears to have pozzolanic properties when ground to a particle size of 3.5 μm.

While incorporating wollastonite as a partial replacement for cement and sand generally enhances strength development, research mentioned above indicates there is an optimal dosage, typically around 10 wt%. Beyond this level, the material's strength starts to decline, and adverse effects on its mechanical properties become noticeable. Therefore, precise dosage control is critical to achieving the desired improvements. The use of wollastonite in concrete remains an area of ongoing study, with particular focus on optimizing its dosage to achieve the best performance outcomes. Mathur et al. [58] found a significant increase when they combined wollastonite and concrete: compressive strength (+28–35 %) and flexural strength (+36–42 %) after a detailed evaluation. Firstly, it optimizes the pore size distribution of the concrete, resulting in superior quality. Secondly, due to its impressive modulus of elasticity (200 GPa), it significantly enhances the toughness and flexural strength of the concrete. Wollastonite is highly beneficial for concrete in two keyways. In fact, Saranyadevi et al. [61] demonstrated that wollastonite can effectively increase the compressive and tensile strength of concrete by an impressive 3.4 %-6.9 % at 28 days. Also, the study conducted by Kogai et al. [59] unequivocally demonstrates that the addition of wollastonite at a dosage of 6 wt% results in concrete mixtures with optimal mechanical properties. This is due to the improvement of internal defects and pore size distribution at the interface of the cement and aggregates, leading to a higher density after forming and a greater degree of interaction between the initial components of the mixture. The addition of low dosages of wollastonite (less than 0.5 wt%) can reduce the internal stress values of concrete, which promotes strength development [60]. Furthermore, the study found that adding 0.25 wt% wollastonite increased compressive strength by 57 % and flexural strength by 12.5 %. These results demonstrate the significant impact that wollastonite can have on the strength of concrete. A recent study [57] demonstrated that replacing cement with wollastonite in the range of 10–15 wt% significantly improves the tensile strength of concrete. It is important to note that further increases in replacement may lead to a slight decrease in strength, which can be attributed to structural loosening.

Wollastonite has a significant impact on both the early-stage and hardened properties of concrete, particularly in terms of shrinkage resistance and durability. Its needle-like structure reduces drying shrinkage by limiting capillary stress, resulting in a 47 % reduction in shrinkage at higher replacement levels (around 30 %) [62]. Additionally, the chemical inertness and needle-like structure of wollastonite enhance the long-term performance of concrete, thereby improving durability [63]. Regarding workability, due to the shape and surface area of wollastonite, it tends to reduce the workability of concrete, leading to an increased water demand. This can be mitigated by using high-performance water-reducing agents. Under these conditions, the optimal replacement level of wollastonite is approximately 10 wt%, at which point the benefits in shrinkage resistance and durability are maximized without significantly affecting workability or strength [63].

In summary, the addition of wollastonite as a partial replacement for cement can significantly enhance the performance of cement-based materials. Research has shown that a replacement ratio of 3–15 wt% of wollastonite can improve the mechanical strength of mortar, with 9–10 wt% being the optimal ratio [51]. This enhancement is mainly due to the pore-filling effect of wollastonite and the ability of its micro-fibrous structure to bridge microcracks, thus increasing the load-bearing capacity of the material. Wollastonite particles have a minor impact on compressive strength. However, using wollastonite with a particle size of 3.5 μm accelerates the cement hydration process by providing additional nucleation sites, thereby enhancing the material properties[55]. This makes wollastonite an excellent choice for improving the structural properties of cement-based materials and preparing more environmentally friendly mortars. Wollastonite can be used as a partial replacement for cement or sand in concrete systems, resulting in a significant improvement in compressive, flexural, and tensile strengths. This is due to wollastonite's ability to enhance the pore distribution and toughness of concrete. It is important to note that a moderate addition of wollastonite (6 wt%) can optimize concrete performance. Avoiding excessive substitution is key to maintaining structural performance. Exercising reasonable control over the use of wollastonite admixture is essential to optimize the mechanical properties of concrete [59].

3. Nano-TiO_2 for carbon capture in cementitious materials

3.1. Properties and photocatalytic mechanism of nano-TiO_2

Nano-TiO_2 is a versatile nanomaterial with a particle size distribution ranging from 1 to 100 nm. It exists in three crystal types: anatase, rutile, and brookite, each with a distinct crystal structure. Specifically, anatase-TiO_2 has indirect bandgap properties, while rutile has direct bandgap properties. Noted that the indirect bandgap structure outperforms the direct bandgap in preventing electron-hole complexation [64,65]. This is the reason why anatase-TiO_2 exhibits higher photocatalytic activity than rutile-TiO_2 [66,67]. Nanoscale TiO_2 exhibits distinct physical and chemical properties in comparison to macroscopic one owing to its smaller particle size. These properties comprise a higher specific surface area, superior photocatalytic activity, and excellent optical properties. As a result, nanoscale TiO_2 finds extensive usage in diverse applications, including environmental purification, coatings, and self-cleaning materials [68–70].

Photocatalysis is a highly efficient and versatile technology that is widely recognized as an environmentally friendly solution to address the greenhouse gas problem. As shown in Fig. 5, the reaction mechanism of TiO_2 materials under photocatalysis is well-established. Solar radiation interacting with titanium dioxide crystals can cause an electron in the valence band to move to the conduction band, creating a photo-generated electron (e^-) -hole (h^+) pair. The hole on the surface of the TiO_2 acts as an oxidizing agent, while the electron in the excited state acts as a reducing agent, as shown in Eq. (6) to (8).

$$TiO_2 + hv \rightarrow e^- + h^+ \quad (6)$$

$$h^+ + OH^- \rightarrow \bullet OH + H^+ \quad (7)$$

$$e^- + O_2^- \rightarrow \bullet O_2^- \quad (8)$$

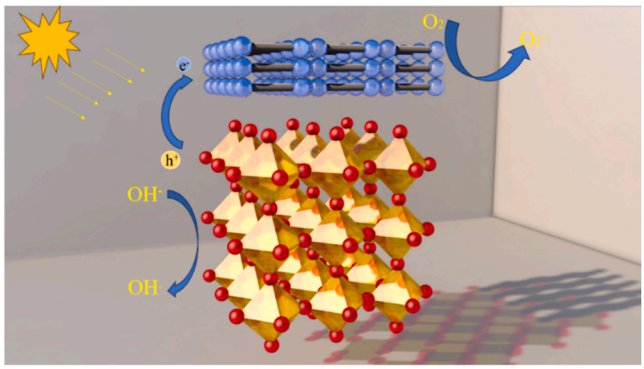

Fig. 5. Photocatalytic TiO_2 reaction mechanism.

TiO_2 acts as a safe photocatalyst. It converts CO_2 into environmentally friendly and harmless substances, thereby safely cleaning the air. This confident conversion process does not cause secondary pollution. The confident application of photocatalytic technology to carbon sequestration was confidently first reported by Fujishima and other researchers in 1979 [71]. TiO_2 was used as a photocatalyst to successfully reduce CO_2 to a substance with low environmental impact, as demonstrated by the reaction in Eqs. (9) to (13) [72]. The presence of water during the photocatalytic reaction converts solar energy to chemical energy by reducing CO_2 to hydrocarbons and oxygen. The conversion process produces substances, such as methanol (CH_3OH) and methane (CH_4), that have significant recycling and reuse value. These substances can directly replace petrol and diesel in the non-fossil fuel resources field [73,74].

$$H_2O + 2h^+ \rightarrow \frac{1}{2}O_2 + 2H^+ \quad (9)$$

$$CO_2 + 2e^- + 2H^+ \rightarrow HCOOH \quad (10)$$

$$HCOOH + 2e^- + 2H^+ \rightarrow HCHO + H_2O \quad (11)$$

$$HCHO + 2e^- + 2H^+ \rightarrow CH_3OH \quad (12)$$

$$CH_3OH + 2e^- + 2H^+ \rightarrow CH_4 + H_2O \quad (13)$$

In summary, the process of photocatalytic degradation of CO_2 involves the movement, reaction, and recombination of charge carriers under light excitation. Highly active materials, such as TiO_2 or ZnO, generate charge carriers when irradiated with light. Electrons fill the valence band of the material, while the conduction band has very few or no electronic ground states. To facilitate the oxidation reaction on the adsorbed material with the aid of light energy, the conduction band must have a negative potential greater than the desired potential [75,76]. The material is then oxidized through surface-bound hydroxyl radicals by the electrons in the valence band. This process requires a sufficient buildup of charge in the conduction band. Electrons migrate across the material's surface and combine with free electrons and charges in the trapping region. This region reacts with substances such as CO_2, producing hydrocarbons [77], as shown in Fig. 6. To ensure smooth progress, it is crucial to maintain a charge complexation rate that is significantly lower than the reaction rate. The compounding process can occur in a photocatalytic reaction when electrons migrate within the material and search for a place to be trapped, or when materials with small band gap energies are used. Charge complexation may result in a small energy release, which can reduce the efficiency of the photocatalytic reaction [78–80]. To conclude, the process of photocatalytic conversion of CO_2 comprises three main phases. Firstly, light generates electron-hole pairs. Secondly, the catalyst surface separates and converts these pairs. Finally, the photogenerated charges undergo a redox reaction with surface adsorbates. It is important to note that this process can occur in both the liquid and gas phases.

3.2. Carbon sequestration capacity of Nano-TiO_2 in cement-based materials

This is of paramount importance considering the pressing global need to reduce carbon emissions and promote environmental sustainability [81–83]. Nano-TiO_2 possess unique photocatalytic properties and can facilitate CO_2 capture and conversion in cement-based materials [84,85]. These studies aim to improve the environmentally friendly properties of the materials and discover novel pathways for the sustainable development of the cement industry. Then we thoroughly examined the capacity of nano-TiO_2 to fix CO_2 in cement-based materials. In their study, Moro et al. [86] demonstrated the significant impact of incorporating TiO_2 nanoparticles on the CO_2 sequestration capacity of cement pastes. This study utilized TGA to evaluate the CO_2 sequestration capacity of cement pastes. By comparing the difference in the $CaCO_3$ content of the samples under normal curing and CO_2 curing conditions, these were able to accurately calculate the amount of CO_2 uptake. The study's results, displayed in Fig. 7(a), clearly demonstrate that the amount of CO_2 uptake increases significantly with increasing nanoTiO_2 content during a 12-hour CO_2 curing process. These findings showcase the effectiveness of incorporating nanoTiO_2 in the mixture for CO_2 uptake. The samples containing 0.5 %, 1 %, and 2 % nanoparticles showed an increase in CO_2 uptake of 18.5 %, 20.5 %, and 38.4 %, respectively, compared to the reference paste without added nano-TiO_2. TiO_2 nanoparticles have been proven to be an effective photocatalyst for promoting carbon sequestration in cement-based materials. Moro et al. [87] investigated the effect of Nano-TiO_2 on the CO_2 sequestration capacity of hardened cement pastes using water-cement ratio (w/c values of 0.45, 0.50, and 0.55, respectively) as an influencing factor. Fig. 7(b) demonstrates a clear relationship between CO_2 uptake after 24 h and the water-cement ratio and percentage of nano-TiO_2. The results confidently indicate that CO_2 uptake increases with an increase in the water-cement ratio. This is due to the higher porosity resulting from the increased

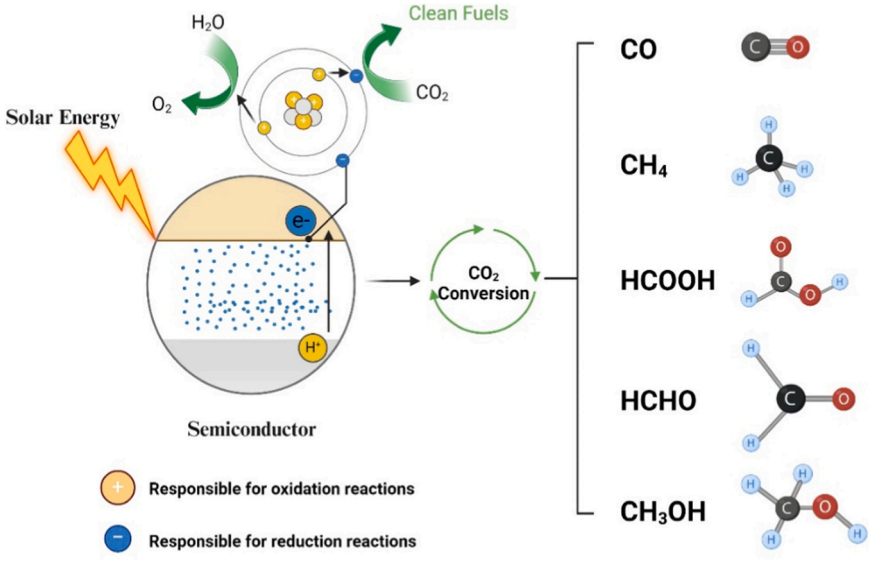

Fig. 6. Photocatalytic promotion of CO_2 reaction and the products.

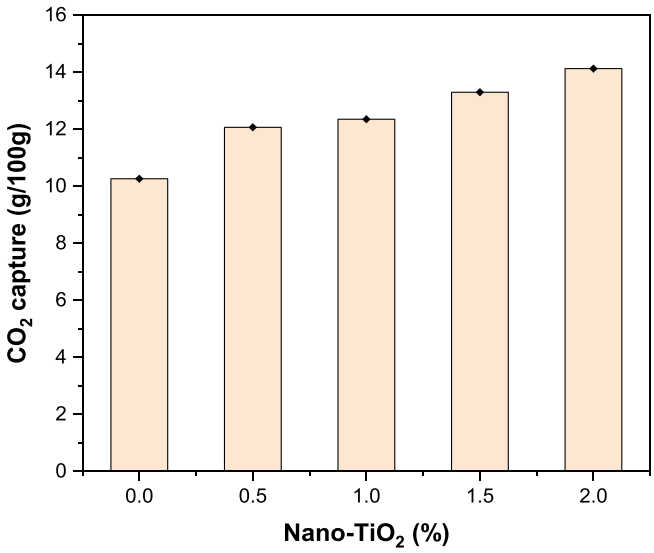

(a) Effect of nano-TiO_2 content

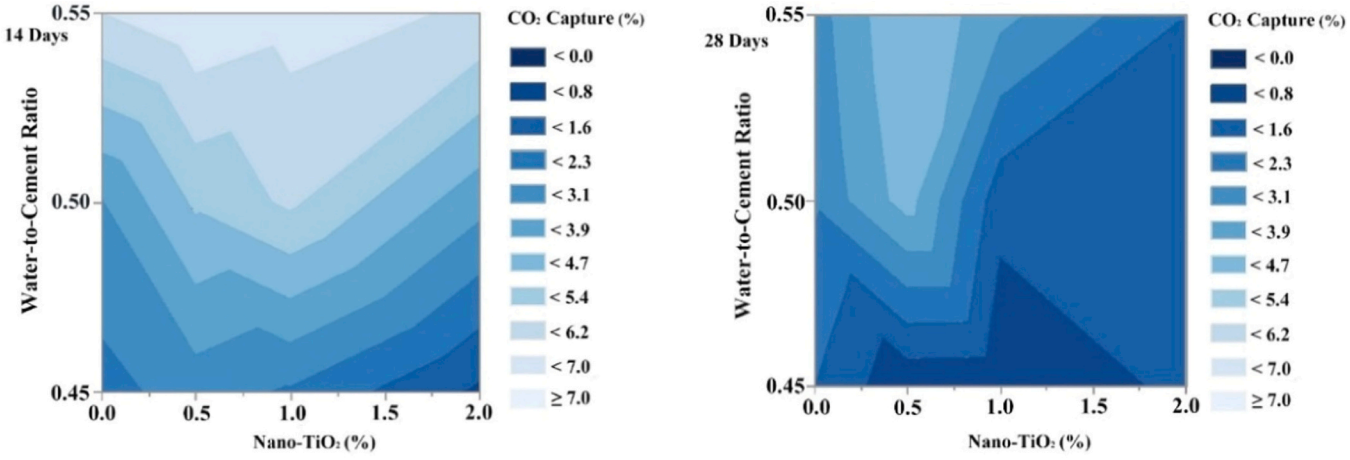

(b) CO_2 uptake (% per cement mass)

Fig. 7. Effect of Nano-TiO_2 content and water-cement ratio of cement paste on carbon capture properties of cement-based materials [86,87].

water-cement ratio, which facilitates the carbon sequestration process by allowing CO_2 to penetrate more easily into the cement stone. However, lower water-cement ratio conditions limit the growth space of the material due to lower porosity, which affects the conversion process of carbonate hydration products to $CaCO_3$.

Xie et al. [88] demonstrated that incorporating TiO_2 nanoparticles into calcium sulphoaluminate cement significantly enhances carbon sequestration (Fig. 8). Carbon sequestration in cement typically occurs via three pathways [89–91]: (i) atmospheric CO_2 diffuses into the material's pore structure; (ii) CO_2 reacts with water in the pores to form carbonic acid; and (iii) the carbonic acid reacts with calcium ions to precipitate $CaCO_3$. This process densifies the cement matrix, enhancing both carbon capture and mechanical properties. In the case of TiO_2 nanoparticle-enhanced cement, the material's carbon sequestration capacity was further improved. The addition of 1 wt% TiO_2 nanoparticles boosted CO_2 capture by 34.8 %, compared to a control sample, by promoting densification of the pore structure and improving CO_2 adsorption. TiO_2 nanoparticles create pore diameters of 6–25 nm, fostering more efficient CO_2 diffusion and reaction. However, when the TiO_2 content exceeds 1 wt%, the reduced porosity negatively impacts the material's sequestration efficiency, contrasting with the positive effects seen at lower concentrations. This showcases how TiO_2 alters the traditional carbonation mechanisms by enhancing pore structure uniformity, but only within optimal limits.

Lopez-Arias et al. [92] investigated the CO_2 sequestration capacity of cement paste containing Nano-TiO_2 using two methods, as shown in Fig. 9: CO_2 detection and the gravimetric method. The CO_2 detection results indicated that higher CO_2 concentrations significantly increased the uptake rate. However, the formation of $CaCO_3$ during carbonation gradually clogged the pores, slowing further CO_2 penetration. The addition of Nano-TiO_2 enhanced CO_2 absorption, increasing uptake by 36.99 % at 25 % CO_2 concentration, 36.31 % at 50 %, and 1.16 % at 100 % CO_2, compared to the control. The gravimetric method also showed a substantial uptake increase (26.80 % at 25 % CO_2, 105.60 % at 50 %, and 137.17 % at 100 %). However, due to water vapor loss during measurement, the gravimetric method tended to underestimate CO_2 uptake, making CO_2 detection the more reliable approach for higher absorption levels.

The carbon fixation effect of TiO_2 nanoparticles in cementitious composites is influenced by several variables, including the incorporation of TiO_2 nanoparticles, the water-cement ratio, and the CO_2 concentration. These variables play a crucial role in determining the

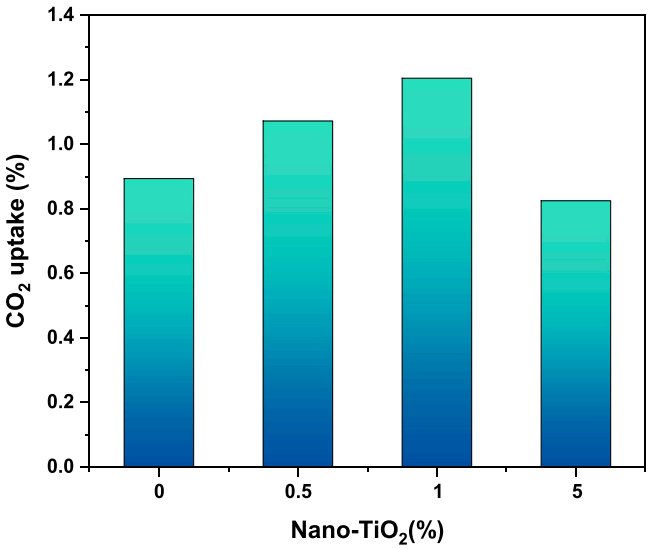

Fig. 8. Effect of Nano-TiO_2 content on carbon capture properties of calcium sulphoaluminate cement [88].

effectiveness of TiO_2 nanoparticles in carbon fixation. The incorporation of nano-TiO_2 significantly enhances the CO_2 uptake capacity of cement-based materials. The optimal CO_2 capture efficiency is demonstrated at a cut-off of 1 wt% incorporation. This effect is attributed to the improvement of the material's microstructure by TiO_2 nanoparticles, which promotes the homogenization and densification of the pores, thus enhancing the CO_2 adsorption capacity. The water-cement ratio is a crucial proportioning parameter of the cement paste that significantly affects the performance of the nano-TiO_2-modified cementitious system. Higher porosity facilitates CO_2 penetration and further carbonation, promoting the process of carbon sequestration. On the other hand, a lower water-cement ratio impedes this process. The concentration of CO_2 has a significant impact on the CO_2 capture capacity of the nano-TiO_2-cementitious system. It is worth noting that the results may vary depending on the method used to assess carbon sequestration capacity, with the CO_2 monitoring method being the most reliable for higher CO_2 uptake levels. To summarize, precise control of the key factors mentioned above effectively enhances the performance of CO_2 fixation in TiO_2-modified cement-based materials. This contributes to the reduction of carbon emissions and enhances the environmental friendliness of the materials.

TiO_2 nanoparticles have proven to significantly improve the CO_2 sequestration of cement-based materials, but their high cost limits their widespread practical application, which has become a major challenge. Currently, the production process for TiO_2 nanoparticles is complex, typically requiring high-temperature calcination (exceeding 1000°C), strict purity control, and high energy consumption (usually requiring multiple refining steps to remove impurities, which increases energy usage and adds to the complexity of the process). As a result, the price of TiO_2 nanoparticles is much higher than that of traditional building materials [93,94]. However, with advancements in technology and production processes, the cost of TiO_2 nanoparticle production has been significantly reduced. Many studies focus on scalable and green synthesis methods, such as flame spray pyrolysis [95] and biologically mediated processes using plant extracts or bacteria [96]. These methods increase production speed and reduce costs through economies of scale. Although the initial cost of TiO_2 nanoparticles is high, their long-term benefits in building materials have been extensively studied. Numerous studies [97–99] support the claim that adding TiO_2 to concrete can reduce maintenance costs and improve environmental outcomes. For instance, TiO_2-modified concrete, with its self-cleaning properties and resistance to degradation, can reduce maintenance expenses by up to 20 % over its lifecycle [100,101].

3.3. Effect of nano-TiO_2 on mechanical properties of cement-based materials

In recent years, researchers have explored the effects of various additives on cement properties to enhance their mechanical properties. Nanoparticles are a cement modifier that can significantly affect the mechanical properties of cement-based materials due to their huge surface area and activity. Their potential in the field of cement research has gained much attention [102]. The physicochemical properties of nano-TiO_2 make it a significant potential for improving cement-based materials. Its effect on the cement matrix, early strength of cement, and promotion of the hydration process of cement have been extensively studied [103–107]. In recent years, studies have shown that nano-TiO_2 has a significant impact on the compressive strength of cement-based materials, as demonstrated in Table 2.

Meng et al. [108] found that nano-TiO_2 significantly improved the early strength of cement mortar, but had little effect on late strength, suggesting its impact is primarily in the initial stages. Yeon Lee et al. [109] further explained this by highlighting that TiO_2 nanoparticles accelerate early hydration and increase the degree of hydration, with the particle size and dispersion being critical factors. Smaller and well-dispersed nanoparticles provide more nucleation sites, which enhances hydration efficiency. Building on this, Wang et al. [110] demonstrated that a 2 wt% nano-TiO_2 content optimizes compressive strength, as higher levels lead to agglomeration, creating weaker clusters that disrupt the microstructure. This was corroborated by Kadhim et al. [111], who noted that exceeding 2 wt% hampers strength development due to these agglomeration effects. Liu et al. [112] also supported these findings by showing that nano-TiO_2 boosts early hydration through nucleation effects, but excessive amounts accelerate hydration too rapidly, resulting in lower overall hydration and reduced strength. Thus, the optimal balance of nano-TiO_2 content is crucial for maximizing early strength without compromising long-term performance.

In the field of concrete, Pathak et al. [113] found that adding 4 wt% nano-TiO_2 improved the mechanical properties of concrete by 3.82 %, largely due to the densification of the microstructure through the nanoparticles' filling effect. However, Selvasofiad et al. [114] identified 2 wt% nano-TiO_2 as the optimal content for achieving the highest compressive strength, suggesting that beyond this level, the benefits diminish. Ren et al. [115] confirmed that 3 wt% nano-TiO_2 significantly enhanced compressive strength by 9 % after 28 days of curing, but higher concentrations, such as 5 wt%, led to reduced strength. This decrease was attributed to the formation of calcium titanate and nanoparticle agglomeration, which can weaken the concrete's microstructure. Melo et al. [116] examined the influence of different TiO_2 types on concrete strength and found that anatase II at 6 wt% content provided the best early strength gains, with a 16 % increase in performance. In contrast, anatase I had a negative impact on strength development due to poor dispersion, and rutile also showed less favorable results compared to anatase II. These findings highlight the critical role of both the type and dosage of nano-TiO_2, where excessive amounts or the use of less effective forms, such as anatase I, can impair the overall strength of the concrete. Optimal use of anatase II, however, can significantly enhance early and long-term strength.

Also, adding an appropriate amount of nano-TiO_2 can significantly improve the workability of concrete, including its flowability, shrinkage, and durability. Rawat et al. [118] found that the optimal dosage is typically 1.5–2 wt% of cement, enhancing mechanical strength and durability. This content also improves concrete's density and crack resistance by reducing air content. However, when the content exceeds 2 wt%, workability decreases, with slump loss reaching 54 % at 3 wt%. Further studies [119] indicate that nano-TiO_2 can suppress belite reactions and slightly reduce calcium silicate precipitation, lowering early shrinkage of cement metrix. Nano-TiO_2 also promotes the formation of

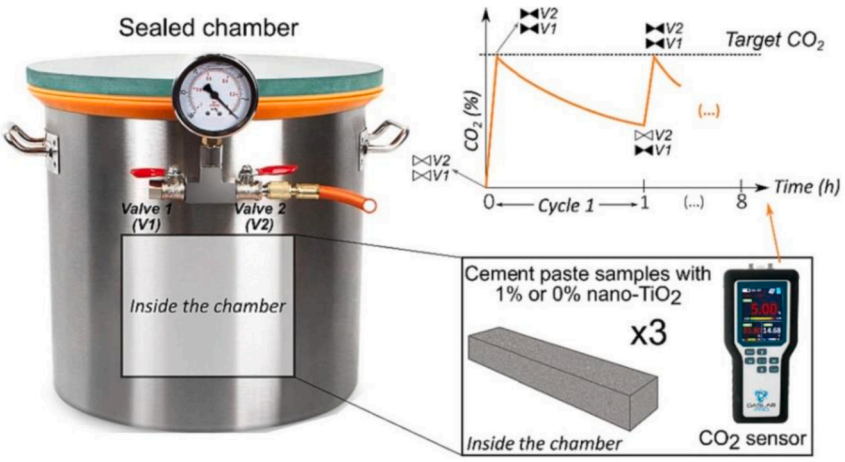

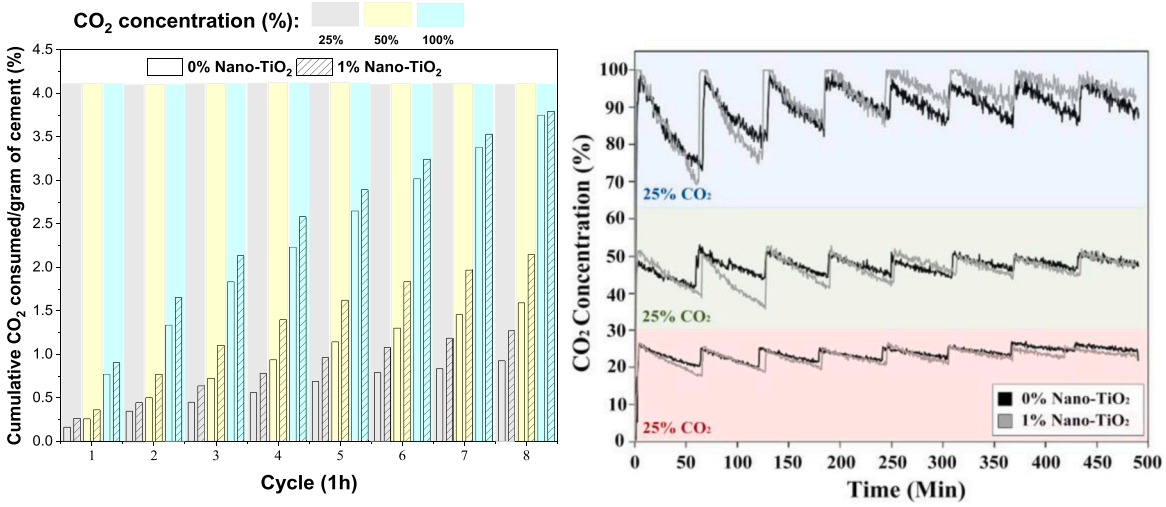

(a) CO_2 monitoring method

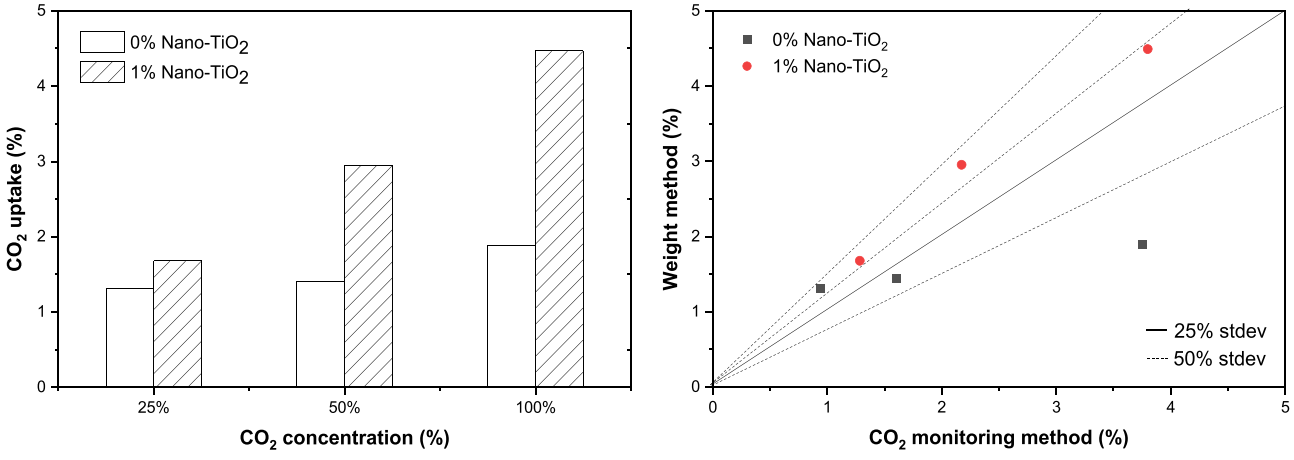

(b) Gravimetric method and comparison of results

Fig. 9. Results of CO_2 exposure of cement pastes containing 0 wt% and 1 wt% nano TiO_2 at three different initial concentrations and data measured using gravimetric methods [92].

Table 2
Effect of Nano-TiO_2 on compressive strength of cement-based materials.

Refs.	Source materials	Sample types	Curing regime (°C)	28 days compressive strength (MPa)
[108]	Nano-TiO_2 (5–10 wt % of cement) + SP	Mortar	Ambient (20)	45–57
[109]	Nano-TiO_2 (5–15 wt % of cement)	Pastes	Ambient (23±2)	40–100
[110]	Nano-TiO_2 (0–5 wt % of cement)	Mortar	Temperature (0−20)	24–67
[111]	Nano-TiO_2 (0–3 wt % of cement)	Mortar	In water	34–36
[112]	Nano-TiO_2 (0–3 wt % of cement)	Pastes	Ambient	60–67
[113]	Nano-TiO_2 (0–5 wt % of cement) + Fly ash (20 wt% of cement)	Concrete	Ambient	38–42
[114]	Nano-TiO_2 (0–4 wt % of cement)	Concrete	In water	60–78
[115]	Nano-TiO_2 (0–5 wt % of cement)	Concrete	Ambient (20 ± 2)	45–50
[116]	Nano-TiO_2 (0–10 wt % of cement	Concrete	humid chamber	Anatase I: 39–42 Anatase II: 43–47 Rutile: 43–45
[117]	Nano-TiO_2 (0–4 wt % of cement)	Concrete	In water	26–30

ettringite, increasing the density and crack resistance of hardened concrete [120,121]. However, when the dosage exceeds 5 wt% of cement, workability and mechanical properties may decline, with reduced flowability, longer setting times, and decreased early strength [122]. Thus, 1.5–2 wt% of cement is considered the optimal range, enhancing performance without negatively affecting early and long-term durability.

In summary. nano-TiO_2 has been shown to improve the early strength of cement as it accelerates the hydration process, particularly when its particle size and dispersion are optimized. An optimal content of 1.5–2 wt% of nano-TiO_2 provides the best balance, enhancing compressive strength and workability without negative side effects like agglomeration, which can weaken the microstructure of concrete. However, higher concentrations (e.g., above 5 wt%) reduce performance due to decreased flowability.

4. GO as a sustainable material for carbon sequestration

4.1. Structure and carbon sequestration mechanism of GO

Graphene is a flat monolayer material with a two-dimensional honeycomb lattice structure. The carbon atoms are connected to three other carbon atoms through sp^2 hybridization orbitals, forming covalent bonds in the plane [123,124]. This results in a regular hexagonal ring structure, which in turn forms an expansive lamellar structure (see Fig. 10) [125,126]. Graphene is a multidimensional carbon material with unique physical and chemical properties that make it a hotspot for emerging nanomaterials research. Its remarkable features include high electrical and thermal conductivity, mechanical strength, and toughness, making it highly suitable for applications in materials science, nanotechnology, and energy storage and conversion [127–129]. In 1860, Brodie, an English chemist, improved upon the method described by previous scholars and determined the molecular weight of graphite by applying strong acids (such as sulphuric and nitric) and oxidizing agents [130]. The method's implementation resulted in an intercalation reaction between the graphite layers and a chemical oxidation of the graphite surface. This ultimately produced GO [131,130,132]. GO has an abundance of oxygen-containing functional groups on its surface, such as hydroxyl (-OH), epoxy (-O-), and carboxyl groups (-COOH). These groups enhance GO's affinity for water and allow it to strongly adsorb various pollutants. This property makes GO an effective material for pollution treatment [133,134].

GO differs significantly from graphene in terms of both structure and properties. It is an oxidized form of graphene, with surfaces and edges enriched with oxide functional groups [135]. These oxygen-containing groups give GO excellent hydrophilicity and binding ability to a wide range of pollutants, enabling it to exhibit high efficiency in removing pollutants from water. In contrast, Graphene is a two-dimensional material made up of a single layer of carbon atoms. It possesses exceptional electrical and thermal conductivity, as well as mechanical strength. However, its hydrophilicity is poor, and its ability to remove pollutants may not be as effective as GO when used directly in water treatment [136,137]. From a physical and chemical property perspective, GO's oxygen-containing groups can be improved through chemical modification to increase hydrophilicity and reactivity. Meanwhile, graphene's high conductivity and strength make it ideal for electrochemical applications and composites. Overall, GO is more effective in water treatment and pollutant removal, while graphene has greater potential in

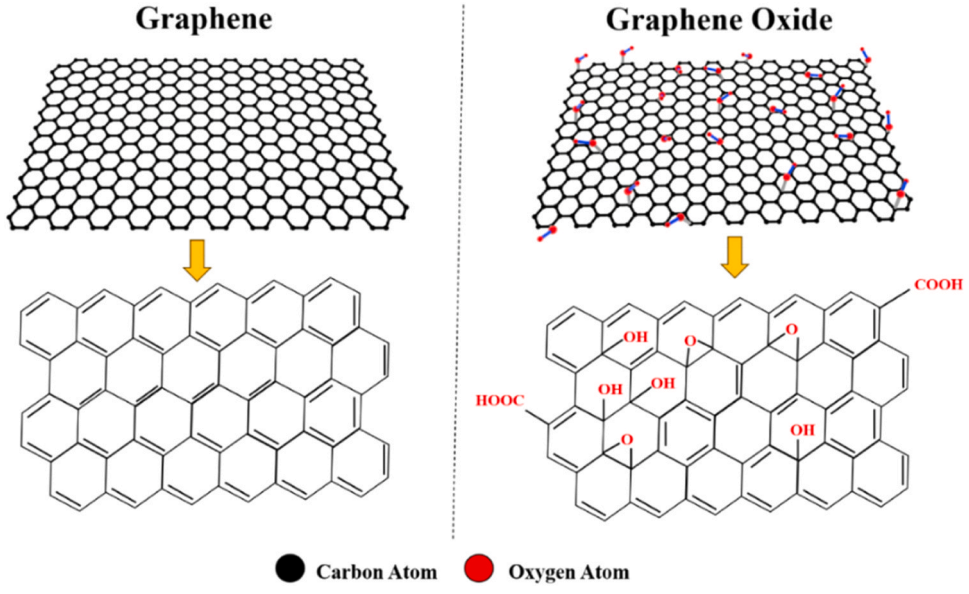

Fig. 10. Molecular structure of graphene and GO.

electronics, energy storage, and reinforced composites.

The principle of carbon sequestration in GO offers an effective method for capturing and storing carbon due to its distinctive chemical structure and high specific surface area. GO surfaces and edges are enriched with oxide functional groups, such as -OH, -O-, and -COOH, which can react with atmospheric CO_2 molecules to form stable chemical bonds, as illustrated in Fig. 11. This process entails the chemisorption of CO_2. CO_2 molecules react with oxygen-containing groups on the surface of GO to form stable carbonates or other compounds, resulting in efficient CO_2 capture and sequestration. Hoyos et al. [138] recently conducted a study on the binding sites of CO_2 molecules with oxide functional groups in GO. The study found that the first position is located between the -OH bottoms, the second position is located at the top of the -OH structure, and the last position is near the right side of the single -OH structure, as shown in Fig. 11 (a) to (c). Research has demonstrated [139,140] that the interlayer spacing of GO increases, providing more sites for trapping CO_2. Furthermore, the physical adsorption process is significantly enhanced by GO's high specific surface area and porous structure, making it highly effective in capturing CO_2. According to Meng et al. [141], pore size is a crucial parameter in the development of efficient carbon-based adsorbent materials for CO_2 capture applications. Eq. (14) shows the mechanism of solid physical adsorbent materials used in the process of capturing CO_2 from combustion.

$$CO_2 + \text{Surface} \leftrightarrow (CO_2) \bullet (\text{Surface}) \tag{14}$$

where the CO_2 adsorption process is mainly driven by van der Waals forces between CO_2 molecules and the adsorbent surface, as well as polar-ionic and polar-polar interactions between them and the adsorbent surface sites [142,143]. Thus, through both chemical and physical mechanisms, GO offers a potentially efficient material solution for CO_2 abatement and sequestration.

4.2. GO's carbon capture efficiency in cement-based systems

In recent years, researchers have explored the use of GO to improve the performance of cement-based materials, particularly its potential for carbon sequestration [144,145]. The aim of this section is to analyze the interaction between GO and cement-based materials. The potential benefits of this innovative material in revolutionizing the construction industry and combating the challenges of global climate change will be explored. Mishra et al. [144] conducted a pilot study that comprehensively assessed the potential application of GO for CO_2 sequestration in cement-based materials. The analysis employed a comparable method to that previously used for nano-TiO_2, which samples were evaluated by TGA. Fig. 12 illustrates the carbon sequestration potential of GO in cement pastes. The experimental results indicate that cement paste samples subjected to the carbonation process for 7 days exhibited 10.4 % CO_2 uptake. However, the introduction of graphene oxide increased the CO_2 uptake rate to 13.4 %, which is approximately 30 % higher than the conventional cement's CO_2 sequestration rate. The researchers observed that when CO_2 diffuses through the cement matrix containing GO, it reacts with calcium ions to produce carbonate ions. The growth of GO lamellae may result in an increase in positive charge, which attracts negatively charged carbonate ions, leading to more precipitation of $CaCO_3$. As precipitation occurs successively, the cement matrix becomes denser. However, the CO_2 uptake decreases when the GO content is increased to a certain level. Therefore, it is recommended that GO be mixed at no more than 0.1 wt% to avoid reducing the carbon sequestration capacity of the cement samples due to excessive precipitates.

Mohammed et al. [146] investigated the long-term anti-carbonation performance of cementitious composites containing GO, as shown in Fig. 13. By measuring carbonation depth, they found that adding GO

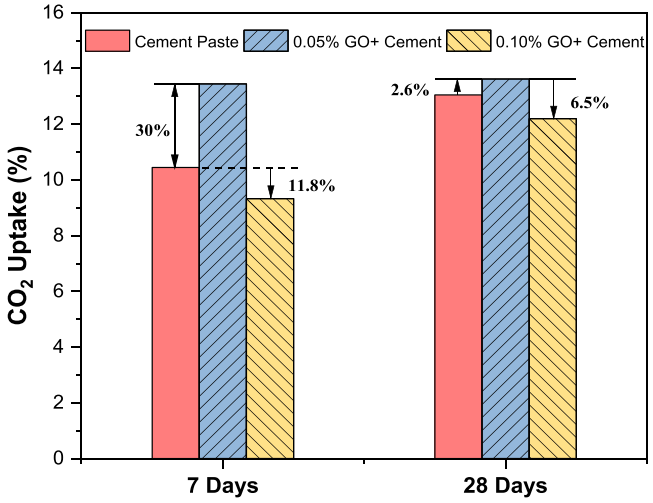

Fig. 12. Carbon sequestration capacity of cement paste samples containing GO [144].

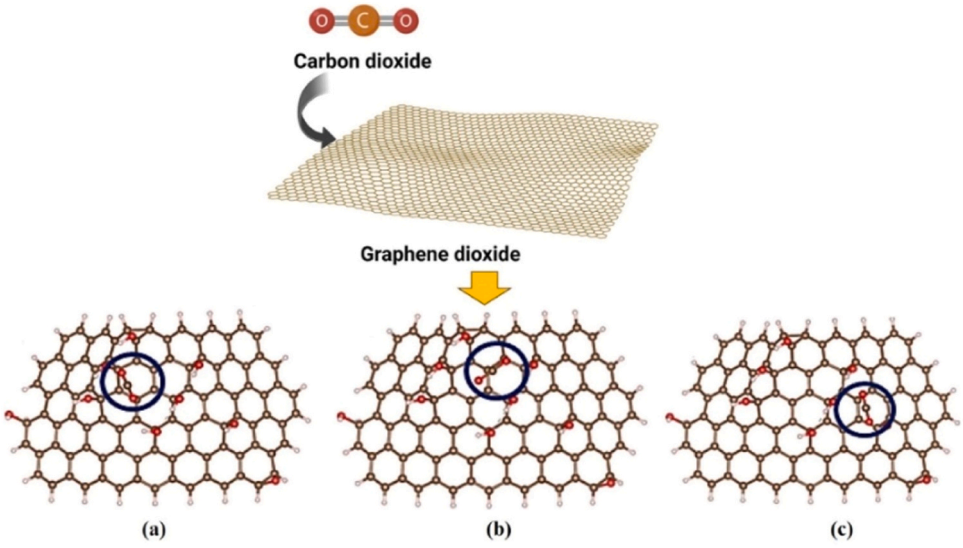

Fig. 11. Graphene oxide carbon sequestration mechanism [138].

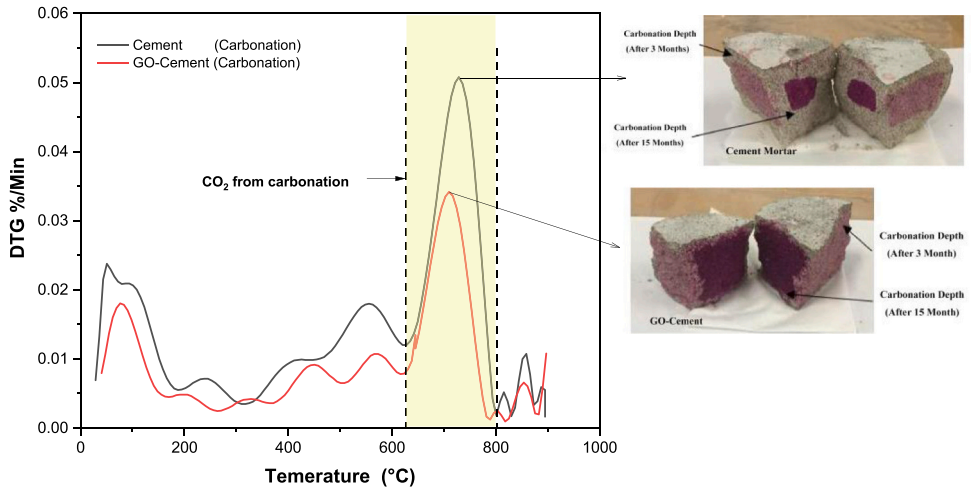

Fig. 13. Characterization of the carbonation resistance of the cement matrix containing GO [146].

significantly enhanced the material's resistance to carbonation. After 15 months, the OPC control group exhibited a carbonation depth of 70 %, while the GO-containing composite showed minimal carbonation progress. TGA further demonstrated that the GO samples produced fewer carbonation products, indicating reduced CO_2 penetration. GO prevents carbonation by its "interlock effect" with calcium and carbonate ions, hindering the reaction and slowing CO_2 diffusion, thus improving the material's carbon sequestration potential.

In summary, GO shows great potential for enhancing carbon sequestration in cementitious materials, as it significantly boosts CO_2 capture and reduces carbonation. Compared to OPC, the addition of GO can increase CO_2 absorption by approximately 30 %. This is due to GO's interaction with calcium ions, which promotes the formation of $CaCO_3$, densifying the cement matrix. This reaction mechanism effectively slows the diffusion of CO_2, improving the material's ability to trap carbon. Although these findings are promising, research in this field remains quite limited. There is a clear need for further investigation to fully understand the mechanisms, optimize the use of GO, and explore its broader applications in carbon reduction strategies for construction materials.

Although GO has demonstrated significant potential in enhancing CO_2 capture in cementitious materials, its high production costs limit widespread application. To address this, researchers have explored the use of renewable resources to produce reduced GO, such as using chestnut-derived bio-waste, which reduces costs and meets environmental goals [147]. Additionally, the pretreatment of graphite with piranha solution reduces oxidation temperature and time, saving energy [148]. Abalonyx has developed a more cost-effective method, potentially reducing the price to €20/kg [149]. Combining GO with lower-cost materials such as fly ash or nano-silica further optimizes costs while maintaining performance [150,151]. In high-performance or environmentally demanding construction materials, such as self-compacting and high-performance concrete, the initial cost increase due to GO can yield higher long-term economic and environmental benefits by improving durability and CO_2 capture.

4.3. Effect of graphene oxide on mechanical properties of cement-based materials

GO, an emerging nanomaterial, is believed to be an ideal candidate for this purpose due to its unique physicochemical properties, including high specific surface area, excellent mechanical strength, and good chemical stability [152–155]. Recent studies have confirmed that the addition of GO to cement-based materials can significantly improve their mechanical properties, particularly their compressive strength.

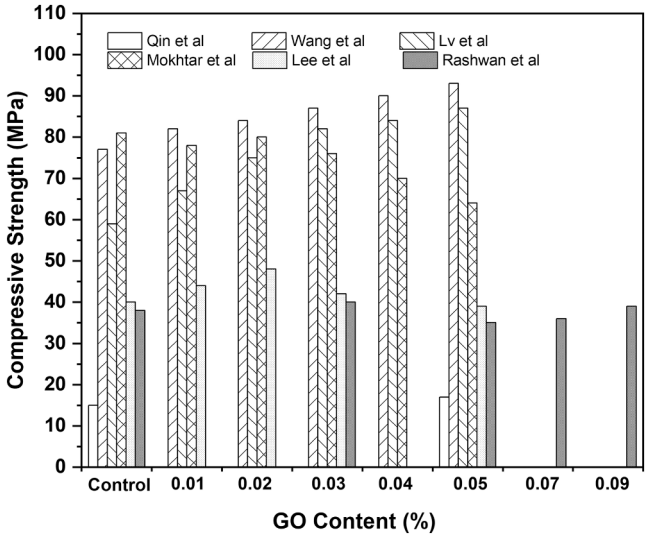

Fig. 14. Effect of GO addition on compressive strength properties of cement pastes (28 days) Qin et al. [156], Wang et al. [157], Lv et al. [158], Mokhtar et al. [159], Lee et al. [160], Reshwan et al. [161].

Fig. 14 illustrates the relationship between GO dosage and the 28-day compressive strength of cement-hardened bodies.

Qin et al. [156] demonstrated that the addition of GO significantly enhances the compressive strength of cement even without any curing process. When 0.5 wt% GO was added, the compressive strength increased by 35.7 % after 28 days, reaching 19.4 MPa. The primary mechanism behind this improvement is that GO acts as a template for hydration products and accelerates the hydration process by providing additional nucleation sites. Wang et al. [157] found that with a GO content of 0.05 wt%, the compressive strength increased by 40.4 %, while the heat of hydration was reduced by 54 %. Similarly, Lv et al. [158] observed a 47.9 % increase in compressive strength at the same dosage, attributing this to the abundant functional groups on the GO surface interacting with cement components, forming nucleation sites that promote the growth of hydration products (Fig. 15). However, when the GO content exceeds 0.05 wt%, the overcrowded nucleation sites lead to less dense local structures, which ultimately reduce the overall strength of the material. Mokhtar et al. [159] further confirmed that 0.02 wt% GO nanoplatelets can increase compressive strength by approximately 13 %. However, exceeding this optimal dosage results in a decrease in strength, as too many nucleation sites can hinder the

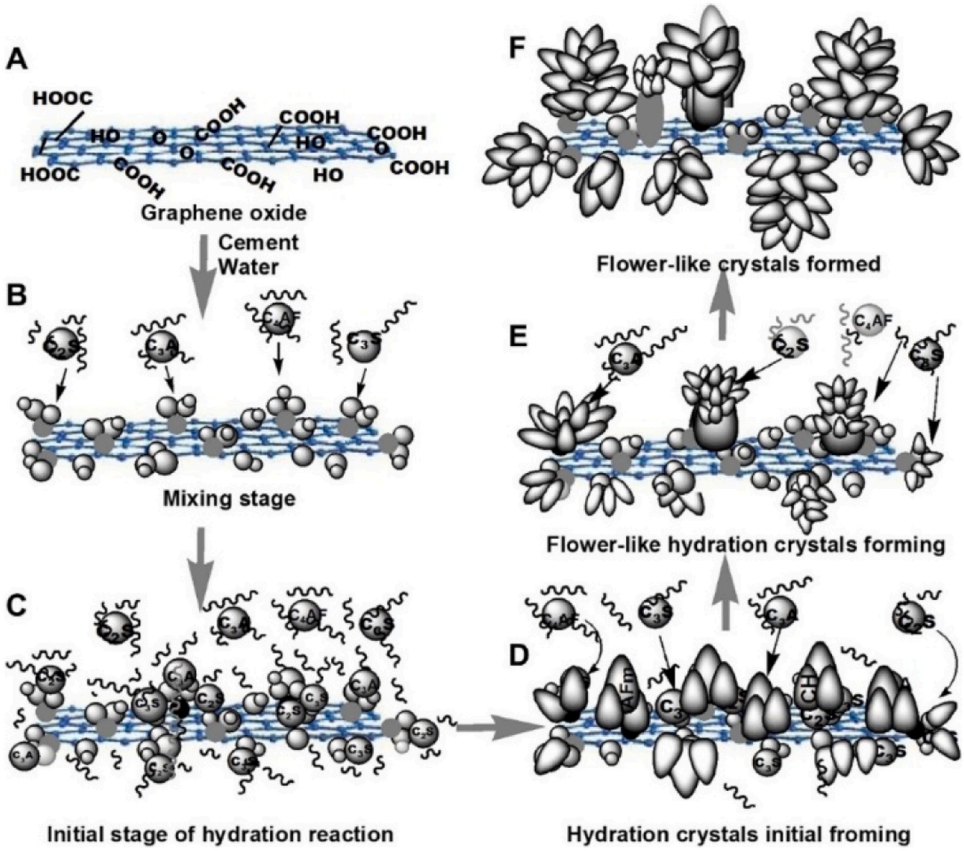

Fig. 15. Sketch of GO-enhanced hydration processes in the cement matrix [158].

formation of a dense structure. Lee and Rashwan et al. [160,161] reached similar conclusions, noting that when the GO content exceeds 0.03 wt%, agglomeration intensifies, leading to increased pore space and weaker mechanical properties.

Table 3 demonstrates the effect of GO admixture on the compressive strength of conventional concrete as well as special categories of concrete in recent years. Reddy et al. [162] demonstrated that the addition of GO can significantly improve the compressive strength of concrete. When the GO dosage ranged between 0.025 and 0.1 wt%, the compressive strength increased by 47 % at 7 days and by 38 % at 28 days. Devi et al. [163] further observed that GO concentrations between 0.02 wt% and 0.08 wt% led to a noticeable improvement in compressive strength, with a 24 % increase observed after 28 days in a mixture containing 0.08 wt% GO. Du et al. [164] confirmed this trend, showing that GO additions in the range of 0.01–0.1 wt% improved compressive strength by 6.8–55.8 %. Although concrete has a wider internal spatial structure compared to cement paste, in fact, some studies have shown [165,166] that GO should not be added at too high a level: around 0.05 wt% is the optimal dosage, while more than 0.1 wt% can adversely affect the mechanical properties. Devi et al. [163] revealed that GO enhances the structure of the interfacial transition zone (ITZ) by promoting the formation of dense hydration products, especially when the GO content reaches 0.06 wt%. However, when the GO content exceeds 0.08 %, the microstructure begins to degrade, hindering further improvements in mechanical strength.

Table 3
Compressive strengths of concrete with different GO content.

Refs.	GO Content (replacement of cement%)	Types	Curing conditions	Compressive Strength (MPa)	
				7 Days	28 Days
[162]	0–0.1 wt%	GO-cement concrete	In water	19–27	26–36
[163]	0.02–0.08 wt %	GO-cement concrete	In water	24–30	33–38
[167]	0–0.2 wt%	GO-cement concrete	—	15–17	24–26
[164]	0–0.1 wt%	GO-cement concrete	In a curing room (temperature: 22 ± 2 °C, relative humidity: 98 %)		54–84
[168]	0–0.075 wt%	GO-UHPC	In a curing room (temperature:20 ± 1°C, relative humidity: >95 %)	—	156–182
[169]	0–0.03 wt%	GO-UHPC	In a curing room (temperature:20 ± 2 °C, relative humidity: >95 %)	90–94	117–122
[170]	0–0.06 wt%	GO-UHPC	—	85–94	123–143

For Ultra High-Performance Concrete (UHPC), Chu et al. [168] found that GO helps improve the pore structure, but the compressive strength does not increase linearly with increasing GO concentration. The optimal GO dosage for UHPC was identified as 0.05 wt%. Yeke et al. [170] also confirmed that adding 0.04 wt% GO increased the compressive strength of UHPC by 15.8 % at 28 days and 14.5 % at 90 days. Yu et al. [171] further elucidated the mechanisms by which GO enhances the mechanical properties of UHPC: 1) The nucleation effect of GO promotes cement hydration and improves the microstructure; 2) GO reduces porosity during crack formation; and 3) The chemical bonding at the GO-matrix interface strengthens the bonding of gel products with GO, enhancing the ductility and tensile strength of the structure. These

mechanisms collectively enhance the overall performance of UHPC. In addition, GO has a significant but complex impact on the workability and durability of concrete. At low content (approximately 0.02–0.04 wt %), GO can improve the workability of concrete by combining with dispersants such as polycarboxylate ether; however, when the content of GO exceeds 0.06 wt%, its large specific surface area increases water demand, thereby reducing workability [172,173]. Also, GO helps reduce shrinkage, especially within the range of 0.04–0.06 wt%. It achieves this by refining the pore structure and improving the bond between the cement matrix and aggregates, thereby controlling moisture loss and shrinkage-related cracking [174]. In terms of durability, the optimal GO content is 0.03–0.06 wt%, within which GO can significantly enhance the crack resistance and corrosion resistance of concrete by refining the pore structure, enhancing hydration reactions, and bridging cracks, with particularly outstanding effects against chloride and sulfate attack [175].

In summary, GO, as an emerging nanomaterial, significantly enhances the mechanical properties, workability, and durability of cementitious materials due to its unique physicochemical properties, particularly its role in nucleation, template effects, crystal growth, and morphology control of hydration products. In cement-based materials, the optimal GO dosage is 0.02–0.05 wt%, with 0.05 wt% showing the most significant improvement in compressive strength. However, exceeding this dosage can lead to overcrowded nucleation sites, limiting the formation of a dense structure. In concrete, a 0.05 wt% GO dosage can also increase compressive strength by up to 55 %. For UHPC, a GO dosage of 0.04–0.05 wt% is ideal for improving pore structure and durability. Regarding workability, GO at 0.02–0.04 wt% can improve flowability when combined with dispersants, but exceeding 0.06 wt% increases water demand and reduces workability. In terms of durability, GO at 0.03–0.06 wt% effectively enhances crack resistance, corrosion resistance, and reduces shrinkage-related cracking. However, higher GO content may increase water demand, worsen pore structure, and negatively affect both workability and long-term durability. While existing studies have demonstrated GO's significant benefits in enhancing strength and structure, further investigation is needed into its specific effects on the morphology and growth space of cement hydration products. In particular, the growth mechanisms of hydration products and their impact on microstructure remain underexplored in current research.

5. Biochar and cellulose fiber: physically adsorbed carbon capture

5.1. Defining biochar and cellulose fiber as carbon adsorbents

Biochar obtained by pyrolysis (i.e., heating biomass such as wood [176,177], crop residues [178], and food waste [179] under anaerobic conditions, as shown in Fig. 16) exhibits remarkable structural stability and resistance to decomposition, allowing it to persist in a wide range of media. Biochar is an excellent CO_2 adsorbent due to the alkaline functional groups on its surface and its high microporous surface area [180,181]. The carbon sequestration potential of biochar varies significantly depending on factors such as the type of feedstock used, its elemental composition, the pyrolysis method applied, and the carbon emission factor used in calculations. While some estimates suggest biochar can sequester around 589 kg of carbon per ton of CO_2, this value is highly dependent on these variables and can vary across different types of biochar[182]; meanwhile, data suggests that sustainable biochar production contributes to annual emission reductions of around 8 % [183]. This property gives biochar an environmental advantage in the construction industry. Structurally, biochar is a highly porous material with a high specific surface area. The pore structure of the biochar is mainly caused by the pyrolysis process. These pores are mainly formed by the release of volatile organic compounds (VOCs) during the pyrolysis process, and the more VOCs released, the larger pores formed in the biochar. The study has shown [184] that increasing the pyrolysis temperature significantly alters its pore structure, leading to an increase in the number of pores, a denser structure, enhanced integrity and a significant increase in porosity as shown in Fig. 16. The pore structure and morphology of biochar, inherited from the characteristics of its raw materials, are the key factors determining its adsorption capacity. This

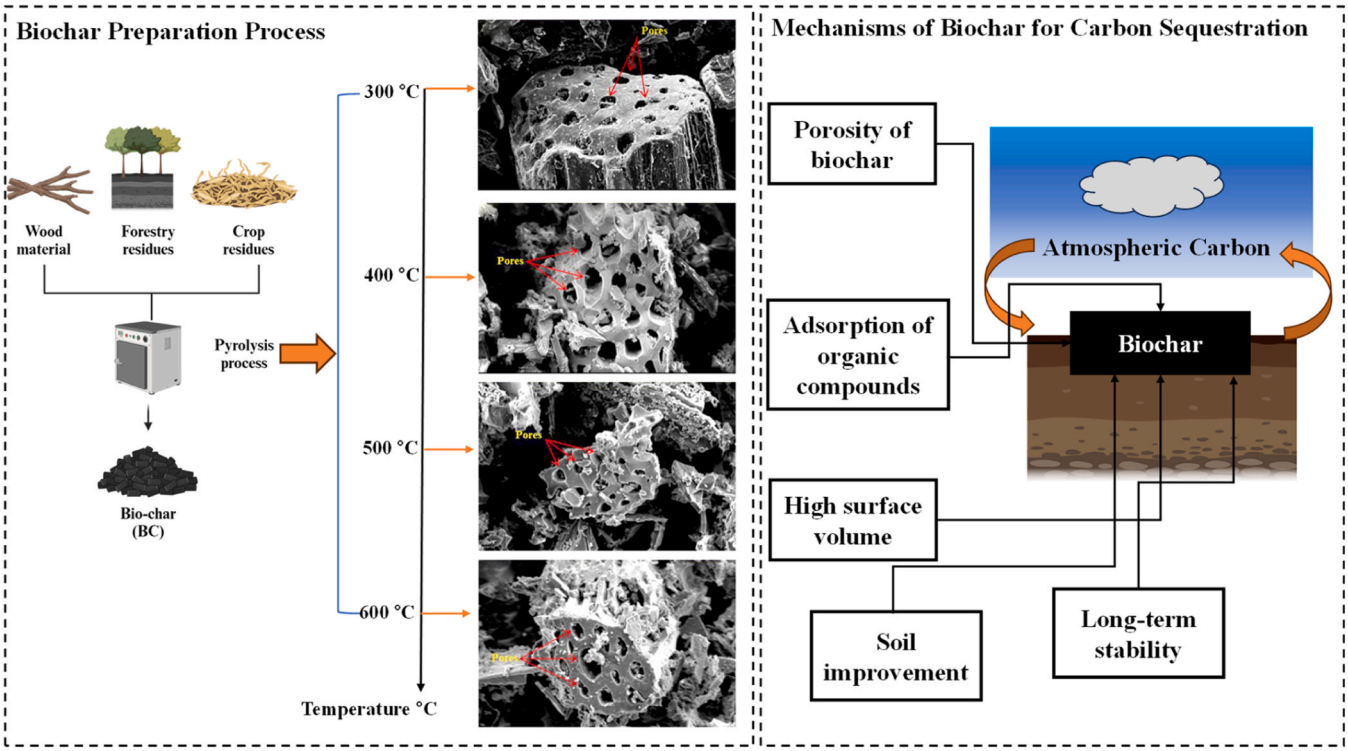

Fig. 16. Biochar preparation process and carbon sequestration mechanism [184,185].

structural characterization provides a basis for a deeper understanding of the role of biochar in carbon capture mechanisms and the exploration of its potential in climate change mitigation.

The mechanism of biochar in carbon sequestration is illustrated in Fig. 16. Firstly, the robust and stable structure of biochar can act as a physical barrier to prevent microbial decomposition of unstable carbon, thus slowing down the process of carbon mineralization. At the same time, its porous nature provides a protective environment for the unstable carbon and effectively maintains its existence in different media for a long period of time. In addition, biochar has a high surface area, which can effectively adsorb unstable carbon molecules and make them adhere to the surface of biochar. Through this adsorption mechanism, the biochar was able to effectively immobilize these carbon molecules in the pores and prevented their rapid decomposition[185,186]. Studies have shown [183] that during the preparation of biochar, about 62–66 % of the CO_2 emission reduction is achieved through sequestration, while the remaining emission reduction is attributed to the adsorption of CO_2 by the microporous structure on the surface of biochar. In summary, biochar contributes to the stable uptake and long-term sequestration of CO_2 in the air through a combination of physical protection, chemical adsorption, and the effects of biological and chemical processes. The combined effect of these mechanisms makes biochar an effective carbon sequestration tool.

Cellulose fiber, as a renewable resource and a sustainable carbon-sequestering material, has significant advantages in terms of large surface area, abundance of storage sites [187]. Fig. 17 illustrates the production process of cellulosic fibers and their carbon sequestration mechanism. The production of cellulosic fibers starts with biomass raw materials such as bark, cotton, bamboo and agricultural by-products, which are first subjected to pre-treatment steps such as acidification, enzyme treatment or microwave heating acidification, and then the production of cellulosic fibers is completed by steps such as alkali treatment and etiolation. The porous structure of cellulose not only provides a large surface area, but also facilitates the adsorption and storage of CO_2. The hydroxyl groups on the cellulose chains act as adsorption sites for CO_2, improving the efficiency of carbon capture [188]. As cellulose is derived from plant biomass, its environmentally friendly nature promotes sustainable development. In addition, cellulose fibers can be synthesized with different types of materials, resulting in porous cellulosic materials with increased surface area and pore structure, further facilitating CO_2 adsorption and storage [189,190].

In summary, both biochar and cellulose fibers are effective materials for implementing 'carbon negative emission' technology for long-term carbon sequestration. However, there are significant differences between the two materials in terms of preparation methods, carbon sequestration mechanisms and sequestration times. Biochar is produced from a variety of biomasses through a pyrolysis process, whereas cellulosic fibers are derived directly from plant biomass. Biochar relies on its physical and chemical stability to sequester carbon, whereas the carbon sequestration mechanism of cellulose fibers is related to the structure of the plant itself. In addition, on the timescale of carbon sequestration, biochar typically has a longer sequestration potential.

5.2. *Carbon sequestration capacity of biochar/cellulose fiber in cement-based materials*

The use of biochar in combination with cement-based materials represents an environmentally friendly waste management and carbon sequestration strategy with positive implications for both environmental protection and industrial development. Although this approach may result in a partial loss of material strength, the benefits of significantly reducing the CO_2 emissions associated with the building and its construction make the addition of biochar an option worth considering[192,193]. The mechanism of carbon fixation in cement-based materials by biochar is mainly based on its porous structure, which provides a large surface area and promotes efficient adsorption of CO_2 in these micropores. In addition, biochar can promote carbonation reactions in the cement matrix. It has been shown that the incorporation of biochar not

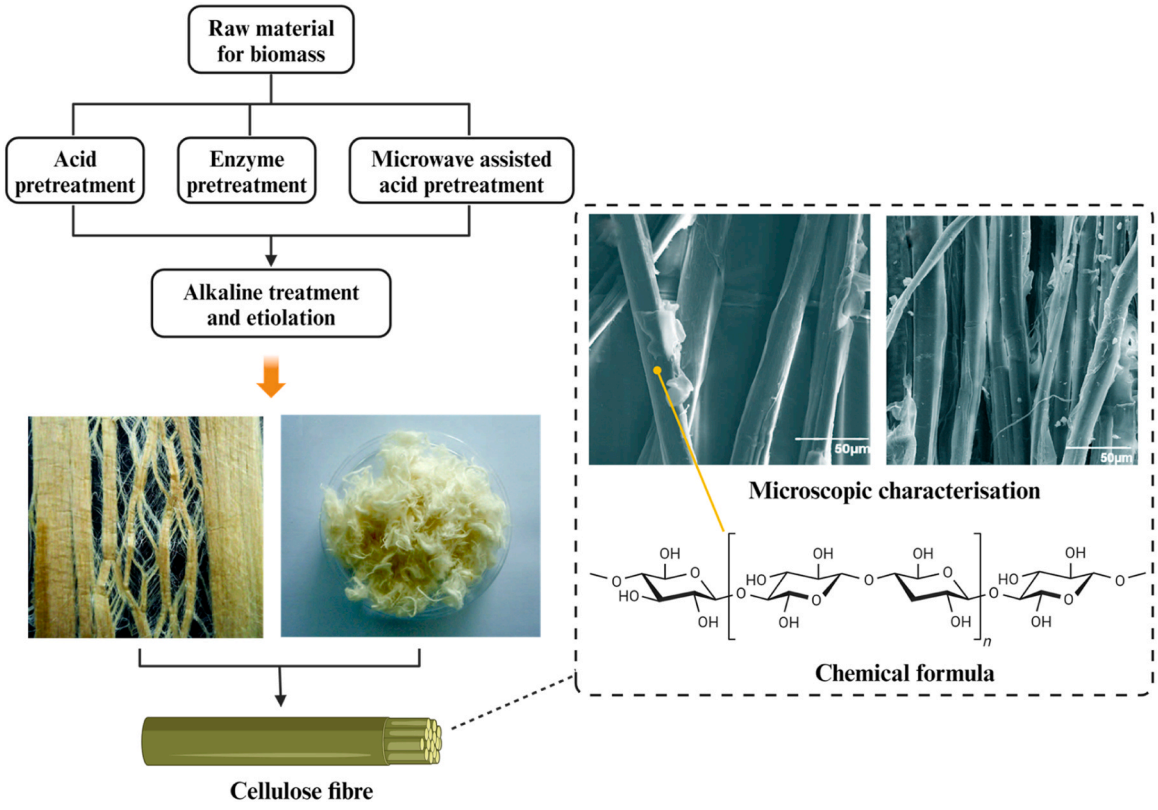

Fig. 17. Cellulose fiber preparation process and carbon sequestration mechanism [191].

only reduces the carbonate mineralization process of C-S-H, but also enhances the mineralization process associated with the carbonation of calcium hydroxide (CH) [194]. This finding indicates that the porous structure and high specific surface area of biochar provide more active sites for the carbonation reaction of CO_2 with CH, thus facilitating more efficient uptake of CO_2 and its conversion to a more stable carbonate form.

The methodology for assessing the carbon sequestration capacity of biochar in cement-based materials is illustrated in Fig. 18. Gupta et al. [195] partially saturated a biochar containing sample by passing pure CO_2 through a sealed glass jar and monitored the CO_2 concentration over a period of three days using two CO_2 sensors. The amount of CO_2 absorbed by the biochar-containing sample was measured using thermal desorption by observing the decrease in CO_2 concentration every two hours and determining the saturation point. This experiment showed that the average adsorption capacity of the sample was 1.67 mmol/g, effectively demonstrating its potential for use in carbon sequestration. Also, in a study by Praneeth et al. [196], they investigated the efficacy of biochar in carbon sequestration by carbonating pre-treated cement paste samples containing biochar in pure CO_2 at a pressure of 1 MPa for 2 h in a controlled environment. The study documented changes in the mass of the samples before and after treatment and found that CO_2 uptake increased significantly with increasing doses of biochar. Particularly in mixtures containing high levels of biochar, the high surface area of biochar provided many adsorption sites for CO_2, significantly increasing its carbon sequestration capacity.

He et al. [197] employed two techniques, the mass gain method and the mass curve method, to assess the carbon sequestration capacity of cellulose fibers in cement-based materials, in Fig. 19 (a). In the mass gain method, CO_2 uptake was quantified by comparing the change in mass of the sample before and after carbonation. However, it is essential to consider the loss of moisture due to the carbonation reaction, as this may affect the accuracy of the results. Furthermore, the CO_2 uptake rate is calculated as the percentage of CO_2 uptake after deducting the pre-carbonation mass and moisture loss from the mass of the sample after carbonation, based on the mass of the dry cement. On the other hand, in the mass profiling method, where the change in mass of the sample is monitored in real time and a gas supply is maintained to stabilize the ambient pressure, an increase in mass indicates that the sample has absorbed CO_2. At the end of the experiment, the gas is released, and the final mass of the system is recorded, which is the sum of the CO_2 absorbed by the sample and the residual gas. To accurately calculate the amount of CO_2 absorbed, the experiment is repeated using a substitute material that does not absorb CO_2 and the mass of residual gas in the container is determined. The carbon sequestration capacity of the sample can be quantified by comparing the difference between the total mass and the residual gas mass. This data is comparable to that obtained by the mass gain method and is independent of the carbon content prior to carbonation. It is worth noting that the authors point out that TGA of the samples for carbonate content was not carried out due to the presence of carbon-rich cellulose fibers. This is since water and CO_2 from cellulose decomposition may be mixed with CO_2 released from carbonate decomposition, making it impossible to accurately differentiate between their sources and thus affecting the accurate determination of carbonate content. The results of the study show that absorption values measured by the mass curve method are usually higher than those measured by the mass gain method, which may be biased lower by vapor loss. The CO_2 uptake of the samples ranged from about 14.3–19.5 % during the 2-hour carbonation period and up to 24.4 % during the 8-hour carbonation period. Micrographs showed the growth of large, dense carbonate crystals with a particle size of 5 μm on the fiber surface, while the cement slurry penetrated the fiber cell walls and voids, with carbonate crystals protruding from the thin cement layer. Different combinations of drying and carbonation were also investigated, such as 150 min oven drying followed by 8 h carbonation and 18 h fan drying followed by 0.5 h carbonation, the latter with CO_2 uptake efficiencies of up to 20 %, demonstrating the potential of cellulose fibers for carbon sequestration in cement-based materials. Also, in a study by Wu et al. [198], natural fibers and activated magnesium cement were used to prepare green building materials for the purpose of CO_2 sequestration in

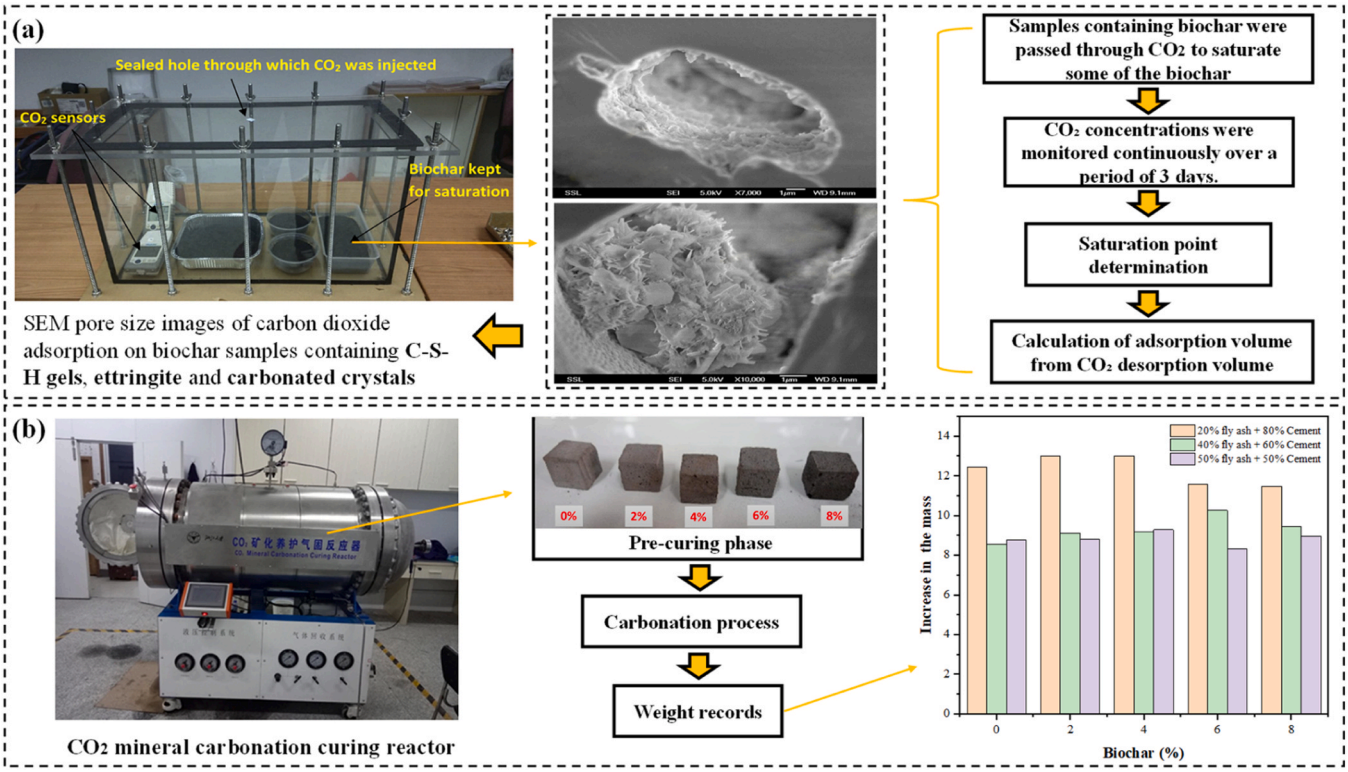

Fig. 18. Methods for characterizing the carbon sequestration capacity of biochar in cement-based materials: (a) by Gupta et al [195];(b) by Praneeth et al [196].

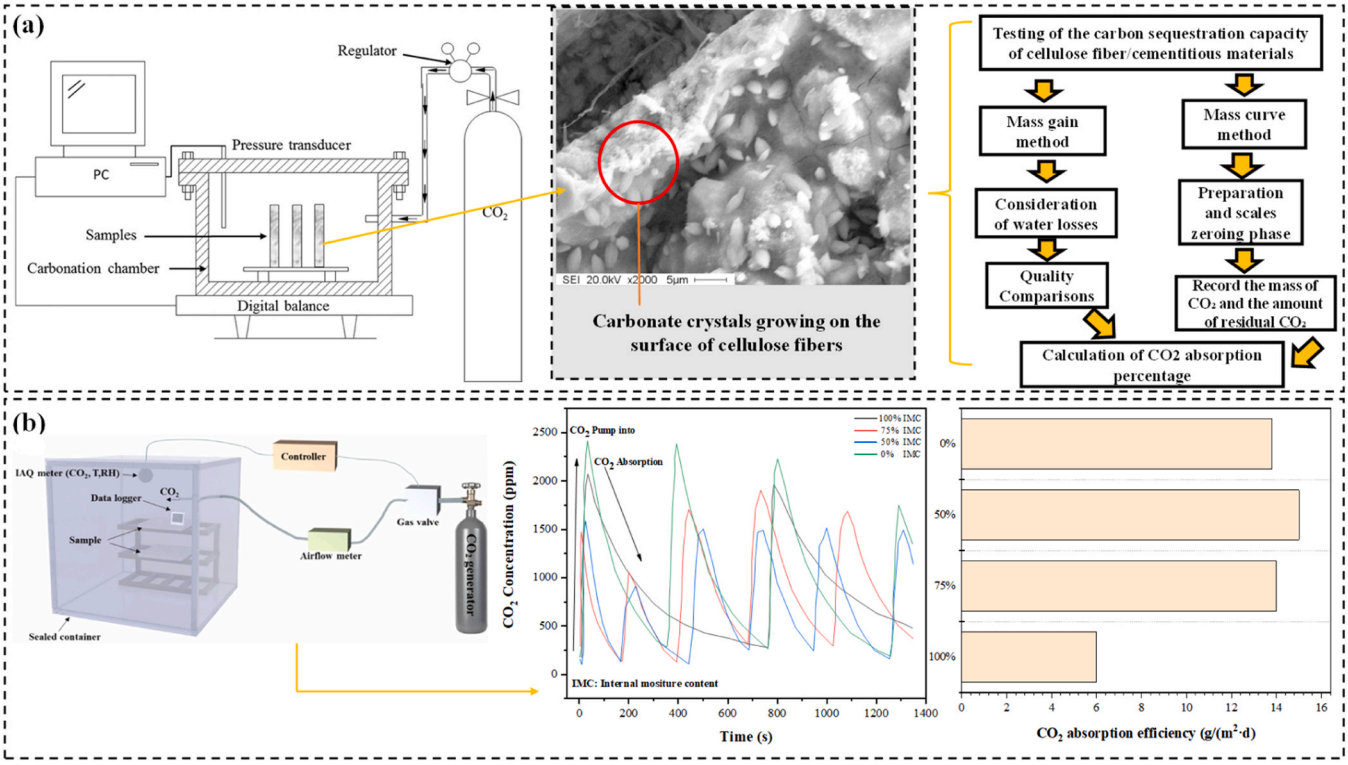

Fig. 19. Methods for characterizing the carbon sequestration capacity of cellulose fiber in cement-based materials: (a) He et al [197]; (b) Wu et al [198].

the air environment. The sequestration capacity of the prepared mortar specimens is illustrated in Fig. 19 (b). During this study, the specimens were placed in closed containers with real-time CO_2 concentration monitoring. This enabled the CO_2 concentration to be maintained at an atmospheric level throughout the experiment, thus allowing the measured data to be used to simulate the CO_2 sequestration effect of the specimens in an indoor environment. The results demonstrate that samples containing natural fibers exhibit an excellent CO_2 sequestration capacity. Furthermore, it was observed that the humidity within the samples exerts a significant influence on the CO_2 sequestration capacity, with higher humidity levels being detrimental to CO_2 sequestration.

Both biochar and cellulose fibers demonstrated considerable carbon sequestration potential in cement-based materials. The CO_2 adsorption capacity of biochar was validated by pyrolysis adsorption, with an average adsorption capacity of 1.67 mmol/g. Cellulosic fibers, in contrast, exhibited good CO_2 uptake as evidenced by the mass gain method and mass curve method for carbon sequestration. Nevertheless, the assessment of the carbon sequestration capacity of cellulose fibers using TGA is challenging due to the potential for inaccurate analysis of carbonate content resulting from their richness in carbon. Biochar exhibits an advantage in terms of carbon sequestration efficiency due to its high surface area, which provides many adsorption sites. In contrast, although cellulose fibers show a similar carbon sequestration capacity, they may differ due to the complexity of the measurement method and

Table 4
Compressive strengths of concrete with biochar and Cellulose fiber.

Biochar content	Curing condition	Sample types	Biochar Preparation Temperature	Compressive strength (MPa)		Refs.
				7 days	28 days	
0–5 wt% of cement	In water	paste	Nitrogen with 500 °C	9–15	23–43	[203]
0–1.5 wt% of cement	In a curing room (temperature: 23 °C, relative humidity: 95 %)	Mortar		21–24	24–31	[204]
0–0.15 wt% of cement (Nano-Biochar)	In water	Mortar	Nitrogen with 500 °C		57–70	[206]
0.1–1 wt% of cement	In the moist environment	Concrete	PL: 450 °C (slow pyrolysis); RH 500 °C (slow pyrolysis); PP (500 °C)	PL: 20–27; RH:19–30; PP:25–30	PL: 28–33; RH: 20–34; PP:28–35	[207]
0–8 wt% of cement		Concrete	550°C	17–23	23–34	[208]
Cellulose fiber	Curing condition	Sample types	Characteristics of fiber types	Compressive strength (MPa)		Refs.
				7 days	28 days	
0–0.7 wt% of cement	In a curing room (temperature: 30 °C, relative humidity: 100 %)	Paste	bamboo fibers	23–30	27–35	[209]
0–0.35 wt% of cement	In a curing room (temperature: 23 °C, relative humidity: > 95 %)	Mortar	Waste cellulose fibers	40–45	44–49	[210]
0–2 wt% of cement	water bath maintained at 20 ± 1 °C	Mortar	Abaca fiber	25–35	27–42	[211]
0.5 wt% of cement	In a curing chamber maintained at 23 ± 2°	Concrete	Cellulose fiber	29–31	35–37	[212]
0.5–3 wt% of cement	In a curing room (temperature: 25 °C, relative humidity: 65 %)	Concrete	Jute, sisal, coconut, and sugarcane fiber			[213]

the different sample treatments. In conclusion, both materials have the potential to enhance the carbon sequestration capacity of cement-based materials. However, the selection of materials and methods should consider the specific application context and objectives.

5.3. Effect of biochar/cellulose fiber on mechanical properties of cement-based materials

As a carbon-negative material, there is a growing interest in the potential use of biochar and its application in cementitious composites, as shown in Table 4. Biochar is increasingly adopted as an additive or as a replacement for cement due to its low thermal conductivity, high chemical stability, and low flammability [199–202]. Ali et al. [203] prepared biochar in a muffle furnace at 500 °C under nitrogen and pressure and used it to investigate its mechanical properties and microstructural changes in cement-based materials. The compressive strength of the cement pastes containing biochar was found to increase significantly at 28 days of curing age compared to the control group. The optimum strength value of 43 MPa was achieved at 3 wt% incorporation at 28 days of curing. This is mainly attributed to the filler effect of the biochar, which can be used to provide nucleation sites for the hydration products, leading to the production of C-S-H gel products used to fill the pores. However, when 5 wt% biochar is added to the cement paste, the accumulation of biochar particles in the cement system occurs due to van der Waals gravity, which leads to a reduction in the formation of hydration products in the mixture and the development of large pores and cracks around the ITZs, thus reducing the macroscopic mechanical properties. Consequently, it is inadvisable to exceed a 5 wt% biochar addition to the cement paste system. Mishra et al. [204] have determined that the optimal biochar content in a cement system is 1 wt%. The addition of 1 wt% biochar resulted in a slight increase in compressive strength of OPC mortar, with values ranging from 5 % to 7.5 %. Given that the biochar did not exhibit any water-hardening properties, the observed increase in strength can be attributed to the filler effect and the fine grain size of the biochar. However, when the biochar dosage was increased to 1.5 wt%, a 26 % reduction in the compressive strength of the specimens was observed at 28 days of age. This reduction was attributed to the mesoporous structure of the biochar, which resulted in the addition of biochar concentrations higher than 1.0 wt% reducing the compressive strength of the OPC mixtures [205].

To gain further insight into the effect of biochar fines on cement pastes, Sisman et al. [206] prepared biochar using two different raw materials: waste sludge (industrial and municipal) and lignocellulose (almond shells). After undergoing pyrolysis at 500 °C, the material was ball-milled and ground to an average particle size of 200 nm. The findings indicate that 0.12 wt% nano-biochar can enhance the compressive strength of cement paste, because of its pore-filling effect. However, above this value, the compressive strength is reduced due to the formation of agglomerates. Indeed, the literature [214,215] indicates that if the quantity of nano-biochar is considerable, biochar agglomerates are formed due to the strong van der Waals forces between the atoms on the surface of the nanoparticles and the electrostatic forces between the nanoparticles. This can result in the formation of weak zones in the cementitious composites. In their study, Akhtar et al. [207] prepared novel biochar-concrete composites using three different types of biochar: poultry litter (PL) biochar, rice husk (RH) biochar, and pulp and paper mill sludge (PP) biochar. The mechanical properties of different specimens were observed, and it was found that the addition of PL, RH, and PP biochar negatively affects the 28-day compressive strength of concrete. The results indicated that the addition of PL biochar resulted in a reduction in the 28-day compressive strength of concrete by between −13 % and −37 %. Similarly, the addition of RH biochar resulted in a reduction in the 28-day compressive strength of concrete by between −9 % and −46 %. Finally, the addition of PP biochar resulted in a reduction in the 28-day compressive strength of concrete by between −7 % and −25 %. In the biochar-concrete system, the filler effect of biochar is more dominant than the volcanic ash effect, yet it contributes little to the hydration products. In fact, it forms a dense structure during the early development, while inhibiting the production of C-S-H gel due to the higher volume occupancy. Aneja et al. [208] also demonstrated that the amount of biochar used to replace the cement fraction should not exceed 4 wt%, as otherwise it will negatively affect the mechanical strength of concrete. Furthermore, excess biochar reduces the formation of C-S-H compounds.

Biochar, due to its porous structure, tends to absorb water and increase the water demand of the mixture, thereby reducing the workability of cementitious materials. The water-to-binder ratio is typically maintained around 0.5 to ensure adequate hydration, but as the biochar content increases, the mixture may become stiffer and require adjustments. If the biochar content exceeds 2 wt%, the mixture may become difficult to handle, and plasticizers are often needed to improve flowability [216,217]. Also, biochar's internal structure can effectively reduce autogenous shrinkage. Its porous nature allows it to store water, which is gradually released during hydration, thereby reducing shrinkage and minimizing cracking in the hardened state. Studies [216,217] have shown that mixtures containing 1–2 wt% biochar can optimize shrinkage control while maintaining structural integrity. In terms of durability, biochar helps increase the electrical resistivity of concrete, reducing the risk of corrosion in reinforced concrete structures. Typically, 1–2 wt% biochar can enhance durability while maintaining good workability and strength. However, biochar content higher than 5 wt% may lead to increased chloride diffusivity, posing long-term durability challenges, especially in corrosive environments [216,218,219]. The appropriate incorporation of biochar enhances the sustainability of cementitious materials and provides significant advantages in reducing shrinkage and improving durability. The optimal biochar content is usually between 1 and 2 wt%, balancing environmental benefits with optimized structural performance.

In conclusion, the optimal value of biochar for concrete strength is contingent upon the nature of the raw material of biochar. Biochar produced from different raw materials exhibits variations in chemical composition, pore structure, and specific surface area, which collectively influence the efficacy of biochar in concrete. For instance, biochar produced from woody materials typically exhibits a high carbon content and porous structure, which can enhance the compactness and compressive strength of concrete [220–222]. Nevertheless, biochar produced from inferior raw materials, such as biomass waste, may contain a greater quantity of impurities and a lower degree of porosity, which reduces its efficacy in enhancing concrete strength [223]. Furthermore, there is a non-linear relationship between the quantity of biochar admixture and the strength of the concrete. A moderate quantity of biochar can fill the voids within concrete, thereby improving its densification and enhancing its strength. However, when the dosage exceeds a certain level, it will begin to hinder the formation of the cement matrix, thus reducing the strength of the concrete. Furthermore, the high porosity of biochar may lead to a weak interface between biochar and cement paste [224]. Consequently, further experiments are required to ascertain the impact of biochar prepared from specific raw materials on the strength of concrete at varying admixtures, with the objective of selecting the optimal admixture to ensure the maintenance or even enhancement of concrete strength while guaranteeing the carbon sequestration effect.

Cellulose fibers are regarded as an optimal reinforcing material due to their distinctive properties, including low density, low cost, a vast range of applications, remarkable specific strength and high specific modulus, particularly their renewability and biodegradability [225,226]. Consequently, numerous researchers have endeavored to utilize cellulose fibers as reinforcement in cementitious composites, including sisal [227], cellulose nanofibers [228], olive pruning fibers [229] and bamboo [230]. These materials have been documented in the literature for their application in cement-based materials. Cellulose fiber cement composites exhibit excellent properties and have the potential to be used

as building materials. However, the cell walls of plant fibers exhibit a high degree of hydrophilicity due to the presence of chemical components such as hydroxyl groups, which may lead to dimensional instability under varying humidity conditions. Consequently, the application of cellulosic fibers in cement-based materials faces a number of challenges, including low interfacial bonding between the fibers and the cement [231], highly porous cellulosic fibers leading to a decrease in the mechanical properties of the cement-based materials [232], and a cement hydration reaction delay [233].

Lee et al. [211] observed that the mechanical strength of banana hemp fiber cement paste exhibited a decreasing trend with increasing fiber content at all curing ages. Samples containing 0.25 wt% exhibited the highest compressive strengths, which were approximately 1–2.5 wt % higher than the control at all ages. The incorporation of natural fibers typically results in an increase in porosity and a concomitant decrease in density, which consequently reduces the compressive strength of the material. Nevertheless, it is important to note that samples containing higher levels of plantain fibers exhibited higher long-term strength growth rates due to the internal curing effect induced by the high-water absorption of plantain fibers. Jaberizadeh et al. [210] found that the addition of low concentrations (0.25 wt%) of waste cellulose fibers to the cementitious system increased the mechanical strength of the samples, with flexural strength increasing by approximately 15–24 % and compressive strength increasing by 3–10 %. However, exceeding this incorporation level negatively affects the mechanical properties of the samples. Conversely, since natural fibers lack a natural affinity with cement, chemical methods (e.g. alkali treatment) can be employed to enhance the interfacial interactions between natural fibers and the cement matrix, thereby improving the mechanical properties of cement-based materials [234,235]. Nevertheless, Li et al. [209] discovered that, despite alkali treatment of bamboo fibers using sodium hydroxide solution, the compressive strength of the samples decreased as the fibre content increased from 0 to 0.7 wt% in the cement paste system. This decrease in strength was attributed to the lower modulus of the bamboo fibers in comparison to the cement matrix. Consequently, the content of cellulose fibers should be kept to a minimum in a cellulose fiber-cement slurry system.

In their study, Singh et al. [212] observed a reduction in the compressive strength of concrete systems by 37.39 % and 25.59 % after 14 and 28 days of curing, respectively, when cellulose fibers were incorporated into the concrete matrix at a concentration of 0.5 wt%. This reduction in strength was attributed to the reduction in compaction that resulted from the addition of cellulose fibers. Conversely, as previously mentioned, cellulose fibers can act as a water storage layer during long-term curing of the concrete samples, thus improving the hydration of unreacted cement particles. This, in turn, allows for further development of strength during the curing period. Similarly, Jamshaid et al. [213] investigated the effect of different types of cellulosic fibers (jute, sisal, coconut and bagasse) on the mechanical properties of concrete. The results demonstrated a non-linear correlation between the mechanical properties of the specimens and the amount of fiber incorporated.

Cellulose fibers, due to their hydrophilicity, reduce the workability of concrete when added in amounts exceeding 0.3 wt%, mainly because the fibers absorb the free water in the mixture. Therefore, to maintain workability, superplasticizer (1 wt%) is typically added to compensate for the decrease in flowability [236,237]. In terms of reducing autogenous shrinkage, cellulose fibers act as internal curing agents, effectively mitigating shrinkage cracking during the early hydration process. The cellulose fibers absorb moisture and gradually release it, providing internal water supply to the concrete, thereby reducing the risk of early cracking caused by autogenous shrinkage. The study has shown [236] that adding 0.5 % to 1.5 wt% of cellulose fibers, especially in high-strength concrete with a low water-to-cement ratio, can significantly reduce autogenous shrinkage. In addition to autogenous shrinkage, cellulose fibers also perform exceptionally well in reducing drying shrinkage. Their sponge-like structure can store moisture and release it slowly during the drying process, maintaining internal humidity and thus reducing the risk of shrinkage cracking. Research has shown [237] that adding approximately 1 wt% of cellulose fibers can effectively control drying shrinkage, helping to maintain internal relative humidity and prevent early cracking. Furthermore, cellulose fibers significantly enhance the crack resistance of concrete. By bridging microcracks, the fibers delay crack propagation and improve the material's crack resistance. Barabanshchikov et al. [238] demonstrated that adding 0.5 % to 1.0 wt% of cellulose fibers can effectively enhance crack resistance.

In conclusion, it is important to exercise caution when incorporating cellulose fibers into cement-based materials, as an excessively high content may lead to a loss of workability, which in turn may result in a deterioration of the mechanical properties [239]. This phenomenon is often attributed to uneven fiber distribution, agglomeration or clogging. It is important to note that the impact of cellulose fibers on the mechanical properties of cement-based materials is inconclusive, with both positive and negative effects. Untreated plant fibers may have a detrimental effect on the mechanical properties due to the presence of internal cavities, high moisture absorption and dimensional instability, and poor adaptation to different matrices. Despite the application of chemical treatments (e.g. alkali treatment), the desired results are difficult to achieve, which is attributed to the low strength and modulus of plant fibers compared to cement particles. Conversely, the use of plant fibers promotes the hydration process of cement and improves the mechanical strength of cement-based materials. This is due to the ability of cellulose fibers to form a water-locking layer, which releases water adsorbed during mixing and enhances continuous internal curing during cement hydration, contributing to prolonged hydration [240,241].

6. Comparative analysis of materials for cement-based carbon sequestration

Wollastonite, Nano-TiO_2, GO, biochar, and cellulose fibers each possess unique carbon sequestration mechanisms and performance enhancement capabilities. In terms of carbon sequestration, these materials have their individual strengths, but a comparison of their performance reveals that some exhibit stronger carbon fixation abilities when used alone, while their effects differ when combined with cementitious materials.

From the perspective of carbon sequestration mechanisms, these materials capture and store CO_2 in cementitious materials through different processes (Fig. 20). Wollastonite sequesters carbon via mineral carbonation, where CO_2 reacts with calcium silicate to form stable $CaCO_3$. This process transforms atmospheric CO_2 into a solid form, providing long-term stability. Nano-TiO_2 utilizes its photocatalytic activity under light exposure to convert CO_2 into $CaCO_3$ and store it within the cement matrix, driven by the electron-hole pairs generated in the titanium dioxide matrix. Similarly, graphene oxide sequesters carbon through chemical adsorption, where CO_2 molecules react with oxygen-containing functional groups (such as hydroxyl and carboxyl groups), forming stable $CaCO_3$ on the surface. Biochar captures CO_2 through its highly porous structure, which adsorbs carbon molecules within its micropores. Additionally, biochar reacts with CO_2 via alkaline functional groups, forming stable $CaCO_3$ and contributing to the carbon sequestration process in cementitious materials. Finally, cellulose fibers sequester carbon by adsorbing CO_2 on their large surface area, thanks to their porous structure and hydroxyl groups, which facilitate physical adsorption and weak chemical bonding with CO_2. The unique mechanisms of each material determine its effectiveness in carbon sequestration, offering distinct advantages in cement applications.

The performance of these materials in enhancing carbon sequestration varies based on their ability to capture CO_2. Wollastonite demonstrates an impressive CO_2 absorption rate of up to 25.3 %, outperforming other composites such as MgO-fly ash-OPC paste. The incorporation of

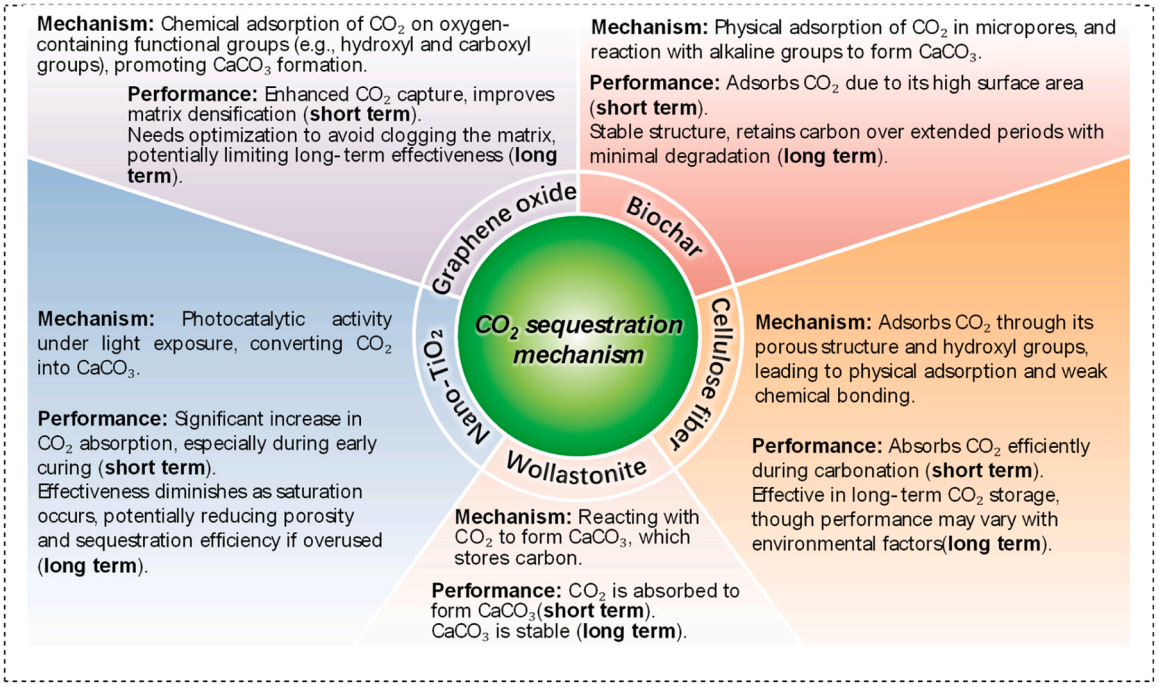

Fig. 20. Mechanisms and performance of carbon sequestration functional materials in cementitious systems.

nano-TiO_2 into cementitious materials can increase CO_2 absorption by 38.4 %, especially during short-term curing processes. GO can boost the carbon sequestration rate by approximately 30 %, interacting with calcium ions to promote the formation of $CaCO_3$, thereby densifying the cement matrix. Biochar, with an average adsorption capacity of 1.67 mmol/g, further enhances the carbon sequestration capability of cement systems by increasing the active surface area available for CO_2 capture. Cellulose fibers exhibit a CO_2 absorption efficiency of up to 24.4 % during prolonged carbonation. Collectively, these materials enhance the carbon capture capacity of cement-based products, with nano-TiO_2 and GO excelling in short-term sequestration, while wollastonite and biochar show strong long-term stability.

On the other hand, the long-term and short-term behaviors of these materials vary significantly. Wollastonite undergoes mineral carbonation to form highly stable $CaCO_3$, ensuring that the sequestered CO_2 is stored for the long term without significant release, making it ideal for applications where durability is critical. Nano-TiO_2, although highly effective in the short term, reaches a saturation point where further additions can reduce porosity and lower sequestration efficiency, thus requiring careful optimization. Similarly, GO can deliver significant carbon capture in the short term, but its dosage must be balanced to avoid clogging the matrix and limiting long-term effectiveness. Biochar, due to its stable structure and high surface area, excels in long-term carbon storage, retaining captured carbon for extended periods with minimal degradation. Cellulose fibers also provide stable long-term CO_2 storage, though their effectiveness can be influenced by environmental factors such as humidity.

To maximize the carbon sequestration rate and mechanical properties of cementitious materials, it is essential to balance the synergies between wollastonite, TiO_2, GO, biochar, and cellulose fibers within the cement matrix. Wollastonite, as a calcium silicate mineral, sequesters CO_2 by converting it into stable $CaCO_3$. This process captures CO_2 and enhances in densifying the cement matrix, improving both compressive and flexural strength. The needle-like structure of wollastonite further acts as a filler, reducing porosity and bridging microcracks, which enhances the material's durability and load-bearing capacity.

Nano-TiO_2 (particularly in the anatase phase) contributes additional synergy through the photocatalytic reduction of CO_2, resulting in its transformation into carbonate compounds. TiO_2 also plays a crucial role in enhancing early hydration due to its high surface area, promoting nucleation and densification of the matrix. GO introduces another layer of synergy. Due to its high specific surface area and oxygen-containing functional groups, GO provides nucleation sites for $CaCO_3$ formation, enhancing CO_2 absorption and further densifying the matrix.

Biochar, with its porous structure and large surface area, greatly enhances carbon sequestration by providing numerous adsorption sites for CO_2. It also improves the pore structure of cementitious materials, promoting better carbonation and densification. Similarly, cellulose fibers reinforce the material by bridging cracks and increasing toughness. Their hydroxyl groups chemically bind with CO_2, while their porous structure aids in additional CO_2 adsorption, further contributing to carbon sequestration. To optimize the combination of these materials, a balanced mixture would include approximately 10 wt% wollastonite, 1–2 wt% TiO_2, 0.05 wt% GO, 1 wt% biochar, and 0.5 wt% cellulose fibers in cementitious materials. These formulations leverage their carbon sequestration capabilities while enhancing mechanical properties through their synergies with cementitious materials, making them suitable for sustainable construction applications.

7. LCA of carbon-sequestering cementitious materials

It is important to analyze the LCA of wollastonite, TiO_2, GO, biochar and cellulose fibers used in the production of green concrete to fully evaluate the environmental impact of the production process of these materials, including energy consumption, greenhouse gas emissions and potential pollution. The LCA analysis will identify and quantify the contribution of these innovative materials to reducing the environmental footprint throughout the life cycle, while improving the performance of the concrete, thus supporting more sustainable strategies for the selection and use of construction materials and advancing the goals of green building and sustainable development. This analysis focuses on both the production and preparation processes. The system boundaries are shown in Fig. 21 and include the extraction of raw materials, their transport, and the process of manufacturing into the different categories of concrete. In addition, we have included the energy required for concrete mixing in the analysis to ensure the comprehensiveness of the

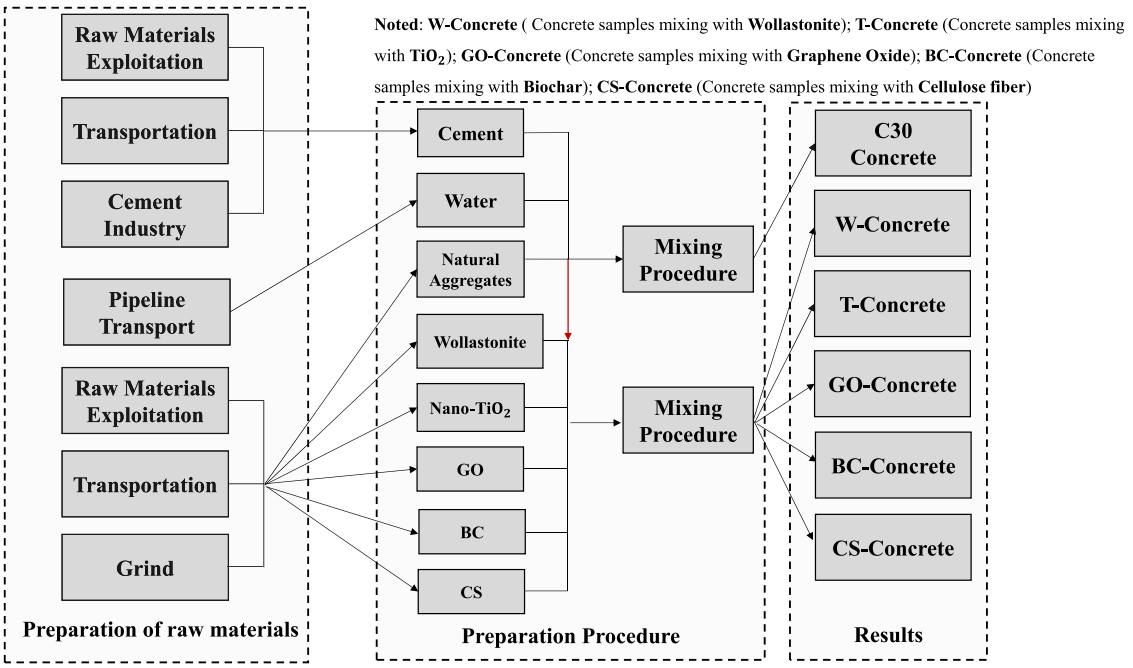

Fig. 21. Boundaries of different categories of green concrete systems.

system boundary. Our aim is to improve overall environmental efficiency and reduce the lifecycle environmental footprint through in-depth analysis and optimization of these key steps. During the analysis process, we looked at the inputs and outputs of each stage of the life cycle. We collected Life Cycle Inventory (LCI) data [242–245] for various elements required to produce concrete, including wollastonite, TiO_2, GO, biochar, cellulose fibers aggregates, cement, as well as concrete production and transport, as shown in Table 5; Table 6 shows the mixing ratios for the different categories of concrete, as well as for the control group (C30 concrete). Also, to ensure comparability, the same transport distances were assumed when comparing the environmental impacts of the different mixes.

Fig. 22 (a) illustrates the GWP performance of the four different types of concrete. The results of the analyses demonstrate that GO-Concrete has the highest GWP in terms of carbon emissions and impact on land due to the use of several chemicals in its production process, including sulphuric acid and sodium nitrate. Furthermore, the high energy consumption of the process contributes to its elevated GWP [246,247]. Secondly, T-Concrete also exhibits high GWP values, primarily because the production of titanium dioxide is an energy-intensive process that involves a sulphate process and several chemical and thermal treatment steps [248,249]. Conversely, CS-Concrete and W-Concrete exhibit lower GWP values, primarily due to the relative simplicity and energy intensity of the extraction and processing of these materials, which do not involve significant land changes during production and extraction. It is noteworthy that BC-Concrete exhibits the highest GWP in terms of bio-emissions. The process of bio-carbon preparation, while capable of locking carbon in solid matter and thus reducing the amount of CO_2 released directly into the atmosphere, is itself a high-energy consumption process accompanied by significant CO_2 emissions. Furthermore, concrete incorporating wollastonite, titanium dioxide, graphene oxide, cellulose fibers and biocarbon demonstrated superior CO_2 capture compared to conventional C30 concrete. This is attributed to the fact that these materials enhance the density, surface area and reactivity of the concrete, with biocarbon concrete exhibiting high stability and excellent adsorption properties, thereby excelling in CO_2 sequestration.

Conversely, Fig. 22 (b) illustrates the combined environmental and human health impacts of the different types of concrete over a 100-year period. The results of the analysis indicate that GO-Concrete and T-Concrete have a more detrimental impact on the environment and human health than C30 concrete. Conversely, W-Concrete has a comparatively lower environmental impact.

Table 5
LCI data for original material as well as transport.

	Production of cement (kg)	Production of natural aggregate (kg)	Production of water (1 m^3)	Production of TiO_2 (kg)	Production of Wollastonite (kg)	Production of GO (kg)	Production of biochar (kg)	Production of cellulose fiber (kg)	Transport (tkm)
Energy (MJ)									
Coal	3.370140								
Natural gas	0.083178			8.9			0.00031	0.0641	
Diesel	0.024369	0.014780		9.3	0.00372		0.641		1.54090
Electricity (kWh)	0.507672		0.48	1.83	0.111	8.31	3.336	0.133	
Emissions to air (g)									
CO	4.203224	0.003475		159			3.46		0.31885
NO_x	2.279068	0.015579		1.44		200	9.73		0.98438
SO_x	3.646948	0.005447		1.28			0.157		0.43094
CH_4	1.002748	0.001296					0.753		0.12386
CO_2	861.2028	1.377926		923			9490		110.770
N_2O	0.000756	0.000055							0.00295

Table 6
C30 concrete and carbon negative concrete ratios.

Types of concrete	Water/cement ratio	Mix proportions (by weight of cement)								
		Cement	Coarse	Fine	Water	Wollastonite	TiO_2	GO	BC	CS
C30	0.65	1	3.5	3	0.65					
W-Concrete	0.65	0.95	3.5	3	0.65	0.05				
T-Concrete	0.65	0.95	3.5	3	0.65		0.05			
GO-Concrete	0.65	0.95	3.5	3	0.65			0.05		
BC-Concrete	0.65	0.95	3.5	3	0.65				0.05	
CS-Concrete	0.65	0.95	3.5	3	0.65					0.05

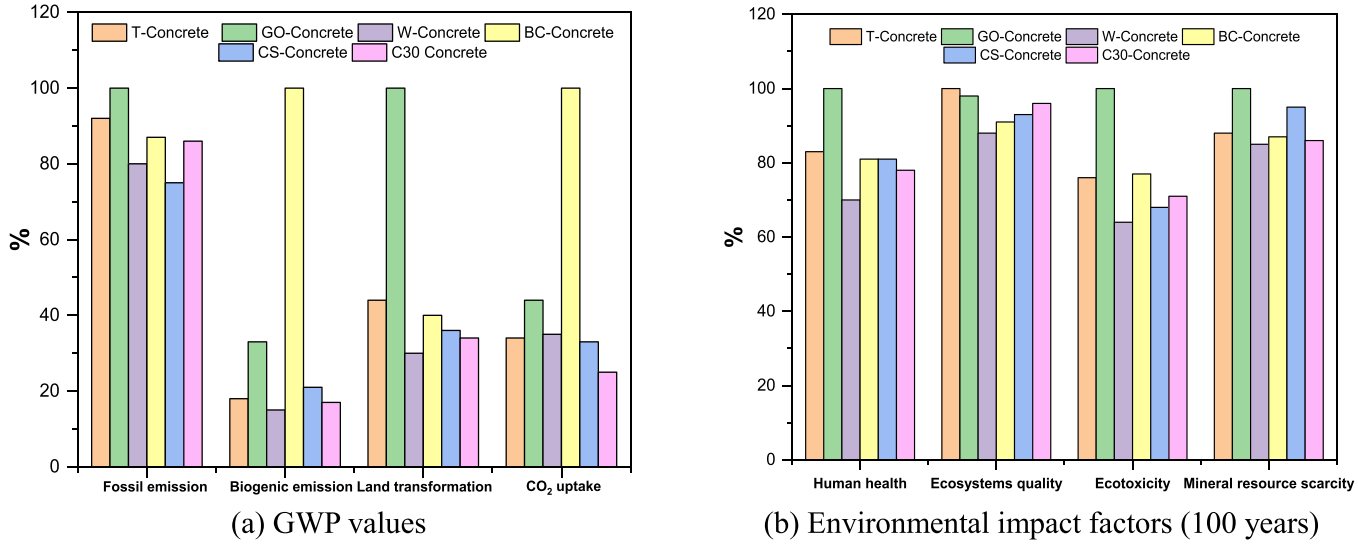

Fig. 22. Life cycle analysis for different types of concrete.

In terms of mineral resources, the production of TiO_2, GO and cellulose fibers consumes a considerable quantity of raw materials. The extraction of TiO_2, in particular, frequently involves large-scale mining activities, which directly results in ecological damage, land degradation and biodiversity loss. Mining not only occupies a considerable amount of land resources, but also permanently alters the original land use and has a long-term impact on the local ecosystem. Regarding environmental pollution, it can be observed that GO-Concrete, T-Concrete and BC-Concrete have a higher environmental impact than C30 concrete, CS-Concrete and W-Concrete. Furthermore, the production of TiO_2 and GO emits hazardous chemicals and wastewater, which react with inorganic ions and molecules in the water. Once discharged into a water body, these wastewaters react with inorganic ions and molecules in the water, thereby affecting the ecosystem. Previous studies have indicated that nanoparticles can accumulate in aquatic environments and interfere with aquatic ecosystems and food chains [250]. Furthermore, the production of biochar is an energy-intensive process, and its pyrolysis generates a variety of pollutants, including hydrocarbons, phenols, and a range of organic compounds [251,252]. Recent studies have revealed that a considerable quantity of phenols was identified in biochar produced from diverse feedstocks, representing approximately 27 % of all hydrocarbons produced [253]. These substances have the potential to cause harm to the environment due to their capacity to induce toxicity through a range of mechanisms, which can affect biological populations and potentially result in carcinogenic and mutagenic effects [254].

Long-term exposure to GO has been demonstrated to reduce mitochondrial function and disrupt cell membranes, resulting in toxicity to skin cells. This is in accordance with the findings of studies on the effects of GO on human health [255]. Meanwhile, TiO_2 nanoparticles have been demonstrated to cause cellular damage, genotoxicity, inflammation and immune responses, primarily by inducing an oxidative stress response. The International Agency for Research on Cancer (IARC) has classified TiO2 nanoparticles as "possibly carcinogenic to humans" [256]. Furthermore, the potential hazards of biochar and cellulosic fibers must be acknowledged, as studies have demonstrated that inhalation of biochar particles or cellulosic fibers during preparation and incorporation can result in serious respiratory diseases such as inflammatory reactions in the lungs or pneumoconiosis [257,258]. In addition, the potential contaminants in biochar may enter groundwater through soil leaching, accumulate in the soil and biomagnify through the food web, thus posing a threat to human health [259,260].

In conclusion, the life cycle assessment of wollastonite, titanium dioxide, graphene oxide, cellulosic fibers and biochar used to produce green concrete revealed significant differences in the contribution of each material to the GWP. While GO-Concrete and T-Concrete exhibited higher values in terms of GWP, this was mainly due to their energy-intensive production processes and the use of hazardous chemicals. However, they demonstrated superior performance in enhancing the CO_2 capture capacity of concrete. BC-Concrete has a significant effect in reducing atmospheric CO_2 concentrations due to its excellent CO_2 sequestration capacity. On the other hand, W-Concrete and CS-Concrete exhibit lower GWP values due to their lower energy consumption and less land impact during production. This suggests that W-Concrete and CS-Concrete are prioritized green materials due to their significant advantages in reducing environmental hazards and promoting the development of green building materials. Nevertheless, although these materials offer the potential to enhance concrete performance and environmental benefits, their production and use also pose significant environmental and health risks. For instance, the production of GO and TiO_2 generates hazardous wastewater that may have long-term impacts on aquatic ecosystems, while the energy-intensive production process of biochar is accompanied by significant CO_2 emissions. Furthermore,

these materials may pose a direct threat to human health during use, including causing lung inflammation and potential carcinogenic risks. Consequently, when advocating the utilization of these eco-friendly materials in concrete, it is imperative to balance their environmental advantages against the potential hazards to ensure that technological advancements are accompanied by the protection of ecosystems and human health [261,262].

8. Conclusions

The construction industry has a key role to play in addressing the challenge of climate change. This study looks at the development of novels, popular building materials and summarizes progress to date. Through the research and application of these materials, we can expect to significantly reduce the environmental impact of construction, encourage the development of sustainable construction materials, and facilitate the formation of greener building standards and policies. In addition, the LCA analyses provide us with an understanding of the importance of sustainable building materials and explore CO_2 sequestration technologies, which provide useful guidance for mitigating global climate change. The conclusions of the paper are as follows:

(1) Wollastonite is highly efficient at carbon sequestration, particularly due to its reaction with CO_2 to form $CaCO_3$. Wollastonite can achieve a carbon sequestration rate of up to 25.3 % in cementitious materials under optimal carbonation conditions. Specifically, replacing 10 wt% of cement with wollastonite reduces the GWP by up to 30 %, cutting CO_2 emissions by 127 kg CO_2-equivalent per cubic meter of concrete. Wollastonite enhances the compressive and flexural strength of cementitious materials, particularly at 9–10 wt% replacement, higher ratios may begin to negatively impact these mechanical properties.
(2) Nano-TiO_2 facilitates carbon sequestration through photocatalytic processes, converting CO_2 into carbonate ions that bond with calcium to form $CaCO_3$. Incorporating 1–2 wt% nano-TiO_2 into cementitious materials can improve CO_2 uptake by 18.5–38.4 %. The optimal dosage is 1.5–2 wt%, which enhances both carbon capture and the mechanical properties of the material without causing particle agglomeration. Nano-TiO_2 also improves the density and pore structure of cement, which aids in the carbonation process and boosts CO_2 capture.
(3) GO's high surface area and functional groups provide excellent carbon capture potential, increasing CO_2 uptake in cementitious materials by approximately 30 % compared to conventional cement. When used in optimal doses of 0.02–0.05 wt%, GO enhances compressive strength, while also promoting carbonation reactions that improve CO_2 sequestration. However, exceeding 0.05 wt% may lead to the creation of too many nucleation sites, hindering the formation of dense hydration products and reducing material strength.
(4) Biochar has a high surface area and porous structure, making it highly effective for carbon capture in cementitious materials, with an average CO_2 adsorption capacity of 1.67 mmol/g. An optimal dosage of 1–5 wt% significantly enhances carbon sequestration efficiency and improves the material's mechanical properties. Above 5 wt%, biochar particles tend to aggregate, reducing hydration efficiency and weakening the microstructure. Biochar also promotes carbonation in cementitious materials, facilitating the formation of stable carbonates and long-term carbon storage
(5) As a renewable resource, cellulose fibers provide effective pathways for CO_2 adsorption through hydroxyl groups in their structure. Adding 0.02–0.05 wt% cellulose fibers to cementitious materials can increase CO_2 uptake by up to 20 %, significantly enhancing carbon capture. These fibers also improve the compressive strength and crack resistance of the materials, although excessive fiber content can negatively affect workability and strength.
(6) A comprehensive examination of the various materials utilized in the fabrication of green concrete has revealed that W-Concrete and CS-Concrete exhibit considerable environmental benefits. Both materials require less energy and have a lower impact on the land during production, resulting in relatively low GWP values. Furthermore, they offer significant advantages in reducing environmental hazards and promoting the development of green building materials, and thus should be prioritized as green materials. Although the production of GO and TiO_2 concretes enhances the CO_2 capture capacity of the materials, the high energy consumption and use of chemicals in their production results in higher GWP values and potentially greater environmental and health risks. Similarly, although BC-Concrete exhibits a high CO_2 sequestration capacity, its production process is energy-intensive and is accompanied by higher carbon emissions.

9. Future research discussion

Although materials such as biochar, nano-TiO_2, GO, and wollastonite have shown significant potential in cementitious materials, future research needs to further explore current challenges and promote the development of new composite materials. Based on the limitations of existing studies, future research directions can focus on the following aspects:

(1) Future research should delve deeper into the synergistic effects when using different materials in combination. For instance, combining biochar with nano-TiO_2 or GO to investigate their combined effects on carbon capture efficiency, strength, and durability. By optimizing the ratios of these materials, it is possible to develop new composites with both high strength and low carbon emissions.
(2) Regarding the optimal dosage of different materials, current studies mainly focus on the individual application of a single material. Future studies could further explore the impact of dosage on the microstructure and pore distribution of concrete. The focus should be on how to finely control the material dosage to regulate the formation of hydration products and porosity, thereby maximizing mechanical performance and carbon sequestration capacity.
(3) Although materials such as nano-TiO_2 and GO exhibit excellent performance, their high production costs limit large-scale applications. Therefore, future research should focus on developing green, sustainable material preparation technologies, such as utilizing industrial by-products or renewable resources to produce low-cost, high-performance carbon sequestration materials.
(4) Current research mainly focuses on the short-term performance of materials. Future studies should strengthen the evaluation of the long-term durability of these materials in complex environments, especially their stability under conditions such as high temperatures and humidity changes. Additionally, their long-term carbon sequestration capacity in practical engineering applications should be investigated.

CRediT authorship contribution statement

Surendra P. Shah: Writing – review & editing, Validation. **Wengui Li:** Writing – review & editing, Writing – original draft, Supervision, Resources, Methodology, Conceptualization. **Kailun Chen:** Writing – review & editing, Writing – original draft, Validation, Methodology, Investigation, Data curation. **Fulin Qu:** Writing – review & editing, Writing – original draft, Validation. **Zihui Sun:** Writing – review & editing, Writing – original draft, Validation.

Declaration of Competing Interest

The authors declare that they have no known competing financial interests or personal relationships that could have appeared to influence the work reported in this paper.

Acknowledgement

The authors acknowledge the support from Australian Research Council (ARC), Australia (FT220100177, LP230100288, DP220101051, DP220100036; IH200100010).

Data availability

Data will be made available on request.

References

[1] National Oceanic, Atmospheric Administration, Annual anomalies in global land and ocean surface temperature from 1880 to 2023, based on temperature departure, National Oceanic and Atmospheric Administration, 2024.
[2] T.A. Jacobson, J.S. Kler, M.T. Hernke, R.K. Braun, K.C. Meyer, W.E. Funk, Direct human health risks of increased atmospheric carbon dioxide, Nat. Sustain 2 (2019) 691–701, https://doi.org/10.1038/s41893-019-0323-1.
[3] K.A. Ali, M.I. Ahmad, Y. Yusup, Issues, impacts, and mitigations of carbon dioxide emissions in the building sector, Sustain. (Switz.) 12 (2020), https://doi.org/10.3390/SU12187427.
[4] O.B. Carcassi, G. Habert, L.E. Malighetti, F. Pittau, Material diets for climate-neutral construction, Environ. Sci. Technol. 56 (2022) 5213–5223, https://doi.org/10.1021/acs.est.1c05895.
[5] J. Kerr, S. Rayburg, M. Neave, J. Rodwell, Comparative analysis of the global warming potential (gwp) of structural stone, concrete and steel construction materials, Sustain. (Switz.) 14 (2022), https://doi.org/10.3390/su14159019.
[6] M.M.A. Klufallah, M. Fadhil Nuruddin, M.F. Khamidi, N. Jamaludin, Assessment of Carbon Emission Reduction for Buildings Projects in Malaysia-A Comparative Analysis, (n.d.). ⟨https://doi.org/10.1051/C⟩.
[7] T. Chen, X. Han, M. Guo, J. Xu, L. Li, L. Qin, X. Gao, CO2 activation of wollastonite cementitious material based on the mineralization-desorption of potassium glycine absorbent, ACS Sustain Chem. Eng. 12 (2024) 8890–8901, https://doi.org/10.1021/acssuschemeng.4c02175.
[8] H. Huang, R. Guo, T. Wang, X. Hu, S. Garcia, M. Fang, Z. Luo, M.M. Maroto-Valer, Carbonation curing for wollastonite-Portland cementitious materials: CO2 sequestration potential and feasibility assessment, J. Clean. Prod. 211 (2019) 830–841, https://doi.org/10.1016/J.JCLEPRO.2018.11.215.
[9] K. Svensson, A. Neumann, F. Feitosa Menezes, C. Lempp, H. Pöllmann, Carbonation of natural pure and impure wollastonite, SN Appl. Sci. 1 (2019), https://doi.org/10.1007/s42452-019-0328-4.
[10] S.Raghavendra Naganna, K. Jayakesh, V.R. Anand, Nano-TiO 2 particles: a photocatalytic admixture to amp up the performance efficiency of cementitious composites, (2046). https://doi.org/⟨10.1007/s12046-020-01515-xS⟩.
[11] L.P. Singh, R. Kumar Dhaka, D. Ali, I. Tyagi, U. Sharma, S.N. Banavath, Remediation of noxious pollutants using nano-titania-based photocatalytic construction materials: a review, (n.d.). ⟨https://doi.org/10.1007/s11356-021-14189-7/Published⟩.
[12] B.E. Arango Hoyos, H.F. Osorio, E.K. Valencia Gómez, J. Guerrero Sánchez, A. P. Del Canto Palominos, F.A. Larrain, J.J. Prías Barragán, Exploring the capture and desorption of CO2 on graphene oxide foams supported by computational calculations, Sci. Rep. 13 (2023), https://doi.org/10.1038/s41598-023-41683-4.
[13] S. Kushwah, S. Singh, R. Agarwal, N.Sanjay Nighot, R. Kumar, H. Athar, S. Naik B, Mixture of biochar as a green additive in cement-based materials for carbon dioxide sequestration, (n.d.). ⟨https://doi.org/10.1186/s40712-024-00170-y⟩.
[14] C.C. Onyekwena, Q. Li, Y. Wang, I.H. Alvi, Y. Hou, C.F. Ukaomah, T. Hakuzweyezu, Impacts of biochar and slag on carbon sequestration potential and sustainability assessment of MgO-stabilized marine soils: insights from MIP analysis, Environ. Sci.: Adv. (2024), https://doi.org/10.1039/d4va00095a.
[15] P.K. Biswas, O. Omole, G. Peterson, E. Cumbo, M. Agarwal, H. Dalir, Carbon and cellulose based nanofillers reinforcement to strengthen carbon fiber-epoxy composites: Processing, characterizations, and applications, Front Mater. 9 (2023), https://doi.org/10.3389/fmats.2022.1089996.
[16] J. Xiao, N. Han, Y. Li, Z. Zhang, S.P. Shah, Review of recent developments in cement composites reinforced with fibers and nanomaterials, Front. Struct. Civ. Eng. 15 (2021), https://doi.org/10.1007/s11709-021-0723-y.
[17] S. Ajabshir, R. Gupta, Effects of pretreatment methods and physical properties of cellulose fibers on compatibility of fiber-cement composites: a review, in: N. Banthia, S. Soleimani-Dashtaki, S. Mindess (Eds.), Smart & Sustainable Infrastructure: Building a Greener Tomorrow, Springer Nature, Switzerland, Cham, 2024, pp. 253–264.
[18] Z. Deng, A.H. Mahmood, W. Dong, D. Sheng, X. Lin, W. Li, Piezoresistive performance of self-sensing bitumen emulsion-cement mortar with multi-walled carbon nanotubes, Cem. Concr. Compos. 153 (2024) 105718.
[19] D. Lu, F. Qu, C. Zhang, Y. Guo, Z. Luo, L. Xu, W. Li, Innovative approaches, challenges, and future directions for utilizing carbon dioxide in sustainable concrete production, J. Build. Eng. 97 (2024) 110904.
[20] Q. Liu, A. Cheng, C. Sun, K. Chen, Y. Wang, W. Li, Effects of aggregate's type and orientation on stress concentration and crack propagation of modeled concrete applied a shear force, J. Build. Eng. 95 (2024) 110340.
[21] Y. Lu, Y. Xu, L. Meng, F. Ouyang, J. Cheng, P. Duan, Y. Zhu, W. Li, Z. Zhang, M. Chen, W. Huang, Role of modified calcium montmorillonite and 5 A zeolite in microstructure and efflorescence formation of metakaolin-based geopolymer, Constr. Build. Mater. 448 (2024) 138258.
[22] X. Wang, Y. Guo, Z. Tao, L. Shi, W. Li, Self-heating performance of phase change cementitious mortar with hybrid carbon-based nanomaterials, J. Energy Storage 104 (2024) 14495.
[23] X. Wang, Y. Huang, L. Shi, S. Zhang, W. Li, Enhanced thermal performance of phase change mortar using multi-scale carbon-based materials, J. Build. Eng. 98 (2024) 111259.
[24] Y. Fan, C. Feng, Z. Hang, L. Shen, W. Li, Optimal design of electrical conductivity of hybrid multi-dimensional carbon fillers reinforced porous cement-based Composites: Experiment and modelling, Compos. Struct. 352 (2025) 118714.
[25] L. Fiocco, H. Elsayed, J.K.M.F. Daguano, V.O. Soares, E. Bernardo, Silicone resins mixed with active oxide fillers and Ca–Mg Silicate glass as alternative/integrative precursors for wollastonite–diopside glass-ceramic foams, J. Non Cryst. Solids 416 (2015) 44–49, https://doi.org/10.1016/J.JNONCRYSOL.2015.03.001.
[26] H.E. Yücel, H.Ö. Öz, M. Güneş, Y. Kaya, Rheological properties, strength characteristics and flexural performances of engineered cementitious composites incorporating synthetic wollastonite microfibers with two different high aspect ratios, Constr. Build. Mater. 306 (2021) 124921, https://doi.org/10.1016/J.CONBUILDMAT.2021.124921.
[27] D. Feng, A. Hicks, Environmental, human health, and CO2 payback estimation and comparison of enhanced weathering for carbon capture using wollastonite, J. Clean. Prod. 414 (2023) 137625, https://doi.org/10.1016/J.JCLEPRO.2023.137625.
[28] Wollastonite: a versatile industrial mineral, United state, 2001. ⟨https://doi.org/10.3133/fs00201⟩.
[29] M.M. Obeid, Crystallization of Synthetic Wollastonite Prepared from Local Raw Materials, Int. J. Mater. Chem. 4 (2014) 79–87, https://doi.org/10.5923/j.ijmc.20140404.01.
[30] Z. He, A. Shen, Z. Lyu, Y. Li, H. Wu, W. Wang, Effect of wollastonite microfibers as cement replacement on the properties of cementitious composites: A review, Constr. Build. Mater. 261 (2020), https://doi.org/10.1016/j.conbuildmat.2020.119920.
[31] R. Shamsudin, F. 'Atiqah Abdul Azam, M.A. Abdul Hamid, H. Ismail, Bioactivity and cell compatibility of β-wollastonite derived from rice husk ash and limestone, Materials 10 (2017), https://doi.org/10.3390/ma10101188.
[32] M. Abdel Wahab, I. Abdel Latif, M. Kohail, A. Almasry, The use of Wollastonite to enhance the mechanical properties of mortar mixes, Constr. Build. Mater. 152 (2017) 304–309, https://doi.org/10.1016/j.conbuildmat.2017.07.005.
[33] F. Haque, R.M. Santos, Y.W. Chiang, CO2 sequestration by wollastonite-amended agricultural soils – an Ontario field study, Int. J. Greenh. Gas. Control 97 (2020) 103017, https://doi.org/10.1016/J.IJGGC.2020.103017.
[34] F. Haque, R.M. Santos, Y.W. Chiang, Optimizing inorganic carbon sequestration and crop yield with wollastonite soil amendment in a microplot study, Front Plant Sci. 11 (2020), https://doi.org/10.3389/fpls.2020.01012.
[35] Z. He, A. Shen, Z. Lyu, Y. Li, H. Wu, W. Wang, Effect of wollastonite microfibers as cement replacement on the properties of cementitious composites: A review, Constr. Build. Mater. 261 (2020), https://doi.org/10.1016/j.conbuildmat.2020.119920.
[36] D.N. Huntzinger, J.S. Gierke, S.K. Kawatra, T.C. Eisele, L.L. Sutter, Carbon dioxide sequestration in cement kiln dust through mineral carbonation, Environ. Sci. Technol. 43 (2009) 1986–1992, https://doi.org/10.1021/es802910z.
[37] H. Huang, T. Wang, B. Kolosz, J. Andresen, S. Garcia, M. Fang, M.M. Maroto-Valer, Life-cycle assessment of emerging CO2 mineral carbonation-cured concrete blocks: Comparative analysis of CO2 reduction potential and optimization of environmental impacts, J. Clean. Prod. 241 (2019) 118359, https://doi.org/10.1016/J.JCLEPRO.2019.118359.
[38] D.P. Siriwardena, S. Peethamparan, Quantification of CO2 sequestration capacity and carbonation rate of alkaline industrial byproducts, Constr. Build. Mater. 91 (2015) 216–224, https://doi.org/10.1016/J.CONBUILDMAT.2015.05.035.
[39] S. Monkman, Y. Shao, Integration of carbon sequestration into curing process of precast concrete, Can. J. Civ. Eng. 37 (2010) 302–310, https://doi.org/10.1139/L09-140.
[40] S. Kashef-Haghighi, S. Ghoshal, CO2 sequestration in concrete through accelerated carbonation curing in a flow-through reactor, : Ind. Eng. Chem. Res (2010) 1143–1149, https://doi.org/10.1021/ie900703d.
[41] H. El-Hassan, Y. Shao, Carbon Storage through Concrete Block Carbonation, J. Clean. Energy Technol. 2 (2014) 287–291, https://doi.org/10.7763/JOCET.2014.V2.141.
[42] W. Ashraf, J. Olek, V. Atakan, Carbonation reaction kinetics, CO2 sequestration capacity, and microstructure of hydraulic and non-hydraulic cementitious binders, : Sustain. Constr. Mater. Technol., Int. Comm. SCMT Conf. (2016), https://doi.org/10.18552/2016/scmt4s303.
[43] H. Huang, R. Guo, T. Wang, X. Hu, S. Garcia, M. Fang, Z. Luo, M.M. Maroto-Valer, Carbonation curing for wollastonite-Portland cementitious materials: CO2 sequestration potential and feasibility assessment, J. Clean. Prod. 211 (2019) 830–841, https://doi.org/10.1016/j.jclepro.2018.11.215.

[44] L. Mo, F. Zhang, D.K. Panesar, M. Deng, Development of low-carbon cementitious materials via carbonating Portland cement–fly ash–magnesia blends under various curing scenarios: a comparative study, J. Clean. Prod. 163 (2017) 252–261, https://doi.org/10.1016/J.JCLEPRO.2016.01.066.

[45] Z. Tu, M.Z. Guo, C.S. Poon, C. Shi, Effects of limestone powder on CaCO3 precipitation in CO2 cured cement pastes, Cem. Concr. Compos 72 (2016) 9–16, https://doi.org/10.1016/J.CEMCONCOMP.2016.05.019.

[46] M. Mahoutian, Y. Shao, Production of cement-free construction blocks from industry wastes, J. Clean. Prod. 137 (2016) 1339–1346, https://doi.org/10.1016/J.JCLEPRO.2016.08.012.

[47] B. Zhan, C.S. Poon, Q. Liu, S. Kou, C. Shi, Experimental study on CO2 curing for enhancement of recycled aggregate properties, Constr. Build. Mater. 67 (2014) 3–7, https://doi.org/10.1016/j.conbuildmat.2013.09.008.

[48] Y. Li, D. Han, H. Wang, H. Lyu, D. Zou, T. liu, Carbonation curing of mortars produced with reactivated cementitious materials for CO2 sequestration, J. Clean. Prod. 383 (2023) 135501, https://doi.org/10.1016/J.JCLEPRO.2022.135501.

[49] M.Z. Kashim, H. Tsegab, O. Rahmani, Z.A. Abu Bakar, S.M. Aminpour, Reaction mechanism of wollastonite in situ mineral carbonation for co2sequestration: effects of saline conditions, temperature, and pressure, ACS Omega 5 (2020) 28942–28954, https://doi.org/10.1021/acsomega.0c02358.

[50] S.K. Saxena, M. Kumar, D.S. Chundawat, N.B. Singh, Utilization of wollastonite in cement manufacturing, Mater. Today Proc. 29 (2020) 733–737, https://doi.org/10.1016/J.MATPR.2020.04.502.

[51] H.E. Yücel, S. Özcan, Strength characteristics and microstructural properties of cement mortars incorporating synthetic wollastonite produced with a new technique, Constr. Build. Mater. 223 (2019) 165–176, https://doi.org/10.1016/J.CONBUILDMAT.2019.06.195.

[52] D. Zhu, A. Wen, A. Tang, Mechanical properties, durability and environmental assessment of low-carbon cementitious composite with natural fibrous wollastonite, Environ. Res 234 (2023) 116552, https://doi.org/10.1016/J.ENVRES.2023.116552.

[53] R.I. Khan, W. Ashraf, Effects of ground wollastonite on cement hydration kinetics and strength development, Constr. Build. Mater. 218 (2019) 150–161, https://doi.org/10.1016/J.CONBUILDMAT.2019.05.061.

[54] Z. hai He, M. lu Shen, J. yan Shi, Ç. Yalçınkaya, S. gui Du, Q. Yuan, Recycling coral waste into eco-friendly UHPC: mechanical strength, microstructure, and environmental benefits, Sci. Total Environ. 836 (2022) 155424, https://doi.org/10.1016/J.SCITOTENV.2022.155424.

[55] R.I. Khan, W. Ashraf, Effects of ground wollastonite on cement hydration kinetics and strength development, Constr. Build. Mater. 218 (2019) 150–161, https://doi.org/10.1016/J.CONBUILDMAT.2019.05.061.

[56] A. Kozin, R. Fediuk, S. Yarusova, P. Gordienko, V. Lesovik, M.A. Mosaberpanah, Y.H.M. Amran, G. Murali, Improvement of mechanical characteristics of mortar by using of wollastonite, Mag. Civ. Eng. 107 (2021), https://doi.org/10.34910/MCE.107.15.

[57] P. Kalla, A. Rana, Y.B. Chad, A. Misra, L. Csetenyi, Durability studies on concrete containing wollastonite, J. Clean. Prod. 87 (2015) 726–734, https://doi.org/10.1016/J.JCLEPRO.2014.10.038.

[58] R. Mathur, A.K. Misra, P. Goel, Influence of wollastonite on mechanical properties of concrete, J. Sci. Ind. Res (India) 66 (2007) 1029–1034.

[59] A. Kogai, A. Puzatova, M. Dmitrieva, Influence of wollastonite on the fine concrete characteristics. AIP Conf Proc, American Institute of Physics Inc, 2023, https://doi.org/10.1063/5.0162979.

[60] S.S. Dobrosmyslov, A.S. Voronin, Y.V. Fadeev, I.G. Endzhievskaya, S.V. Khartov, Theoretical and experimental study of the effect of wollastonite on the physical and mechanical properties of concrete. J Phys Conf Ser, IOP Publishing Ltd, 2021, https://doi.org/10.1088/1742-6596/2094/2/022077.

[61] D. Saranyadevi, P. Sabareeswaran, P. Paramaguru, M. Surya Prakash, Study on mechanical properties of M30 grade concrete with replacement of cement by wollastonite. Lecture Notes in Civil Engineering, Springer Science and Business Media Deutschland GmbH, 2021, pp. 63–70, https://doi.org/10.1007/978-981-15-5001-0_6.

[62] M. Abdel Wahab, I. Abdel Latif, M. Kohail, A. Almasry, The use of Wollastonite to enhance the mechanical properties of mortar mixes, Constr. Build. Mater. 152 (2017) 304–309, https://doi.org/10.1016/j.conbuildmat.2017.07.005.

[63] M. Dutkiewicz, H.E. Yücel, F. Yıldızhan, Evaluation of the performance of different types of fibrous concretes produced by using wollastonite, Materials 15 (2022), https://doi.org/10.3390/ma15196904.

[64] J. Zhang, P. Zhou, J. Liu, J. Yu, New understanding of the difference of photocatalytic activity among anatase, rutile and brookite TiO2, Phys. Chem. Chem. Phys. 16 (2014) 20382–20386, https://doi.org/10.1039/c4cp02201g.

[65] D.R. Eddy, M.D. Permana, L.K. Sakti, G.A.N. Sheha, G.A.N. Solihudin, S. Hidayat, T. Takei, N. Kumada, I. Rahayu, Heterophase polymorph of TiO2 (Anatase, Rutile, Brookite, TiO2 (B)) for Efficient Photocatalyst: Fabrication and Activity, Nanomaterials 13 (2023), https://doi.org/10.3390/nano13040704.

[66] J. Wu, Y. Luo, Z. Qin, Composite-modified nano-TiO2 for the degradation of automobile exhaust in tunnels, Constr. Build. Mater. 408 (2023) 133805, https://doi.org/10.1016/J.CONBUILDMAT.2023.133805.

[67] J. Jiang, X. Dong, H. Wang, F. Wang, Y. Li, Z. Lu, Enhanced mechanical and photocatalytic performance of cement mortar reinforced by nano-TiO2 hydrosol-coated sand, Cem. Concr. Compos 137 (2023) 104906, https://doi.org/10.1016/J.CEMCONCOMP.2022.104906.

[68] L. Yang, A. Hakki, L. Zheng, M.R. Jones, F. Wang, D.E. Macphee, Photocatalytic concrete for NOx abatement: supported TiO2 efficiencies and impacts, Cem. Concr. Res 116 (2019) 57–64, https://doi.org/10.1016/J.CEMCONRES.2018.11.002.

[69] Z. Wang, Q. Yu, F. Gauvin, P. Feng, R. Qianping, H.J.H. Brouwers, Nanodispersed TiO2 hydrosol modified Portland cement paste: the underlying role of hydration on self-cleaning mechanisms, Cem. Concr. Res 136 (2020) 106156, https://doi.org/10.1016/J.CEMCONRES.2020.106156.

[70] D.E. MacPhee, A. Folli, Photocatalytic concretes — The interface between photocatalysis and cement chemistry, Cem. Concr. Res 85 (2016) 48–54, https://doi.org/10.1016/J.CEMCONRES.2016.03.007.

[71] C.M. Aitchison, Y. Zhang, W. Lu, I. McCulloch, Photocatalytic CO2 reduction by topologically matched polymer-polymer heterojunction nanosheets, Faraday Discuss. 250 (2023) 251–262, https://doi.org/10.1039/d3fd00143a.

[72] T. Inoue, A. Fujishima, S. Konishi, K. Honda, Photoelectrocatalytic reduction of carbon dioxide in aqueous suspensions of semiconductor powders, Nature 277 (1979) 637–638, https://doi.org/10.1038/277637a0.

[73] J. Yu, J. Low, W. Xiao, P. Zhou, M. Jaroniec, Enhanced Photocatalytic CO2-Reduction Activity of Anatase TiO2 by Coexposed {001} and {101} Facets, J. Am. Chem. Soc. 136 (2014) 8839–8842, https://doi.org/10.1021/ja5044787.

[74] L. Liu, H. Zhao, J.M. Andino, Y. Li, Photocatalytic CO2 reduction with H2O on TiO2 nanocrystals: comparison of anatase, rutile, and brookite polymorphs and exploration of surface chemistry, ACS Catal. 2 (2012) 1817–1828, https://doi.org/10.1021/cs300273q.

[75] E. Karamian, S. Sharifnia, On the general mechanism of photocatalytic reduction of CO2, J. CO2 Util. 16 (2016) 194–203, https://doi.org/10.1016/J.JCOU.2016.07.004.

[76] M. Tahir, N.S. Amin, Advances in visible light responsive titanium oxide-based photocatalysts for CO2 conversion to hydrocarbon fuels, Energy Convers. Manag 76 (2013) 194–214, https://doi.org/10.1016/J.ENCONMAN.2013.07.046.

[77] H. He, P. Zapol, L.A. Curtiss, Computational screening of dopants for photocatalytic two-electron reduction of CO 2 on anatase (101) surfaces, Energy Environ. Sci. 5 (2012) 6196–6205, https://doi.org/10.1039/c2ee02665a.

[78] J. Mao, T. Peng, X. Zhang, K. Li, L. Zan, Selective methanol production from photocatalytic reduction of CO2 on BiVO4 under visible light irradiation, Catal. Commun. 28 (2012) 38–41, https://doi.org/10.1016/J.CATCOM.2012.08.008.

[79] C.C. Yang, J. Vernimmen, V. Meynen, P. Cool, G. Mul, Mechanistic study of hydrocarbon formation in photocatalytic CO2 reduction over Ti-SBA-15, J. Catal. 284 (2011) 1–8, https://doi.org/10.1016/J.JCAT.2011.08.005.

[80] A. Nikokavoura, C. Trapalis, Alternative photocatalysts to TiO2 for the photocatalytic reduction of CO2, Appl. Surf. Sci. 391 (2017) 149–174, https://doi.org/10.1016/J.APSUSC.2016.06.172.

[81] M.I. Sohail, A.A. Waris, M.A. Ayub, M. Usman, M. Zia ur Rehman, M. Sabir, T. Faiz, Environmental application of nanomaterials: a promise to sustainable future, Compr. Anal. Chem. 87 (2019) 1–54, https://doi.org/10.1016/BS.COAC.2019.10.002.

[82] F. Xi, S.J. Davis, P. Ciais, D. Crawford-Brown, D. Guan, C. Pade, T. Shi, M. Syddall, J. Lv, L. Ji, L. Bing, J. Wang, W. Wei, K.-H. Yang, B. Lagerblad, I. Galan, C. Andrade, Y. Zhang, Z. Liu, Substantial global carbon uptake by cement carbonation, Nat. Geosci. 9 (2016) 880–883, https://doi.org/10.1038/ngeo2840.

[83] F. Althoey, W.S. Ansari, M. Sufian, A.F. Deifalla, Advancements in low-carbon concrete as a construction material for the sustainable built environment, Dev. Built Environ. 16 (2023) 100284, https://doi.org/10.1016/J.DIBE.2023.100284.

[84] Y. Wei, H. Meng, Q. Wu, X. Bai, Y. Zhang, TiO2-based photocatalytic building material for air purification in sustainable and low-carbon cities: a review, Catalysts 13 (2023), https://doi.org/10.3390/catal13121466.

[85] M. Hu, S. Li, X. Chen, S. Sui, L. Jin, Y. Geng, J. Jiang, Influences of titanium dioxide nanoparticles on regulation of crystalline growth and early carbonation of cementitious composites, Ceram. Int 49 (2023) 37366–37376, https://doi.org/10.1016/J.CERAMINT.2023.09.061.

[86] C. Moro, V. Francioso, M. Velay-Lizancos, Impact of nano-TiO2 addition on the reduction of net CO2 emissions of cement pastes after CO2 curing, Cem. Concr. Compos 123 (2021) 104160, https://doi.org/10.1016/J.CEMCONCOMP.2021.104160.

[87] C. Moro, V. Francioso, M. Velay-Lizancos, Modification of CO2 capture and pore structure of hardened cement paste made with nano-TiO2 addition: Influence of water-to-cement ratio and CO2 exposure age, Constr. Build. Mater. 275 (2021) 122131, https://doi.org/10.1016/J.CONBUILDMAT.2020.122131.

[88] J. Xie, F. Yang, N. Tan, W. Wang, W. Wang, Z. Wang, Calcium sulphoaluminate cement from solid waste with nano-TiO2 addition for high-efficiency CO2 capture, Constr. Build. Mater. 367 (2023) 130267, https://doi.org/10.1016/J.CONBUILDMAT.2022.130267.

[89] M. Saillio, V. Baroghel-Bouny, S. Pradelle, M. Bertin, J. Vincent, J.B. d'Espinose de Lacaillerie, Effect of supplementary cementitious materials on carbonation of cement pastes, Cem. Concr. Res 142 (2021) 106358, https://doi.org/10.1016/J.CEMCONRES.2021.106358.

[90] K. Chen, W.T. Lin, W. Liu, Microstructures and mechanical properties of sodium-silicate-activated slag/co-fired fly ash cementless composites, J. Clean. Prod. 277 (2020) 124025, https://doi.org/10.1016/J.JCLEPRO.2020.124025.

[91] K. Chen, W.T. Lin, W. Liu, Effect of NaOH concentration on properties and microstructure of a novel reactive ultra-fine fly ash geopolymer, Adv. Powder Technol. 32 (2021) 2929–2939, https://doi.org/10.1016/J.APT.2021.06.008.

[92] M. Lopez-Arias, C. Moro, V. Francioso, H.H. Elgaali, M. Velay-Lizancos, Effect of nanomodification of cement pastes on the CO2 uptake rate, Constr. Build. Mater. 404 (2023) 133165, https://doi.org/10.1016/J.CONBUILDMAT.2023.133165.

[93] A.L. Castro, M.R. Nunes, A.P. Carvalho, F.M. Costa, M.H. Florêncio, Synthesis of anatase TiO2 nanoparticles with high temperature stability and photocatalytic activity, Solid State Sci. 10 (2008) 602–606, https://doi.org/10.1016/J.SOLIDSTATESCIENCES.2007.10.012.

[94] M.M. Viana, V.F. Soares, N.D.S. Mohallem, Synthesis and characterization of TiO2 nanoparticles, Ceram. Int 36 (2010) 2047–2053, https://doi.org/10.1016/J.CERAMINT.2010.04.006.
[95] A. Kumar, R. Wang, K.A. Orton, K.M. Van Allsburg, C. Mukarakate, E.C. Wegener, Q. Wu, S.E. Habas, K.Z. Pupek, J.A. Libera, F.G. Baddour, Synthesis, performance evaluation, and economic assessment of tailored Pt/TiO2 catalysts for selective biomass vapour upgrading via a scalable flame spray pyrolysis route, Catal. Sci. Technol. 13 (2023) 4941–4954, https://doi.org/10.1039/D3CY00550J.
[96] J. Wang, Z. Wang, W. Wang, Y. Wang, X. Hu, J. Liu, X. Gong, W. Miao, L. Ding, X. Li, J. Tang, Synthesis, modification and application of titanium dioxide nanoparticles: a review, Nanoscale 14 (2022) 6709–6734, https://doi.org/10.1039/D1NR08349J.
[97] F. Hamidi, F. Aslani, Tio2-based photocatalytic cementitious composites: Materials, properties, influential parameters, and assessment techniques, Nanomaterials 9 (2019), https://doi.org/10.3390/nano9101444.
[98] A.M. Castro-Hoyos, M.A. Rojas Manzano, A. Maury-Ramírez, Challenges and Opportunities of Using Titanium Dioxide Photocatalysis on Cement-Based Materials, Coatings 12 (2022), https://doi.org/10.3390/coatings12070968.
[99] Y. Wei, Q. Wu, H. Meng, Y. Zhang, C. Cao, Recent advances in photocatalytic self-cleaning performances of TiO2-based building materials, RSC Adv. 13 (2023) 20584–20597, https://doi.org/10.1039/d2ra07839b.
[100] R. Kumar, G. Chandgude, P. Gond, A. Shete, S. Jadhav, A. Professor APCOER, S. of APCOER, Titanium dioxide-an experimental study of self-cleaning concrete (M25 Grande), Int. J. Creat. Res. Thoughts 11 (2023) 2320–2882. ⟨www.ijcrt.org⟩.
[101] R. Kumar, G. Chandgude, P. Gond, A. Shete, S. Jadhav, A. Professor APCOER, S. of APCOER, A review on titanium dioxide-a study self-cleaning concrete, Int. J. Creat. Res. Thoughts 11 (2023) 2320–2882. ⟨www.ijcrt.org⟩.
[102] G.F. Huseien, A Review on Concrete Composites Modified with Nanoparticles, J. Compos. Sci. 7 (2023), https://doi.org/10.3390/jcs7020067.
[103] J. Chen, S.C. Kou, C.S. Poon, Hydration and properties of nano-TiO2 blended cement composites, Cem. Concr. Compos 34 (2012) 642–649, https://doi.org/10.1016/J.CEMCONCOMP.2012.02.009.
[104] J. Sun, X. Cao, Z. Xu, Z. Yu, Y. Zhang, G. Hou, X. Shen, Contribution of core/shell TiO2@SiO2 nanoparticles to the hydration of Portland cement, Constr. Build. Mater. 233 (2020) 117127, https://doi.org/10.1016/J.CONBUILDMAT.2019.117127.
[105] G. dos S. Batista, A.S. Takimi, E.M. da Costa, Hardened oil well cement paste modified with TiO2@SiO2 nanoparticles: Physical and chemical properties, Constr. Build. Mater. 367 (2023) 130282, https://doi.org/10.1016/J.CONBUILDMAT.2022.130282.
[106] F. Yang, J. Xie, W. Wang, W. Wang, Z. Wang, The role of nano-TiO2 on the mechanical properties and hydration behavior of C2S, C3S and C4A3$\bar{S}$, Constr. Build. Mater. 388 (2023) 131558 https://doi.org/10.1016/J.CONBUILDMAT.2023.131558.
[107] J. Sun, L. Tian, Z. Yu, Y. Zhang, C. Li, G. Hou, X. Shen, Studies on the size effects of nano-TiO2 on Portland cement hydration with different water to solid ratios, Constr. Build. Mater. 259 (2020) 120390, https://doi.org/10.1016/J.CONBUILDMAT.2020.120390.
[108] T. Meng, Y. Yu, X. Qian, S. Zhan, K. Qian, Effect of nano-TiO2 on the mechanical properties of cement mortar, Constr. Build. Mater. 29 (2012) 241–245, https://doi.org/10.1016/J.CONBUILDMAT.2011.10.047.
[109] B.Y. Lee, A.R. Jayapalan, K.E. Kurtis, Effects of nano-TiO2 on properties of cement-based materials, Mag. Concr. Res. 65 (2013) 1293–1302, https://doi.org/10.1680/macr.13.00131.
[110] L. Wang, H. Zhang, Y. Gao, Effect of TiO_2 Nanoparticles on Physical and Mechanical Properties of Cement at Low Temperatures, Adv. Mater. Sci. Eng. 2018 (2018) 8934689, https://doi.org/10.1155/2018/8934689.
[111] M.J. Kadhim, R.S. Al-Jadiri, M.A.A.L. Wahab Ali, Study the Effect of Addition nano-TiO2 by Dispersion Method on the Some Mechanical Properties and Durability of Cement Mortar, IOP Conf. Ser. Mater. Sci. Eng. 518 (2019) 032027, https://doi.org/10.1088/1757-899X/518/3/032027.
[112] M. Liu, H. Xiao, R. Liu, J. Liu, Dispersion characteristics of various contents of nano-TiO2 and its effect on the properties of cement-based composite, Struct. Concr. 19 (2018) 1301–1308, https://doi.org/10.1002/suco.201800110.
[113] S.S. Pathak, G.R. Vesmawala, Effect of nano TiO2 on mechanical properties and microstructure of concrete, Mater. Today Proc. 65 (2022) 1915–1921, https://doi.org/10.1016/J.MATPR.2022.05.161.
[114] S.D.A. Selvasofia, E. Sarojini, G. Moulica, S. Thomas, M. Tharani, P. T. Saravanakumar, P.M. Kumar, Study on the mechanical properties of the nanoconcrete using nano-TiO2 and nanoclay, Mater. Today Proc. 50 (2022) 1319–1325, https://doi.org/10.1016/J.MATPR.2021.08.242.
[115] J. Ren, Y. Lai, J. Gao, Exploring the influence of SiO2 and TiO2 nanoparticles on the mechanical properties of concrete, Constr. Build. Mater. 175 (2018) 277–285, https://doi.org/10.1016/J.CONBUILDMAT.2018.04.181.
[116] J.V. Staub de Melo, G. Trichês, Study of the influence of nano-TiO2 on the properties of Portland cement concrete for application on road surfaces, Road. Mater. Pavement Des. 19 (2018) 1011–1026, https://doi.org/10.1080/14680629.2017.1285811.
[117] K. Behfarnia, A. Keivan, THE EFFECTS OF TiO2 AND ZnO NANOPARTICLES ON PHYSICAL AND MECHANICAL PROPERTIES OF NORMAL CONCRETE, 2013. ⟨www.SID.ir⟩.
[118] S.G. Garima Rawat, Yogesh Iyer Murthy, , Durability Aspects of Concrete Containing Nano- Titanium Dioxide, Acids Mater. J. 120 (2023) 25–35, https://doi.org/10.14359/51738490.
[119] R. Kurihara, I. Maruyama, Impact of TiO2 nanoparticles on drying shrinkage of hardened cement paste, J. Adv. Concr. Technol. 16 (2018) 272–281, https://doi.org/10.3151/jact.16.272.
[120] Q. Liu, Q. Jiang, M. Huang, J. Xin, P. Chen, The fresh and hardened properties of 3D printing cement-base materials with self-cleaning nano-TiO2:An exploratory study, J. Clean. Prod. 379 (2022) 134804, https://doi.org/10.1016/J.JCLEPRO.2022.134804.
[121] M. Atiq Orakzai, Hybrid effect of nano-alumina and nano-titanium dioxide on Mechanical properties of concrete, Case Stud. Constr. Mater. 14 (2021) e00483, https://doi.org/10.1016/J.CSCM.2020.E00483.
[122] K.P. Bautista-Gutierrez, A.L. Herrera-May, J.M. Santamaría-López, A. Honorato-Moreno, S.A. Zamora-Castro, Recent progress in nanomaterials for modern concrete infrastructure: Advantages and challenges, Materials 12 (2019), https://doi.org/10.3390/ma12213548.
[123] A.K. Geim, K.S. Novoselov, The rise of graphene, Nat. Mater. 6 (2007) 183–191, https://doi.org/10.1038/nmat1849.
[124] M. Han, Y. Muhammad, Y. Wei, Z. Zhu, J. Huang, J. Li, A review on the development and application of graphene based materials for the fabrication of modified asphalt and cement, Constr. Build. Mater. 285 (2021) 122885, https://doi.org/10.1016/J.CONBUILDMAT.2021.122885.
[125] Z. Zhen, H. Zhu, Structure and Properties of Graphene, Graph.: Fabr., Charact., Prop. Appl. (2018) 1–12, https://doi.org/10.1016/B978-0-12-812651-6.00001-X.
[126] J.M. Macleod, F. Rosei, Molecular self-assembly on graphene, Small 10 (2014) 1038–1049, https://doi.org/10.1002/smll.201301982.
[127] Z. Li, L. Deng, I.A. Kinloch, R.J. Young, Raman spectroscopy of carbon materials and their composites: Graphene, nanotubes and fibres, Prog. Mater. Sci. 135 (2023) 101089, https://doi.org/10.1016/j.pmatsci.2023.101089.
[128] R. Singh, M.S. Samuel, M. Ravikumar, S. Ethiraj, M. Kumar, Graphene materials in pollution trace detection and environmental improvement, Environ. Res 243 (2024) 117830, https://doi.org/10.1016/J.ENVRES.2023.117830.
[129] I.N. Rolemberg Prudente, H. Campos dos Santos, C. da Cunha Nascimento, I. de, F. Gimenez, G.R. Santana Andrade, W. Acchar, L. Silva Barreto, Anti-biofouling properties of graphene-based nanoadditives in cementitious mortars, J. Build. Eng. 74 (2023) 106837, https://doi.org/10.1016/J.JOBE.2023.106837.
[130] B.C. Brodie, XXIII.—Researches on the atomic weight of graphite, Q. J. Chem. Soc. Lond. 12 (1860) 261–268, https://doi.org/10.1039/QJ8601200261.
[131] D.R. Dreyer, R.S. Ruoff, C.W. Bielawski, From conception to realization: An historial account of graphene and some perspectives for its future, Angew. Chem. - Int. Ed. 49 (2010) 9336–9344, https://doi.org/10.1002/anie.201003024.
[132] S.N. Alam, N. Sharma, L. Kumar, Synthesis of graphene oxide (GO) by modified hummers method and its thermal reduction to obtain reduced graphene oxide (rGO)*, Graphene 06 (2017) 1–18, https://doi.org/10.4236/graphene.2017.61001.
[133] S. Eigler, A. Hirsch, Chemistry with graphene and graphene oxide - challenges for synthetic chemists, Angew. Chem. - Int. Ed. 53 (2014) 7720–7738, https://doi.org/10.1002/anie.201402780.
[134] A. Avornyo, C.V. Chrysikopoulos, Applications of graphene oxide (GO) in oily wastewater treatment: recent developments, challenges, and opportunities, J. Environ. Manag. 353 (2024) 120178, https://doi.org/10.1016/J.JENVMAN.2024.120178.
[135] D.R. Dreyer, R.S. Ruoff, C.W. Bielawski, From Conception to Realization: An Historial Account of Graphene and Some Perspectives for Its Future, Angew. Chem. Int. Ed. 49 (2010) 9336–9344, https://doi.org/10.1002/anie.201003024.
[136] N.M.S. Hidayah, W.-W. Liu, C.-W. Lai, N.Z. Noriman, C.-S. Khe, U. Hashim, H. C. Lee, Comparison on graphite, graphene oxide and reduced graphene oxide: synthesis and characterization, AIP Conf. Proc. 1892 (2017) 150002, https://doi.org/10.1063/1.5005764.
[137] H. Yang, H. Hu, Z. Ni, C.K. Poh, C. Cong, J. Lin, T. Yu, Comparison of surface-enhanced Raman scattering on graphene oxide, reduced graphene oxide and graphene surfaces, Carbon N. Y 62 (2013) 422–429, https://doi.org/10.1016/J.CARBON.2013.06.027.
[138] B.E. Arango Hoyos, H.F. Osorio, E.K. Valencia Gómez, J. Guerrero Sánchez, A. P. Del Canto Palominos, F.A. Larrain, J.J. Prías Barragán, Exploring the capture and desorption of CO2 on graphene oxide foams supported by computational calculations, Sci. Rep. 13 (2023) 14476, https://doi.org/10.1038/s41598-023-41683-4.
[139] S.Y. Lee, S.J. Park, A review on solid adsorbents for carbon dioxide capture, J. Ind. Eng. Chem. 23 (2015) 1–11, https://doi.org/10.1016/J.JIEC.2014.09.001.
[140] S. Gadipelli, Z.X. Guo, Graphene-based materials: Synthesis and gas sorption, storage and separation, Prog. Mater. Sci. 69 (2015) 1–60, https://doi.org/10.1016/J.PMATSCI.2014.10.004.
[141] L.Y. Meng, S.J. Park, Effect of exfoliation temperature on carbon dioxide capture of graphene nanoplates, J. Colloid Interface Sci. 386 (2012) 285–290, https://doi.org/10.1016/J.JCIS.2012.07.025.
[142] A. Samanta, A. Zhao, G.K.H. Shimizu, P. Sarkar, R. Gupta, Post-Combustion CO2 Capture Using Solid Sorbents: A Review, Ind. Eng. Chem. Res 51 (2012) 1438–1463, https://doi.org/10.1021/ie200686q.
[143] J.P. Severinghaus, M.O. Battle, Fractionation of gases in polar ice during bubble close-off: New constraints from firn air Ne, Kr and Xe observations, Earth Planet Sci. Lett. 244 (2006) 474–500, https://doi.org/10.1016/J.EPSL.2006.01.032.
[144] G. Mishra, A. Warda, S.P. Shah, Carbon sequestration in graphene oxide modified cementitious system, J. Build. Eng. 62 (2022) 105356, https://doi.org/10.1016/J.JOBE.2022.105356.

[145] A. Bagheri, E. Negahban, A. Asad, H.A. Abbasi, S.M. Raza, Graphene oxide-incorporated cementitious composites: a thorough investigation, Mater. Adv. 3 (2022) 9040–9051, https://doi.org/10.1039/d2ma00169a.
[146] A. Mohammed, J.G. Sanjayan, A. Nazari, N.T.K. Al-Saadi, The role of graphene oxide in limited long-term carbonation of cement-based matrix, Constr. Build. Mater. 168 (2018) 858–866, https://doi.org/10.1016/J.CONBUILDMAT.2018.02.082.
[147] A. Shah, H. Singh, P. Prajongtat, M.C. Joshi, S. Hannongbua, N. Chattham, Y. K. Kim, S. Kumar, D.P. Singh, Scalable production of reduced graphene oxide via biowaste valorisation: an efficient oxygen reduction reaction towards metal-free electrocatalysis, N. J. Chem. 47 (2022) 1360–1370, https://doi.org/10.1039/d2nj05082j.
[148] Z. Benzait, P. Chen, L. Trabzon, Enhanced synthesis method of graphene oxide, Nanoscale Adv. 3 (2021) 223–230, https://doi.org/10.1039/d0na00706d.
[149] Letizia Diamante, Large scale production of graphene oxide and its derivatives, Graph. Flagship (2021).
[150] Y. Gao, G. Li, W. Chen, X. Shi, C. Gong, Q. Shao, Y. Liu, Graphene oxide coated fly ash for reinforcing dynamic tensile behaviours of cementitious composites, Constr. Build. Mater. 411 (2024) 134289, https://doi.org/10.1016/J.CONBUILDMAT.2023.134289.
[151] C.M. Damian, M.I. Necolau, I. Neblea, E. Vasile, H. Iovu, Synergistic effect of graphene oxide functionalized with SiO2 nanostructures in the epoxy nanocomposites, Appl. Surf. Sci. 507 (2020) 145046, https://doi.org/10.1016/J.APSUSC.2019.145046.
[152] I. Abdulkadir, B.S. Mohammed, A.M. Al-Yacouby, E.L. Woen, T. Tafsirojjaman, Tailoring an engineered cementitious composite with enhanced mechanical performance at ambient and elevated temperatures using graphene oxide and crumb rubber, J. Mater. Res. Technol. 28 (2024) 4508–4530, https://doi.org/10.1016/J.JMRT.2024.01.059.
[153] K. Ghouchani, H. Abbasi, E. Najaf, Some mechanical properties and microstructure of cementitious nanocomposites containing nano-SiO2 and graphene oxide nanosheets, Case Stud. Constr. Mater. 17 (2022) e01482, https://doi.org/10.1016/J.CSCM.2022.E01482.
[154] P. Li, J. Liu, S. Im, S. Cho, S. Bae, Graphene nanoribbons as a novel nanofiller for enhancing the mechanical and electrical properties of cementitious composites, Constr. Build. Mater. 406 (2023) 133273, https://doi.org/10.1016/J.CONBUILDMAT.2023.133273.
[155] J. Ying, Z. Xie, B. Chen, Z. Jiang, Z. Tian, J. Xiao, Multi-scale experimental studies on mechanical properties of three-dimensional porous graphene cementitious composite, Cem. Concr. Compos 147 (2024) 105412, https://doi.org/10.1016/J.CEMCONCOMP.2023.105412.
[156] H. Qin, W. Wei, Y. Hang Hu, Synergistic effect of graphene-oxide-doping and microwave-curing on mechanical strength of cement, J. Phys. Chem. Solids 103 (2017) 67–72, https://doi.org/10.1016/J.JPCS.2016.12.009.
[157] Q. Wang, J. Wang, C.X. Lu, B.W. Liu, K. Zhang, C.Z. Li, Influence of graphene oxide additions on the microstructure and mechanical strength of cement, N. Carbon Mater. 30 (2015) 349–356, https://doi.org/10.1016/S1872-5805(15)60194-9.
[158] S. Lv, Y. Ma, C. Qiu, T. Sun, J. Liu, Q. Zhou, Effect of graphene oxide nanosheets of microstructure and mechanical properties of cement composites, Constr. Build. Mater. 49 (2013) 121–127, https://doi.org/10.1016/J.CONBUILDMAT.2013.08.022.
[159] M.M. Mokhtar, S.A. Abo-El-Enein, M.Y. Hassaan, M.S. Morsy, M.H. Khalil, Mechanical performance, pore structure and micro-structural characteristics of graphene oxide nano platelets reinforced cement, Constr. Build. Mater. 138 (2017) 333–339, https://doi.org/10.1016/J.CONBUILDMAT.2017.02.021.
[160] S.J. Lee, S.H. Jeong, D.U. Kim, J.P. Won, Effects of graphene oxide on pore structure and mechanical properties of cementitious composites, Compos Struct. 234 (2020) 111709, https://doi.org/10.1016/J.COMPSTRUCT.2019.111709.
[161] M.M. Rashwan, M.F.M. Fahmy, A. Abdullah, M. Hesham, EFFECT OF GRAPHENE OXIDE ON THE MECHANICAL STRENGTH AND MICROSTRUCTURE OF CEMENTITIOUS MATERIALS, Jes. J. Eng. Sci. 48 (2020) 32–43, https://doi.org/10.21608/jesaun.2020.109052.
[162] P.V.R.K. Reddy, D.R. Prasad, Investigation on the impact of graphene oxide on microstructure and mechanical behaviour of concrete, J. Build. Pathol. Rehabil. 7 (2022) 30, https://doi.org/10.1007/s41024-022-00166-1.
[163] S.C. Devi, R.A. Khan, Effect of graphene oxide on mechanical and durability performance of concrete, J. Build. Eng. 27 (2020) 101007, https://doi.org/10.1016/J.JOBE.2019.101007.
[164] S. Du, Z. Tang, J. Zhong, Y. Ge, X. Shi, Effect of admixing graphene oxide on abrasion resistance of ordinary portland cement concrete, AIP Adv. 9 (2019) 105110, https://doi.org/10.1063/1.5124388.
[165] Z. Lu, D. Hou, H. Ma, T. Fan, Z. Li, Effects of graphene oxide on the properties and microstructures of the magnesium potassium phosphate cement paste, Constr. Build. Mater. 119 (2016) 107–112, https://doi.org/10.1016/J.CONBUILDMAT.2016.05.060.
[166] Z. Pan, L. He, L. Qiu, A.H. Korayem, G. Li, J.W. Zhu, F. Collins, D. Li, W.H. Duan, M.C. Wang, Mechanical properties and microstructure of a graphene oxide–cement composite, Cem. Concr. Compos 58 (2015) 140–147, https://doi.org/10.1016/J.CEMCONCOMP.2015.02.001.
[167] M. Devasena, J. Karthikeyan, M.E. Student, INVESTIGATION ON STRENGTH PROPERTIES OF GRAPHENE OXIDE CONCRETE, Int. J. Eng. Sci. Invent. Res. Dev. I (2015) 307. ⟨www.ijesird.com⟩.
[168] H. Chu, Y. Zhang, F. Wang, T. Feng, L. Wang, D. Wang, Effect of graphene oxide on mechanical properties and durability of ultra-high-performance concrete prepared from recycled sand, Nanomaterials 10 (2020) 1–17, https://doi.org/10.3390/nano10091718.
[169] L. Lu, D. Ouyang, Properties of cement mortar and ultra-high strength concrete incorporating graphene oxide nanosheets, Nanomaterials 7 (2017), https://doi.org/10.3390/nano7070187.
[170] L. Yeke, Z. Yu, Effect of graphene oxide on mechanical properties of UHPC and analysis of micro-control mechanism, Mater. Res Express 8 (2021), https://doi.org/10.1088/2053-1591/ac2015.
[171] L. Yu, S. Bai, X. Guan, Effect of graphene oxide on microstructure and micromechanical property of ultra-high performance concrete, Cem. Concr. Compos 138 (2023) 104964, https://doi.org/10.1016/J.CEMCONCOMP.2023.104964.
[172] X. Hong, J.C. Lee, B. Qian, Mechanical Properties and Microstructure of High-Strength Lightweight Concrete Incorporating Graphene Oxide, Nanomaterials 12 (2022) 833, https://doi.org/10.3390/nano12050833.
[173] H. Zeng, S. Qu, Y. Qin, Microstructure and transport properties of cement-based material enhanced by graphene oxide, Mag. Concr. Res. 73 (2021) 1011–1024, https://doi.org/10.1680/jmacr.19.00558.
[174] Z. Chen, Y. Xu, J. Hua, X. Wang, L. Huang, X. Zhou, Mechanical properties and shrinkage behavior of concrete-containing graphene-oxide nanosheets, Materials 13 (2020), https://doi.org/10.3390/ma13030590.
[175] D. Udumulla, T. Ginigaddara, T. Jayasinghe, P. Mendis, S. Baduge, Effect of Graphene Oxide Nanomaterials on the Durability of Concrete: A Review on Mechanisms, Provisions, Challenges, and Future Prospects, Materials 17 (2024), https://doi.org/10.3390/ma17102411.
[176] A. Promraksa, N. Rakmak, Biochar production from palm oil mill residues and application of the biochar to adsorb carbon dioxide, Heliyon 6 (2020), https://doi.org/10.1016/j.heliyon.2020.e04019.
[177] P.D. Dissanayake, S.W. Choi, A.D. Igalavithana, X. Yang, D.C.W. Tsang, C. H. Wang, H.W. Kua, K.B. Lee, Y.S. Ok, Sustainable gasification biochar as a high efficiency adsorbent for CO2 capture: A facile method to designer biochar fabrication, Renew. Sustain. Energy Rev. 124 (2020) 109785, https://doi.org/10.1016/J.RSER.2020.109785.
[178] Y.J. Zhou, K.I. Zheng, G. Targher, C.D. Byrne, M.H. Zheng, Non-invasive diagnosis of non-alcoholic steatohepatitis and liver fibrosis, Lancet Gastroenterol. Hepatol. 6 (2021) 9–10, https://doi.org/10.1016/S2468-1253(20)30308-3.
[179] A.D. Igalavithana, S.W. Choi, P.D. Dissanayake, J. Shang, C.H. Wang, X. Yang, S. Kim, D.C.W. Tsang, K.B. Lee, Y.S. Ok, Gasification biochar from biowaste (food waste and wood waste) for effective CO2 adsorption, J. Hazard Mater. 391 (2020) 121147, https://doi.org/10.1016/J.JHAZMAT.2019.121147.
[180] J. Liu, G. Liu, W. Zhang, Z. Li, H. Jin, F. Xing, A new approach to CO2 capture and sequestration: A novel carbon capture artificial aggregates made from biochar and municipal waste incineration bottom ash, Constr. Build. Mater. 398 (2023) 132472, https://doi.org/10.1016/J.CONBUILDMAT.2023.132472.
[181] S. Gupta, H.W. Kua, C.Y. Low, Use of biochar as carbon sequestering additive in cement mortar, Cem. Concr. Compos 87 (2018) 110–129, https://doi.org/10.1016/J.CEMCONCOMP.2017.12.009.
[182] S. Fang, L. Zhao, G. Rong, B. Chen, X. Xu, H. Qiu, X. Cao, Converting coastal silt into subgrade soil with biochar as reinforcing agent, CO2 adsorbent, and carbon sequestrating material, J. Environ. Manag. 344 (2023) 118394, https://doi.org/10.1016/J.JENVMAN.2023.118394.
[183] K.G. Roberts, B.A. Gloy, S. Joseph, N.R. Scott, J. Lehmann, Life Cycle Assessment of Biochar Systems: Estimating the Energetic, Economic, and Climate Change Potential, Environ. Sci. Technol. 44 (2010) 827–833, https://doi.org/10.1021/es902266r.
[184] A.Y. Elnour, A.A. Alghyamah, H.M. Shaikh, A.M. Poulose, S.M. Al-Zahrani, A. Anis, M.I. Al-Wabel, Effect of pyrolysis temperature on biochar microstructural evolution, physicochemical characteristics, and its influence on biochar/polypropylene composites, Appl. Sci. (Switz.) 9 (2019), https://doi.org/10.3390/app9061149.
[185] S. Li, D. Tasnady, Biochar for Soil Carbon Sequestration: Current Knowledge, Mechanisms, and Future Perspectives, C. -J. Carbon Res. 9 (2023), https://doi.org/10.3390/c9030067.
[186] A. Al-Rumaihi, M. Alherbawi, G. Mckay, H. Mackey, P. Parthasarathy, T. Al-Ansari, Assessing plastic and biomass-based biochar's potential for carbon sequestration: an energy-water-environment approach, Front. Sustain. 4 (2023), https://doi.org/10.3389/frsus.2023.1200094.
[187] K.A. Adegoke, K.O. Oyedotun, J.O. Ighalo, J.F. Amaku, C. Olisah, A.O. Adeola, K. O. Iwuozor, K.G. Akpomie, J. Conradie, Cellulose derivatives and cellulose-metal-organic frameworks for CO2 adsorption and separation, J. CO2 Util. 64 (2022) 102163, https://doi.org/10.1016/J.JCOU.2022.102163.
[188] M. Zhang, T. Xu, Q. Zhao, K. Liu, D. Liang, C. Si, Cellulose-based materials for carbon capture and conversion, Carbon Capture Sci. Technol. 10 (2024) 100157, https://doi.org/10.1016/J.CCST.2023.100157.
[189] W. Luo, W. Lu, Q. Xiang, L. Zhan, X. Yang, H. Jiang, C. Xu, H. He, Engineering a photothermal responsive cellulose carbon capture material for solar-driven CO2 desorption, Chem. Eng. J. 489 (2024) 151144, https://doi.org/10.1016/J.CEJ.2024.151144.
[190] B. Liu, H. Zeng, S. Wang, Y. Pang, C. Qin, C. Liang, C. Huang, S. Yao, Efficient degradation of lignin by chlorine dioxide and preparation of high purity pulp fiber, Int J. Biol. Macromol. 266 (2024) 131003, https://doi.org/10.1016/J.IJBIOMAC.2024.131003.
[191] L. Qu, M. Tian, X. Guo, N. Pan, X. Zhang, S. Zhu, Preparation and Properties of Natural Cellulose Fibres from Broussonetia papyrifera (L.) Vent. Bast. FIBRES & TEXTILES in Eastern, 2014..

[192] J. Liu, G. Liu, W. Zhang, Z. Li, F. Xing, L. Tang, Application potential analysis of biochar as a carbon capture material in cementitious composites: A review, Constr. Build. Mater. 350 (2022) 128715, https://doi.org/10.1016/J.CONBUILDMAT.2022.128715.
[193] A.M.N. Aman, A. Selvarajoo, T.L. Lau, W.H. Chen, Biochar as cement replacement to enhance concrete composite properties: a review, Energy 15 (2022), https://doi.org/10.3390/en15207662.
[194] S. Song, Z. Liu, G. Liu, X. Cui, J. Sun, Application of biochar cement-based materials for carbon sequestration, Constr. Build. Mater. 405 (2023) 133373, https://doi.org/10.1016/J.CONBUILDMAT.2023.133373.
[195] S. Gupta, H.W. Kua, C.Y. Low, Use of biochar as carbon sequestering additive in cement mortar, Cem. Concr. Compos 87 (2018) 110–129, https://doi.org/10.1016/J.CEMCONCOMP.2017.12.009.
[196] S. Praneeth, R. Guo, T. Wang, B.K. Dubey, A.K. Sarmah, Accelerated carbonation of biochar reinforced cement-fly ash composites: Enhancing and sequestering CO2 in building materials, Constr. Build. Mater. 244 (2020) 118363, https://doi.org/10.1016/J.CONBUILDMAT.2020.118363.
[197] Z. He, Y. Jia, S. Wang, M. Mahoutian, Y. Shao, Maximizing CO2 sequestration in cement-bonded fiberboards through carbonation curing, Constr. Build. Mater. 213 (2019) 51–60, https://doi.org/10.1016/J.CONBUILDMAT.2019.04.042.
[198] B. Wu, Y.W. Chung, Y. Tang, J. Qiu, Effect of internal moisture content (IMC) on the CO2 sequestration efficiency of hollow natural fiber (HNF)-reinforced reactive magnesia cement (RMC) composites, Constr. Build. Mater. 428 (2024) 136339, https://doi.org/10.1016/J.CONBUILDMAT.2024.136339.
[199] O. Zaid, F. Alsharari, M. Ahmed, Utilization of engineered biochar as a binder in carbon negative cement-based composites: A review, Constr. Build. Mater. 417 (2024) 135246, https://doi.org/10.1016/J.CONBUILDMAT.2024.135246.
[200] S. Gupta, A. Kashani, Utilization of biochar from unwashed peanut shell in cementitious building materials – effect on early age properties and environmental benefits, Fuel Process. Technol. 218 (2021) 106841, https://doi.org/10.1016/J.FUPROC.2021.106841.
[201] S. Gupta, A. Kashani, A.H. Mahmood, T. Han, Carbon sequestration in cementitious composites using biochar and fly ash – Effect on mechanical and durability properties, Constr. Build. Mater. 291 (2021) 123363, https://doi.org/10.1016/J.CONBUILDMAT.2021.123363.
[202] M. Sisman, E. Teomete, J. Yanik, U. Malayoglu, The effect of nano-biochar produced from various raw materials on flow and mechanical properties of mortar, Constr. Build. Mater. 416 (2024) 135040, https://doi.org/10.1016/J.CONBUILDMAT.2024.135040.
[203] D. Ali, R. Agarwal, M. Hanifa, P. Rawat, R. Paswan, D. Rai, I. Tyagi, B. Srinivasarao Naik, A. Pippal, Thermo-physical properties and microstructural behaviour of biochar-incorporated cementitious material, J. Build. Eng. 64 (2023) 105695, https://doi.org/10.1016/J.JOBE.2022.105695.
[204] G. Mishra, P.A. Danoglidis, S.P. Shah, M.S. Konsta-Gdoutos, Carbon capture and storage potential of biochar-enriched cementitious systems, Cem. Concr. Compos 140 (2023) 105078, https://doi.org/10.1016/J.CEMCONCOMP.2023.105078.
[205] W. Liu, K. Li, S. Xu, Utilizing bamboo biochar in cement mortar as a bio-modifier to improve the compressive strength and crack-resistance fracture ability, Constr. Build. Mater. 327 (2022) 126917, https://doi.org/10.1016/J.CONBUILDMAT.2022.126917.
[206] M. Sisman, E. Teomete, J. Yanik, U. Malayoglu, The effect of nano-biochar produced from various raw materials on flow and mechanical properties of mortar, Constr. Build. Mater. 416 (2024) 135040, https://doi.org/10.1016/J.CONBUILDMAT.2024.135040.
[207] A. Akhtar, A.K. Sarmah, Novel biochar-concrete composites: manufacturing, characterization and evaluation of the mechanical properties, Sci. Total Environ. 616–617 (2018) 408–416, https://doi.org/10.1016/J.SCITOTENV.2017.10.319.
[208] A. Aneja, R.L. Sharma, H. Singh, Mechanical and durability properties of biochar concrete, Mater. Today Proc. 65 (2022) 3724–3730, https://doi.org/10.1016/J.MATPR.2022.06.371.
[209] M. Li, S. Zhou, X. Guo, Effects of alkali-treated bamboo fibers on the morphology and mechanical properties of oil well cement, Constr. Build. Mater. 150 (2017) 619–625, https://doi.org/10.1016/J.CONBUILDMAT.2017.05.215.
[210] M.M. Jaberizadeh, P.A. Danoglidis, S.P. Shah, M.S. Konsta-Gdoutos, Eco-efficient cementitious composites using waste cellulose fibers: Effects on autogenous shrinkage, strength and energy absorption capacity, Constr. Build. Mater. 408 (2023) 133504, https://doi.org/10.1016/J.CONBUILDMAT.2023.133504.
[211] G.W. Lee, Y.C. Choi, Effect of abaca natural fiber on the setting behavior and autogenous shrinkage of cement composite, J. Build. Eng. 56 (2022) 104719, https://doi.org/10.1016/J.JOBE.2022.104719.
[212] H. Singh, R. Gupta, Influence of cellulose fiber addition on self-healing and water permeability of concrete, Case Stud. Constr. Mater. 12 (2020) e00324, https://doi.org/10.1016/J.CSCM.2019.E00324.
[213] H. Jamshaid, R.K. Mishra, A. Raza, U. Hussain, M.L. Rahman, S. Nazari, V. Chandan, M. Muller, R. Choteborsky, Natural Cellulosic Fiber Reinforced Concrete: Influence of Fiber Type and Loading Percentage on Mechanical and Water Absorption Performance, Materials 15 (2022), https://doi.org/10.3390/ma15030874.
[214] D. Cuthbertson, U. Berardi, C. Briens, F. Berruti, Biochar from residual biomass as a concrete filler for improved thermal and acoustic properties, Biomass-.-. Bioenergy 120 (2019) 77–83, https://doi.org/10.1016/J.BIOMBIOE.2018.11.007.
[215] Y. Qin, X. Pang, K. Tan, T. Bao, Evaluation of pervious concrete performance with pulverized biochar as cement replacement, Cem. Concr. Compos 119 (2021) 104022, https://doi.org/10.1016/J.CEMCONCOMP.2021.104022.
[216] X. Yang, X.Y. Wang, Hydration-strength-durability-workability of biochar-cement binary blends, J. Build. Eng. 42 (2021), https://doi.org/10.1016/j.jobe.2021.103064.
[217] S.S. Senadheera, S. Gupta, H.W. Kua, D. Hou, S. Kim, D.C.W. Tsang, Y.S. Ok, Application of biochar in concrete – a review, Cem. Concr. Compos 143 (2023), https://doi.org/10.1016/j.cemconcomp.2023.105204.
[218] B.A. Akinyemi, A. Adesina, Recent advancements in the use of biochar for cementitious applications: a review, J. Build. Eng. 32 (2020), https://doi.org/10.1016/j.jobe.2020.101705.
[219] H. Maljaee, R. Madadi, H. Paiva, L. Tarelho, V.M. Ferreira, Incorporation of biochar in cementitious materials: a roadmap of biochar selection, Constr. Build. Mater. 283 (2021), https://doi.org/10.1016/j.conbuildmat.2021.122757.
[220] M.M. Almeron, S.D. Ferreira, P.H. Mareze, M. Godinho, Mechanical and acoustic performance of mortar with partial replacement by biochar from civil construction wood waste at advanced ages, Constr. Build. Mater. 428 (2024) 136281, https://doi.org/10.1016/J.CONBUILDMAT.2024.136281.
[221] M.R. Zakaria, M.A. Ahmad Farid, Y. Andou, I. Ramli, M.A. Hassan, Production of biochar and activated carbon from oil palm biomass: Current status, prospects, and challenges, Ind. Crops Prod. 199 (2023) 116767, https://doi.org/10.1016/J.INDCROP.2023.116767.
[222] A. Bala, S. Gupta, Engineered bamboo and bamboo-reinforced concrete elements as sustainable building materials: A review, Constr. Build. Mater. 394 (2023) 132116, https://doi.org/10.1016/J.CONBUILDMAT.2023.132116.
[223] Y. Jia, H. Li, X. He, P. Li, Z. Wang, Effect of biochar from municipal solid waste on mechanical and freeze–thaw properties of concrete, Constr. Build. Mater. 368 (2023) 130374, https://doi.org/10.1016/J.CONBUILDMAT.2023.130374.
[224] L. Chen, T. Zhou, J. Yang, J. Qi, L. Zhang, T. Liu, S. Dai, Y. Zhao, Q. Huang, Z. Liu, B. Li, A review on the roles of biochar incorporated into cementitious materials: Mechanisms, application and perspectives, Constr. Build. Mater. 409 (2023) 134204, https://doi.org/10.1016/J.CONBUILDMAT.2023.134204.
[225] W. Yao, Z. Li, Flexural behavior of bamboo–fiber-reinforced mortar laminates, Cem. Concr. Res 33 (2003) 15–19, https://doi.org/10.1016/S0008-8846(02)00909-2.
[226] X. Xie, Z. Zhou, M. Jiang, X. Xu, Z. Wang, D. Hui, Cellulosic fibers from rice straw and bamboo used as reinforcement of cement-based composites for remarkably improving mechanical properties, Compos B Eng. 78 (2015) 153–161, https://doi.org/10.1016/J.COMPOSITESB.2015.03.086.
[227] R.D. Toledo Filho, K. Ghavami, M.A. Sanjuán, G.L. England, Free, restrained and drying shrinkage of cement mortar composites reinforced with vegetable fibres, Cem. Concr. Compos 27 (2005) 537–546, https://doi.org/10.1016/J.CEMCONCOMP.2004.09.005.
[228] S.W.M. Supit, T. Nishiwaki, F.U.A. Shaikh, K. Boonserm, S.A. Rahman, Influences of hybrid fiber-reinforcement using wollastonite and cellulose nanofibers on strength and microstructure characterization of ultra-high-performance mortar, Constr. Build. Mater. 423 (2024) 135802, https://doi.org/10.1016/J.CONBUILDMAT.2024.135802.
[229] M.A. Gómez-Casero, L. Pérez-Villarejo, E. Castro, D. Eliche-Quesada, Reinforcement of alkali-activated cements based matrices using olive pruning fibres as an alternative to traditional fibres, Sustain Chem. Pharm. 37 (2024) 101433, https://doi.org/10.1016/J.SCP.2024.101433.
[230] M. Fei, W. Fu, X. Zheng, Y. Chen, W. Liu, R. Qiu, Enhancing cement composite interface with waterglass modification on bamboo fiber: A viable and effective approach, Constr. Build. Mater. 411 (2024) 134338, https://doi.org/10.1016/J.CONBUILDMAT.2023.134338.
[231] Properties and interfacial performances with magnesium phosphate cement of coir fiber treated by an efficient water bath method: Effect of immersion temperatures and times, Constr Build Mater 429 (2024) 136443. ⟨https://doi.org/10.1016/J.CONBUILDMAT.2024.136443⟩.
[232] N. Gamage, Y. Patrisia, C. Gunasekara, D.W. Law, S. Houshyar, S. Setunge, Shrinkage induced crack control of concrete integrating synthetic textile and natural cellulosic fibres: comparative review analysis, Constr. Build. Mater. 427 (2024) 136275, https://doi.org/10.1016/J.CONBUILDMAT.2024.136275.
[233] E.O. Cruz, P.R. Vlasak, X.L. Osorios Barajas, G. Rocha de Paula, C. Alexandre Fioroni, H. Savastano, Novel surface functionalization of cellulose fibers with polyurethane prepolymers in fiber cement composites: impact on final properties and potential benefits for the production process, Constr. Build. Mater. 409 (2023) 133934, https://doi.org/10.1016/J.CONBUILDMAT.2023.133934.
[234] A. Hakamy, F.U.A. Shaikh, I.M. Low, Thermal and mechanical properties of hemp fabric-reinforced nanoclay–cement nanocomposites, J. Mater. Sci. 49 (2014) 1684–1694, https://doi.org/10.1007/s10853-013-7853-0.
[235] J. Zhao, Y. Yao, Q. Cui, X.M. Wang, Optimization of processing variables and mechanical properties in rubber-wood particles reinforced cement based composites manufacturing technology, Compos B Eng. 50 (2013) 193–201, https://doi.org/10.1016/J.COMPOSITESB.2012.10.024.
[236] S. Feng, J. Lyu, H. Xiao, J. Feng, Application of cellulose fibre in ultra-high-performance concrete to mitigate autogenous shrinkage, J. Sustain Cem. Based Mater. 12 (2023) 842–855, https://doi.org/10.1080/21650373.2022.2119618.
[237] S. Kawashima, S.P. Shah, Early-age autogenous and drying shrinkage behavior of cellulose fiber-reinforced cementitious materials, Cem. Concr. Compos 33 (2011) 201–208, https://doi.org/10.1016/j.cemconcomp.2010.10.018.
[238] Y. Barabanshchikov, H. Pham, K. Usanova, Influence of microfibrillated cellulose additive on strength, elastic modulus, heat release, and shrinkage of mortar and concrete, Materials 14 (2021), https://doi.org/10.3390/ma14226933.
[239] C.L. Hwang, V.A. Tran, J.W. Hong, Y.C. Hsieh, Effects of short coconut fiber on the mechanical properties, plastic cracking behavior, and impact resistance of

cementitious composites, Constr. Build. Mater. 127 (2016) 984–992, https://doi.org/10.1016/J.CONBUILDMAT.2016.09.118.
[240] S. Ma, D. Hou, P. Bao, D. Wang, Influence of alkali-resistant glass fiber on seismic performance of precast ceramsite concrete sandwich wall panels, Structures 38 (2022) 94–107, https://doi.org/10.1016/J.ISTRUC.2022.01.081.
[241] H. Wu, A. Shen, Q. Cheng, Y. Cai, G. Ren, H. Pan, S. Deng, A review of recent developments in application of plant fibers as reinforcements in concrete, J. Clean. Prod. 419 (2023) 138265, https://doi.org/10.1016/J.JCLEPRO.2023.138265.
[242] S. Marinković, V. Radonjanin, M. Malešev, I. Ignjatović, Comparative environmental assessment of natural and recycled aggregate concrete, Waste Manag. 30 (2010) 2255–2264, https://doi.org/10.1016/j.wasman.2010.04.012.
[243] M. Garfí, E. Cadena, D. Sanchez-Ramos, I. Ferrer, Life cycle assessment of drinking water: Comparing conventional water treatment, reverse osmosis and mineral water in glass and plastic bottles, J. Clean. Prod. 137 (2016) 997–1003, https://doi.org/10.1016/j.jclepro.2016.07.218.
[244] L. Serrano-Luján, S. Víctor-Román, C. Toledo, O. Sanahuja-Parejo, A.E. Mansour, J. Abad, A. Amassian, A.M. Benito, W.K. Maser, A. Urbina, Environmental impact of the production of graphene oxide and reduced graphene oxide, SN Appl. Sci. 1 (2019) 179, https://doi.org/10.1007/s42452-019-0193-1.
[245] Y.D. Hernandez-Charpak, A.M. Mozrall, N.J. Williams, T.A. Trabold, C.A. Diaz, Biochar as a sustainable alternative to carbon black in agricultural mulch films, Environ. Res 246 (2024) 117916, https://doi.org/10.1016/J.ENVRES.2023.117916.
[246] J. Song, X. Wang, C.-T. Chang, Preparation and characterization of graphene oxide, J. Nanomater 2014 (2014) 276143, https://doi.org/10.1155/2014/276143.
[247] D. Chen, H. Feng, J. Li, Graphene oxide: preparation, functionalization, and electrochemical applications, Chem. Rev. 112 (2012) 6027–6053, https://doi.org/10.1021/cr300115g.
[248] C. Tian, A novel preparation of high purity TiO2 from industrial low concentration TiOSO4 solution via short sulfate process, Mater. Sci. Semicond. Process 137 (2022) 106166, https://doi.org/10.1016/J.MSSP.2021.106166.
[249] J. Tian, L. Chen, J. Dai, X. Wang, Y. Yin, P. Wu, Preparation and characterization of TiO2, ZnO, and TiO2/ZnO nanofilms via sol–gel process, Ceram. Int 35 (2009) 2261–2270, https://doi.org/10.1016/J.CERAMINT.2008.12.010.
[250] N. Malhotra, O.B. Villaflores, G. Audira, P. Siregar, J.S. Lee, T.R. Ger, C.Der Hsiao, Toxicity studies on graphene-based nanomaterials in aquatic organisms: Current understanding, Molecules 25 (2020), https://doi.org/10.3390/molecules25163618.
[251] N.R. Schwartz, A.D. Paulsen, M.J. Blaise, A.L. Wagner, P.E. Yelvington, Analysis of emissions from combusting pyrolysis products, Fuel 274 (2020) 117863, https://doi.org/10.1016/J.FUEL.2020.117863.
[252] H. Zhou, C. Wu, A. Meng, Y. Zhang, P.T. Williams, Effect of interactions of biomass constituents on polycyclic aromatic hydrocarbons (PAH) formation during fast pyrolysis, J. Anal. Appl. Pyrolysis 110 (2014) 264–269, https://doi.org/10.1016/J.JAAP.2014.09.007.
[253] M.S. Safdari, M. Rahmati, E. Amini, J.E. Howarth, J.P. Berryhill, M. Dietenberger, D.R. Weise, T.H. Fletcher, Characterization of pyrolysis products from fast pyrolysis of live and dead vegetation native to the Southern United States, Fuel 229 (2018) 151–166, https://doi.org/10.1016/J.FUEL.2018.04.166.
[254] B.-K. Lee, Sources, Distribution and Toxicity of Polyaromatic Hydrocarbons (PAHs) in Particulate Matter, in: V. Villanyi (Ed.), Air Pollution, IntechOpen, Rijeka, 2010, https://doi.org/10.5772/10045.
[255] A.N. Ghulam, O.A.L. Dos Santos, L. Hazeem, B.P. Backx, M. Bououdina, S. Bellucci, Graphene Oxide (GO) Materials—Applications and Toxicity on Living Organisms and Environment, J. Funct. Biomater. 13 (2022), https://doi.org/10.3390/jfb13020077.
[256] M. Skocaj, M. Filipic, J. Petkovic, S. Novak, Titanium dioxide in our everyday life; Is it safe? Radio. Oncol. 45 (2011) 227–247, https://doi.org/10.2478/v10019-011-0037-0.
[257] R.T. Cullen, B.G. Miller, A.D. Jones, J.M.G. Davis, Toxicity of cellulose fibres, Ann. Occup. Hyg. 46 (2002) 81–84, https://doi.org/10.1093/annhyg/mef628.
[258] E.M. De Capitani, E. Algranti, A.M.Z. Handar, A.M.A. Altemani, R.G. Ferreira, A. B. Balthazar, E.M.F.P. Cerqueira, J.S. Ota, Wood charcoal and activated carbon dust pneumoconiosis in three workers, Am. J. Ind. Med 50 (2007) 191–196, https://doi.org/10.1002/ajim.20418.
[259] O.J. Uski, M.S. Happo, P.I. Jalava, T. Brunner, J. Kelz, I. Obernberger, J. Jokiniemi, M.R. Hirvonen, Acute systemic and lung inflammation in C57Bl/6J mice after intratracheal aspiration of particulate matter from small-scale biomass combustion appliances based on old and modern technologies, Inhal. Toxicol. 24 (2012) 952–965, https://doi.org/10.3109/08958378.2012.742172.
[260] S.V. Vassilev, D. Baxter, L.K. Andersen, C.G. Vassileva, An overview of the composition and application of biomass ash.: Part 2. Potential utilisation, technological and ecological advantages and challenges, Fuel 105 (2013) 19–39, https://doi.org/10.1016/J.FUEL.2012.10.001.
[261] G.M. Zannerni, K.P. Fattah, A.K. Al-Tamimi, Ambient-cured geopolymer concrete with single alkali activator,Sustain, Mater. Technol. 23 (2020) e00131.
[262] A.S. El-Dieb, D.M. Kanaan, Ceramic waste powder an alternative cement replacement – Characterization and evaluation, Sustain. Mater. Technol. 17 (2018) e00063.